Matematisk-fysiske Skrifter
udgivet af
Det Kongelige Danske Videnskabernes Selskab
Bind **1**, nr. 8

Mat. Fys. Skr. Dan. Vid. Selsk. **1**, no. 8 (1959)

THE INTRINSIC STATES OF ODD-A NUCLEI HAVING ELLIPSOIDAL EQUILIBRIUM SHAPE

BY

BEN R. MOTTELSON AND SVEN GÖSTA NILSSON

København 1959
i kommission hos Ejnar Munksgaard

DET KONGELIGE DANSKE VIDENSKABERNES SELSKAB udgiver følgende publikationsrækker:

THE ROYAL DANISH ACADEMY OF SCIENCES AND LETTERS *issues the following series of publications:*

	Bibliographical Abbreviation
Oversigt over Selskabets Virksomhed (8°) *(Annual in Danish)*	Overs. Dan. Vid. Selsk.
Historisk-filosofiske Meddelelser (8°)	Hist. Filos. Medd. Dan. Vid. Selsk.
Historisk-filosofiske Skrifter (4°) *(History, Philology, Philosophy, Archeology, Art History)*	Hist. Filos. Skr. Dan. Vid. Selsk
Matematisk-fysiske Meddelelser (8°)	Mat. Fys. Medd. Dan. Vid. Selsk
Matematisk-fysiske Skrifter (4°) *(Mathematics, Physics, Chemistry, Astronomy, Geology)*	Mat. Fys. Skr. Dan. Vid. Selsk.
Biologiske Meddelelser (8°)	Biol. Medd. Dan. Vid. Selsk.
Biologiske Skrifter (4°) *(Botany, Zoology, General Biology)*	Biol. Skr. Dan. Vid. Selsk.

Selskabets sekretariat og postadresse: Dantes Plads 5, København V.

The address of the secretariate of the Academy is:
Det Kongelige Danske Videnskabernes Selskab,
Dantes Plads 5, København V, Denmark.

Selskabets kommissionær: EJNAR MUNKSGAARD's Forlag, Nørregade 6, København K.

The publications are sold by the agent of the Academy:
EJNAR MUNKSGAARD, *Publishers,*
6 Nörregade, København K, Denmark.

Matematisk-fysiske Skrifter
udgivet af
Det Kongelige Danske Videnskabernes Selskab
Bind **1**, nr. 8

Mat. Fys. Skr. Dan. Vid. Selsk. **1**, no. 8 (1959)

THE INTRINSIC STATES OF ODD-A NUCLEI HAVING ELLIPSOIDAL EQUILIBRIUM SHAPE

BY

BEN R. MOTTELSON AND SVEN GÖSTA NILSSON

København 1959
i kommission hos Ejnar Munksgaard

PRINTED IN DENMMARK
BIANCO LUNOS BOGTRYKKERI A-S

CONTENTS

Synopsis.

In the regions $A \sim 25$, $150 < A < 190$ and $A > 222$, it is known that the nuclear shape deviates essentially from spherical. In this paper, the odd-A nuclei in these regions are considered and a classification of the observed intrinsic excitations is attempted on the basis of an independent-particle description of the last odd nucleon. The evidence available on beta and gamma transitions, nuclear moments, and properties of the rotational spectra are discussed in terms of this classification of the states.

I. INTRODUCTION

Whenever we observe nuclear configurations with sufficiently many particles outside of closed shells, it is found that the nuclear shape deviates essentially from spherical symmetry. A very simple type of excitation is then possible corresponding to the rotation of the nucleus in space without changing the shape or intrinsic configuration[1]. In the regions $A \sim 25$, $150 < A < 190$, and $A > 222$, the nuclear spectra exhibit such rotational bands associated with each intrinsic state[2]. The structure of the observed rotational bands (i. e., the energy dependence, $I(I+1)$, and the spin sequence, $I = 0, 2, 4, 6 \ldots$ for even-even nuclei) implies that the nuclear equilibrium shape is axially symmetric and symmetric with respect to reflection in a plane perpendicular to the symmetry axis and passing through the center of the system. The existence of a symmetry axis implies that, for each rotational band, there will be a constant of the motion, K, representing the component of the total angular momentum along the symmetry axis. In the nucleus, there is no collective rotational motion around the symmetry axis and so the angular momentum, K, in each rotational band is a characteristic of the intrinsic configuration associated with that band. Similarly, the reflection symmetry of the nucleus implies that the rotational motion always has even parity and, thus, the parity of all the states in a rotational band is the same and is equal to the parity of the intrinsic configuration. The coupling scheme appropriate to such non-spherical, axially symmetric nuclei is illustrated in Fig. 1.

Having classified the observed spectra into the intrinsic states and the corresponding rotational excitations associated with each such state, the next step in the interpretation of these spectra is to obtain a more detailed description of the intrinsic motion. In the present paper, we attempt an interpretation of the available data on the intrinsic states of the non-spherical odd-A nuclei, assuming an independent-particle model for the intrinsic motion.

We thus consider the motion of the nucleons in an axially symmetric, but non-spherical nuclear potential. The calculations of the single-particle spectra and wave

[1] For a systematic discussion of the nuclear rotational spectra, cf. ALDER et al. (1956), in the following referred to as ABH.

[2] *Note added in proof:* In a recent work by KURATH and PIČMAN (to appear in Nuclear Phys.), it is shown that this coupling scheme can also be applied to the nuclei in the region $4 < A < 16$. The results are very similar to those obtained from a description of the states in terms of the $1p$ single-particle configurations, in which the coupling scheme is intermediate between LS and jj.

functions have been published previously[1]. In such calculations, there appear a number of parameters which describe the radial dependence of the potential and the spin orbit force. These have been adjusted, first, so that they reproduce the available empirical evidence about the sequence of single-particle orbitals in a spherical potential (i. e., the evidence obtained from the spins and parities of levels near to closed-shell configurations). Finally, small adjustments in the available parameters

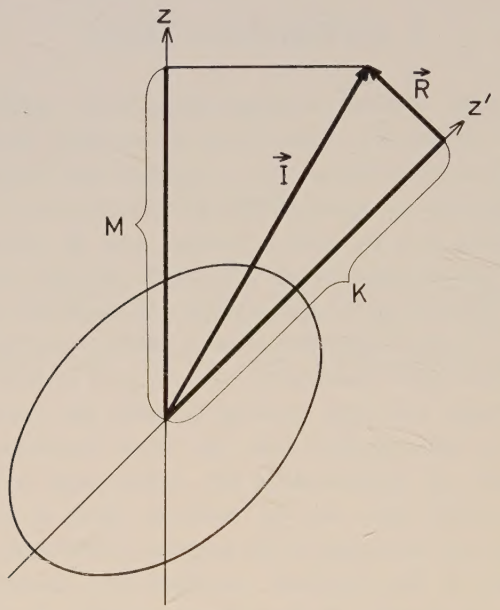

Fig. 1. *Angular momentum coupling scheme for deformed nuclei.* The total angular momentum, I, has the component M along the fixed z-axis and the component K along the nuclear symmetry axis, z'. The collective rotational angular momentum, R, is perpendicular to the nuclear symmetry axis; thus, K is entirely a property of the intrinsic motion.

have been made in order to reproduce as well as possible the observed intrinsic spectra of the non-spherical nuclei. The calculated single-particle spectra are plotted in Figs. 2, 3, 4, 5, and 6 as a function of the parameter δ, which characterizes the eccentricity of the nuclear potential[2].

Assuming the nuclear potential and charge distribution to have the same shape, the quantity δ can be determined directly from an electric quadrupole moment measurement or from a measurement of the $E2$ transition probability between two states in

[1] S. G. Nilsson (1955); in the following, this reference will be cited as SGN. A preliminary report of the present classification was published in B. R. Mottelson and S. G. Nilsson (1955a) which will be referred to as MN. Similar calculations have also been made by S. Moszkowski (1955a) and K. Gottfried (1956).

[2] Some of these level diagrams and the corresponding wave functions have been published previously (SGN and MN). In a number of cases, additional calculations have been made in order to complete those reported in these references; the new energies and wave functions are given in the Appendix.

a rotational band. These quantities may be expressed in terms of the intrinsic quadrupole moment, Q_0, which is given in terms of δ by the relation[1]

$$Q_0 = \frac{4}{5}\delta Z R_0^2\left(1+\frac{1}{2}\delta+\ldots\right), \tag{1}$$

where Z is the nuclear charge number and R_0 the mean charge radius of the nucleus. It is also possible to make a theoretical estimate of δ as the value of the eccentricity which minimizes the total nuclear energy (cf. § IV).

Two orbits will have the same energy if they are identical, except for the sense (right handed or left handed) in which the particle moves around the symmetry axis. Thus, each level in Figs. 2—6 is two-fold degenerate, corresponding to the possibilities $+K$ and $-K$.

Besides K and the parity, $\Pi = \pm$, a number of other quantum numbers are necessary to distinguish the different single-particle states in a non-spherical field. In Figs. 2—6, we have used the "asymptotic" quantum numbers which would characterize these states in the limit where the nuclear potential becomes a very anisotropic, axially symmetric, harmonic oscillator. In this limit, one has the quantum numbers, N, the total number of nodes in the wave function, n_z, the number of nodal planes perpendicular to the symmetry axis, and Λ, the component of the particle's orbital angular momentum along the symmetry axis. These quantum numbers are written in square brackets, as $[Nn_z\Lambda]$, beside each orbit in Figs. 2—6. While these quantum numbers would exactly characterize the nuclear states in the limit mentioned above, the actual proper states usually contain components with other values of n_z and Λ. However, for values of $\delta \sim 0.3$, the calculated states usually correspond to the asymptotic states with an accuracy of the order of 90 % or better. Thus, selection rules associated with these asymptotic quantum numbers may be expected to play an important role in determining the strengths of nuclear transitions between different intrinsic states. The asymptotic quantum numbers have the further advantage that they characterize the actual states in the region of interest, ($\delta \gtrsim 0.15$), in a manner that is independent of the detailed assumptions made about the order of levels for $\delta = 0$.

In the following section (§ II), we discuss the available level spectra of the odd-A nuclei possessing non-spherical equilibrium shapes. Where detailed evidence is available on the spins and parities of the nuclear states, the data provide a direct test of the theoretical spectra of Figs. 2—6. Where such evidence is not available,

[1] The parameter δ used in the present paper equals exactly the parameter δ used by MN and the parameter ε of SGN. It can be expressed in terms of the various deformation parameters used in the references indicated below by means of the following relations, correct to first order:

$\delta \simeq 0.95\,\beta$ (A. Bohr, 1952).
$\delta \simeq \delta$ (SGN).
$\delta \simeq \frac{\Delta R}{R}$ (A. Bohr and B. Mottelson, 1955b).
$\delta \simeq \eta\cdot\varkappa$ (SGN).

we have used Figs. 2—6 as a guide in the classification of the available information. In § III, we discuss the moments of inertia of the odd-A nuclei. The rather large variations in these moments of inertia in going from one intrinsic state to another are found to be well accounted for on the basis of the classification of the intrinsic states given in § II. The theoretical estimate of the equilibrium deformation is considered in § IV. Finally, in § V, we summarize the main conclusions that can be drawn from the present analysis.

II. INTERPRETATION OF THE OBSERVED LEVEL SPECTRA

In this section, we attempt a systematic discussion of the available evidence on the ground states and excited levels in the odd-A nuclei in the regions where the nuclei are found to have large equilibrium deformations, i. e., $A \sim 25$, $150 < A < 190$, and $A > 225$. We begin the section by a number of short paragraphs in which we review certain selection rules and definitions of the nuclear parameters relevant to the discussion of these spectra.

A. Summary of parameters used in discussing the spectra of non-spherical nuclei.

a) *Rotational bands* (see footnote 1 on p. 5.)

As mentioned in the Introduction, it is a characteristic feature of the spectra we shall discuss that there is a rotational band associated with each intrinsic configuration. The energy within such a band is approximately given by

$$E_{\mathrm{rot}} = \frac{\hbar^2}{2\Im}\left\{I(I+1) + a(-)^{I+1/2}\left(I+\frac{1}{2}\right)\delta_{K\,1/2}\right\}. \qquad (2)$$

The last term in (2) reflects a decoupling effect which occurs only for configurations with $K = 1/2$. The magnitude of this effect is determined by the parameter a which depends on the details of the intrinsic motion and can be explicitly calculated in terms of the wave functions of the last odd nucleon (the expression for a in terms of the wave function for the last odd nucleon may be found, for example, in SGN; cf. Table VIII for a comparison of the calculated and measured a-values). The effective moment of inertia, $\Im$, appearing in (2) is found to be systematically larger in odd-A nuclei than in the ground-state rotational band of neighbouring even-even nuclei; also, there are appreciable variations in $\Im$ from one rotational band to another in the odd-A nuclei. This effect is discussed in § III. Besides the regularities implied by the energy

spectrum (2), there are a number of simple intensity rules governing the relative intensity of nuclear transitions which lead to different members of a rotational band. These relations have been experimentally tested for alpha, beta and gamma transitions as well as for deuteron stripping reactions. It is found that, whenever the absolute transition intensity is of the order of magnitude or greater than that which would be predicted for a single-particle transition, the experimentally observed transition rates follow well the theoretical intensity rules. However, when the absolute intensity is appreciably smaller than the single-particle estimate, the relative intensities may differ from those predicted by as much as an order of magnitude. Such deviations reflect the fact that the highly hindered transitions are extremely sensitive to very small admixtures in the nuclear wave function.

An especially simple consequence of the intensity rules is the existence of selection rules associated with the quantum number K. For a transition of multipole order λ from a level in a rotational band characterized by K_i to a level in a band characterized by K_f, we must have

$$| K_i - K_f | \leq \lambda \tag{3}$$

or the transition will be "K-forbidden". It is found that, for transitions which violate (3), the lifetime is from ten to a hundred times longer for each degree of K-forbiddenness. Thus, for example, the most highly K-forbidden transition reported occurs in Hf^{180}, where $K_i = 8$ (or possibly 9), $K_f = 0$, and $\lambda = 1$. The transition is thus 7 times K-forbidden and the measured half-life is about 10^{15} times longer than the single-particle estimate (cf. also Table V which contains a comparison of relative intensities of gamma transitions in Al^{25}).

b) *Selection rules associated with the intrinsic structure.*

As discussed in the Introduction, the intrinsic nuclear states for a sufficiently deformed potential may be approximately characterized by the quantum numbers N, n_z, and Λ in addition to K and the parity Π. There are a number of selection rules associated with these asymptotic quantum numbers (Alaga, 1955). The selection rules appropriate to gamma transitions are collected in Table I, while those for beta transitions are given in Table II. We shall use the following abbreviations to indicate the classification of beta and gamma transitions:

a = allowed beta transition, i. e., $\Delta I = 0$, or 1 (no).
1 = first forbidden beta transitions with $\Delta I = 0$, or 1 (yes).
1^* = alpha-type first forbidden beta transition, i. e., $\Delta I = 2$ (yes).
$E\lambda$ = gamma transition of electric 2^λ-pole.
$M\lambda$ = gamma transition of magnetic 2^λ-pole.
u = the transition does not violate the asymptotic selection rules of Table I or II (i. e., unhindered).
h = the transition violates the selection rules of Table I or II (i. e., hindered).

TABLE I. *Selection rules for electromagnetic single-proton transitions in terms of the asymptotic quantum numbers.*

Multipole	ΔK	Operator	$\Delta\Lambda$	Δn_z	ΔN
$E1$	1	$x+iy$	1	0	± 1
	0	z	0	1	1
				-1	-1
$M1$	1	l_+	1	1	0, (2)
				-1	0, (-2)
		s_+	0	0	0
	0	l_z	0	0	0
		s_z	0	0	0
$E2$	2	$(x+iy)^2$	2	0	0, ± 2
	1	$z(x+iy)$	1	1	0, 2
				-1	0, -2
	0	z^2	0	0	0
				2	2
				-2	-2
		x^2+y^2	0	0	0, ± 2
$M2$	2	$(x+iy)\,l_+$	2	1	± 1, (3)
				-1	± 1, (-3)
		$(x+iy)s_+$	1	0	± 1
	1	$(x+iy)l_z$	1	0	± 1
		zl_+	1	0	± 1
				2	± 1, (3)
				-2	± 1, (-3)
		$(x+iy)s_z$	1	0	± 1
		zs_+	0	1	1
				-1	-1
	0	$\{(x+iy)l_-\}$ $\{(x-iy)l_+\}$	0	1	± 1, (3)
				-1	± 1, (-3)
		$(x+iy)s_-$	1	0	± 1
		$(x-iy)s_+$	-1	0	± 1
		$\{zl_z\}$ $\{zs_z\}$	0	1	1
				-1	-1
$E3$	3	$(x+iy)^3$	3	0	± 1, ± 3
	2	$z(x+iy)^2$	2	1	± 1, 3
				-1	± 1, -3
	1	$z^2(x+iy)$	1	0	± 1
				2	1, 3
				-2	-1, -3
		$(x^2+y^2)(x+iy)$	1	0	± 1, ± 3
	0	z^3	0	1	1
				-1	-1
				3	3
				-3	-3
		$z(x^2+y^2)$	0	1	± 1, 3
				-1	± 1, -3

Multipole	ΔK	Operator	$\Delta\Lambda$	Δn_z	ΔN
$M3$	3	$(x+iy)^2 l_+$	3	1	0, ± 2, (4)
				-1	0, ± 2, (-4)
		$(x+iy)^2 s_+$	2	0	0, ± 2
	2	$z(x+iy)\,l_+$	2	0	0, ± 2
				2	0, 2, (4)
				-2	0, -2, (-4)
		$(x+iy)^2 l_z$	2	0	0, ± 2
		$z(x+iy)\,s_+$	1	1	0, 2
				-1	0, -2
		$(x+iy)^2 s_z$	2	0	0, ± 2
	1	$(x+iy)^2 l_-$	1	1	0, ± 2, (4)
				-1	0, ± 2, (-4)
		$z(x+iy)\,l_z$	1	1	0, 2
				-1	0, -2
		$z^2 l_+$	1	1	0, 2
				3	2, (4)
				-1	0, -2
				-3	-2, (-4)
	1	$(x^2+y^2)\,l_+$	1	1	0, ± 2, (4)
				-1	0, ± 2, (-4)
		$(x+iy)^2 s_-$	2	0	0, ± 2
		$z(x+iy)\,s_z$	1	1	0, 2
				-1	0, -2
		$z^2 s_+$	0	0	0
				2	2
				-2	-2
		$(x^2+y^2)\,s_+$	0	0	0, ± 2
	0	$\{z(x+iy)\,l_-\}$ $\{z(x-iy)\,l_+\}$	0	0	0, ± 2
				2	0, 2, (4)
				-2	0, -2, (-4)
		$z^2 l_z$	0	0	0
				2	2
				-2	-2
		$(x^2+y^2)\,l_z$	0	0	0, ± 2
		$z(x+iy)\,s_-$	1	1	0, 2
				-1	0, -2
		$z(x-iy)\,s_+$	-1	1	0, 2
				-1	0, -2
		$z^2 s_z$	0	0	0
				2	2
				-2	-2
		$(x^2+y^2)\,s_z$	0	0	0, ± 2

TABLE II. *Selection rules for beta transitions in terms of the asymptotic quantum numbers N, n_z, and Λ.*

Transition	ΔK	Operator	$\Delta\Lambda$	Δn_z	ΔN
Allowed (a)	0	1	0	0	0
		σ_z	0	0	0
	1	σ_+	0	0	0
First forbidden (1)	0	z	0	1 −1	1 −1
		$\sigma_z z, \sigma_z \nabla_z$	0	1 −1	1 −1
		$\sigma_+(x-iy)$, $\sigma_+ \nabla_-$	−1	0	±1
		$\sigma_-(x+iy)$, $\sigma_- \nabla_+$	1	0	±1
	1	$(x+iy)$	1	0	±1
		$\sigma_+ z$, $\sigma_+ \nabla_z$	0	1 −1	1 −1
		$\sigma_z(x+iy)$, $\sigma_z \nabla_+$	1	0	±1
First forbidden with α-type shape (1*)	0	$\sigma_z z$	0	1 −1	1 −1
		$\sigma_+(x-iy)$	−1	0	±1
		$\sigma_-(x+iy)$	1	0	±1
	1	$\sigma_+ z$	0	1 −1	1 −1
		$\sigma_z(x+iy)$	1	0	±1
	2	$\sigma_+(x+iy)$	1	0	±1

The organization of the table is identical to that of Table I. These selection rules were first given by G. ALAGA (1955 and 1957).

To TABLE I, p. 10.

The entries of the table are ordered according to multipolarity and change in angular momentum component ΔK between initial and final states. Column three then contains the corresponding multipole operator. The selection rules in terms of Λ, the component of orbital angular momentum along the nuclear symmetry axis z', N, the total number of nodes in the harmonic oscillator wave function, and n_z, the number of nodal planes perpendicular to the z'-axis are given in columns four, six and five, respectively. The transitions in parenthesis are expected to be weaker than the other transitions indicated, by a factor proportional to δ (see Appendix I in SGN). These rules have previously been discussed by S. G. NILSSON (1955b), CHASMAN and RASMUSSEN (1956), and G. ALAGA (1957).

It might at first be expected that the $E\lambda$ transition of an odd neutron should be appreciably slower than the corresponding transition of an odd proton. However, for $E1$, the center of mass correction implies that the matrix element for a nucleon of charge e_p is proportional to $\left(e_p - \frac{Ze}{A}\right)$ and is thus not significantly different in magnitude for a neutron and a proton. For $E2$ transitions, it is known that the last odd nucleon induces a quadrupole moment in the rest of the nucleus, which is responsible for an appreciable fraction of the transition intensity; this effect can be expressed in terms of an effective charge which can be roughly estimated to be $e_{\text{eff}} \sim \left(e_p + \frac{Ze}{A}\right)$, which is thus not too different for neutrons and protons. A similar effect is expected for $E\lambda$ transitions with $\lambda \geq 3$. The situation with respect to the orbital contribution to odd-neutron $M\lambda$ transitions is not so clear.

In order to be able to discuss quantitatively the relative strength of gamma transitions, we define a hindrance factor H which measures the ratio of the observed lifetime to that expected for a single-proton transition, using the estimate of Moszkowski (1955b). The summary of observed beta and gamma transitions, given in § V and illustrated in Figs. 13—15, seems to indicate that the transitions which are classified as hindered, according to Tables I and II, are systematically slower than corresponding transitions which are unhindered. The hindrance is found to be on the average of the order of a factor of 100, but is appreciably greater in some cases.

c) *Alpha decay.*

In the region of heavy elements, the alpha-decay data provide an important source of evidence for the classification of the intrinsic states. The alpha decay of the even-even nuclei is known to follow a very regular systematics in which the lifetime-energy relationship of the ground-state transition agrees well with the simple barrier penetration theory (for recent summaries, see Fröman, 1957, and Perlman and Rasmussen, 1957). It is therefore convenient to compare the partial half-life, $T_{1/2}^{(i)}$, of the alpha group i in an odd-A nucleus, with the value $T_{1/2}^{(0)}$ that would be expected for a ground-state transition of the same energy in an even-even nucleus. We thus define a hindrance factor, F, as

$$F = \frac{T_{1/2}^{(i)}}{T_{1/2}^{(0)}}. \tag{4}$$

It is found that the values of F range from 1 up to more than 10^4. However, there is in each odd-A nucleus one transition with $F \sim 1$ (the favoured transition) and this transition leads to a state in the daughter which has exactly the same intrinsic configuration for the last odd particle as the ground state configuration of the parent[1] (Bohr, Fröman, and Mottelson, 1955, and J. O. Newton, 1955). There does not yet exist any detailed interpretation of the variations in the observed F-values associated with transitions in which the orbit of the last odd nucleon changes.

d) *Magnetic moments.*

The magnetic moment of a nuclear state characterized by I and K can be written

$$\mu = g_R \frac{I(I+1) - K^2}{I+1} + g_K \frac{K^2}{I+1} \qquad K \neq 1/2. \tag{5}$$

For $K = 1/2$, a slightly more complicated expression must be used (see, e. g., SGN). The rotational g-factor, g_R, describes the ratio of charge to mass in the nuclear rotational motion and is expected to have approximately the value Z/A aside from shell structure effects and a possible systematic difference in the radial distribution of protons and neutrons. The intrinsic g-factor, g_K, depends on the intrinsic configuration.

The $M1$ transition rate between different states of a rotational band depends

[1] There are a few cases in odd-A nuclei in which two different alpha groups are observed with $F \sim 1$. These cases seem to occur in spectra where one expects two near-lying intrinsic states that are strongly mixed through the effect of the Coriolis force (cf. the alpha decay of U^{235} and Np^{237}).

on $(g_K - g_R)^2$ and, thus, a measurement of the absolute $M1$ transition rate and of the ground state magnetic moment makes possible a determination of g_K and g_R, separately. A number of such determinations (cf. F. K. McGowan and P. H. Stelson, 1957, and ABH) yield values of g_R which are on the average $(g_R)_{ave} \approx 0.3$, although the experimental accuracy is as yet rather poor. Also, recent direct determinations of g_R (Scharenberg and Goldring, 1958) from magnetic moment measurements on states with $K = 0$, i. e., excited states in the rotational bands of even-even nuclei, yield a value of $g_R = 0.2$ for Nd^{150}, Sm^{152}, and Sm^{154}.

In the interpretation of the ground state magnetic moments, we have calculated g_K from the wave function of the last odd nucleon and assumed a value of $g_R = Z/A$ for the collective g-factor. The uncertainty in the calculated value of the magnetic moment associated with the uncertainty in the assumed value of g_R is rather small. The calculated and measured magnetic moments are summarized in Table VII and Figs. 11—12.

We shall discuss separately the level schemes for each mass number in the regions where the nuclei are known to have non-spherical equilibrium shapes. In the captions to the figures, we give the references to the experimental work from which the level schemes were taken. The abbreviations employed are:

half-lives are given in *y* years, *d* days, *h* hours, *s* seconds;
the *Q values* for the ground state transitions are indicated by Q_β for beta decay, Q_{ec} for electron capture decay, Q_α for alpha decay;
beta decay log ft-values are given for each beta group and are indicated by underlining;
hindrance factors for alpha decay, as defined in § II c, are given for each alpha group and are enclosed within curly brackets, { };
excitation energies are given in keV except for the spectra with $A = 25$, where the unit is MeV;
the *spin I*, *parity II*, and *assumed K-value* of the states are written at the side of each level in the order *IKII*;
the *classification* of the intrinsic states is written in square brackets as $[Nn_z\Lambda]$ (cf. the definition of these asymptotic quantum numbers in the Introduction). This classification is usually written only for the first member of the corresponding rotational band.

In order to indicate approximately the amount of experimental data available on a given nuclear level, we have, somewhat arbitrarily, assigned the following grades:

A: sufficient evidence available to establish the existence of the level and also to indicate quite strongly the spin and parity value.
B: position of the level well established, but the available data does not uniquely determine the spin and parity.
C: position of the level based largely on conjecture guided by established systematics or an energy fit with otherwise unassigned gamma rays.

In cases where the complexity of the full level scheme obscures the band structure, we have drawn a seperate figure to illustrate the classification of the observed levels into rotational bands.

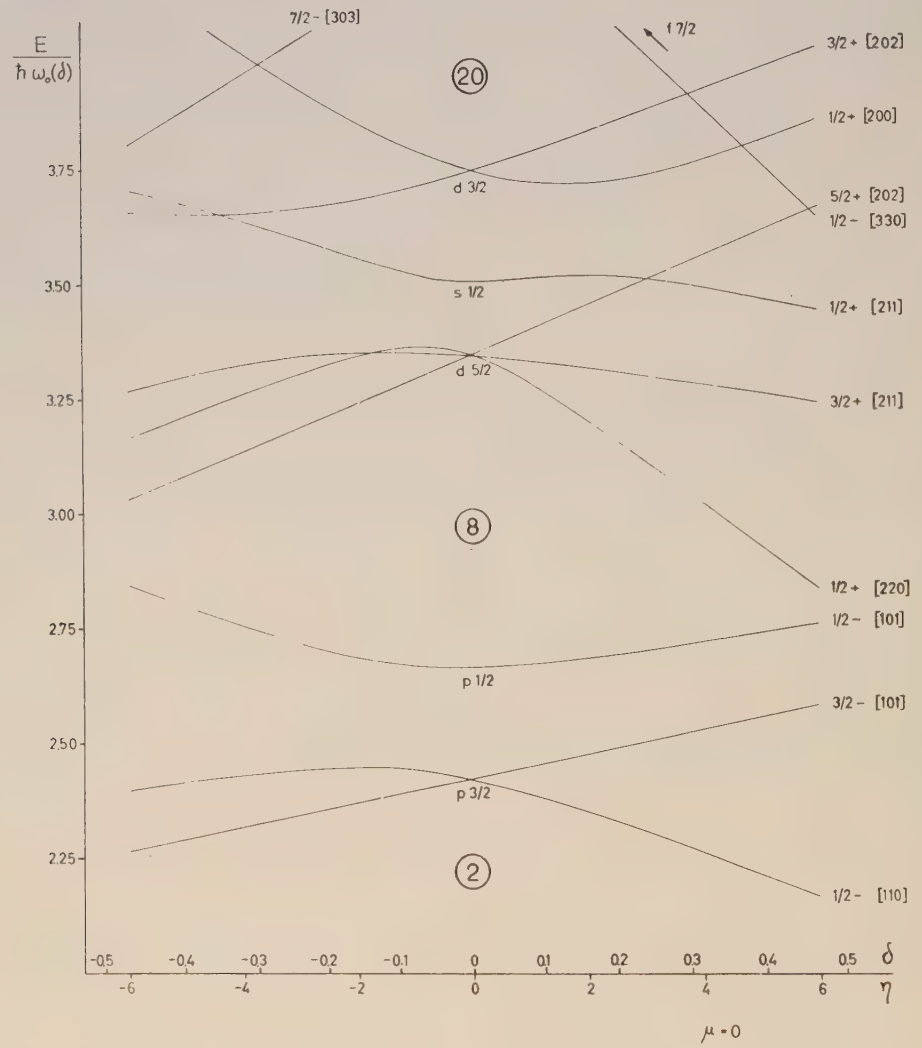

Fig. 2. *Single-particle levels in the regions* $8 < Z < 20$ *and* $8 < N < 20$, corresponding to the choice of potential parameters: $\mu = 0$ and $\varkappa = 0.08$. The corresponding wave functions are listed in (SGN). [This figure differs slightly from fig. 5 of (SGN) because of the different value of $\varkappa$ employed in the present paper.]

B. Level schemes:

a) *Region of* $A \sim 25$.

A number of authors have recently discussed the application of the present coupling scheme to the interpretation of the nuclei ranging from F^{19} to Si^{29} (Paul,

1956; Rakavy, 1957; Sheline, 1956; Bromley et al., 1957; Litherland et al., 1958). Although, in most cases, the experimental data are not sufficiently complete to provide a very critical test of the model, it appears that these considerations do provide a satisfactory basis for interpreting most of the available evidence in this region. The interpretation of the spectrum of F^{19} in terms of this coupling scheme is especially interesting, since the spectrum of this nucleus has also been successfully interpreted on the basis of the spherical shell model (Elliot and Flowers, 1955; Redlich, 1955). A comparison of the two interpretations has led to a better understanding of

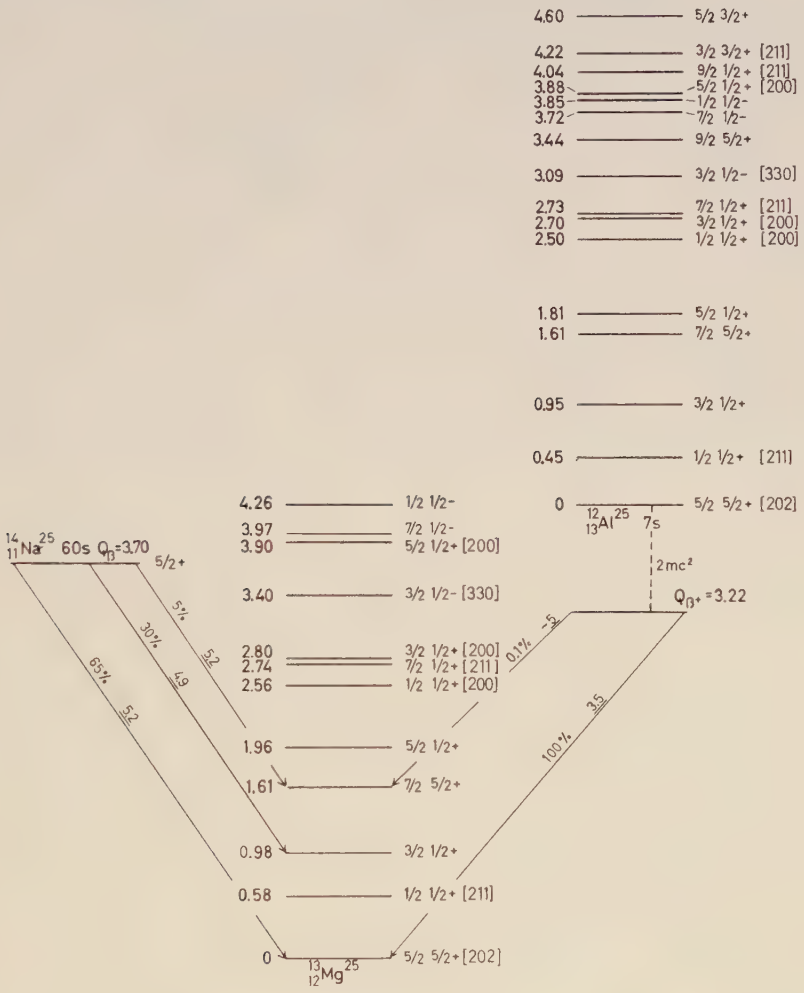

Fig. A = 25.

The experimental data for Al^{25} and Mg^{25} have been systematically summarized by P. M. Endt and C. M. Braams, (1957), Revs. Mod. Phys. **29**, 683. Additional data are given by Litherland, Gove, and Ferguson (1958), Bull. Am. Phys. Soc. **II:3**, 37. For a more detailed theoretical analysis, see Litherland, McManus, Paul, Bromley, and Gove (1958), Canad. Journ. Phys. **36**, 378.

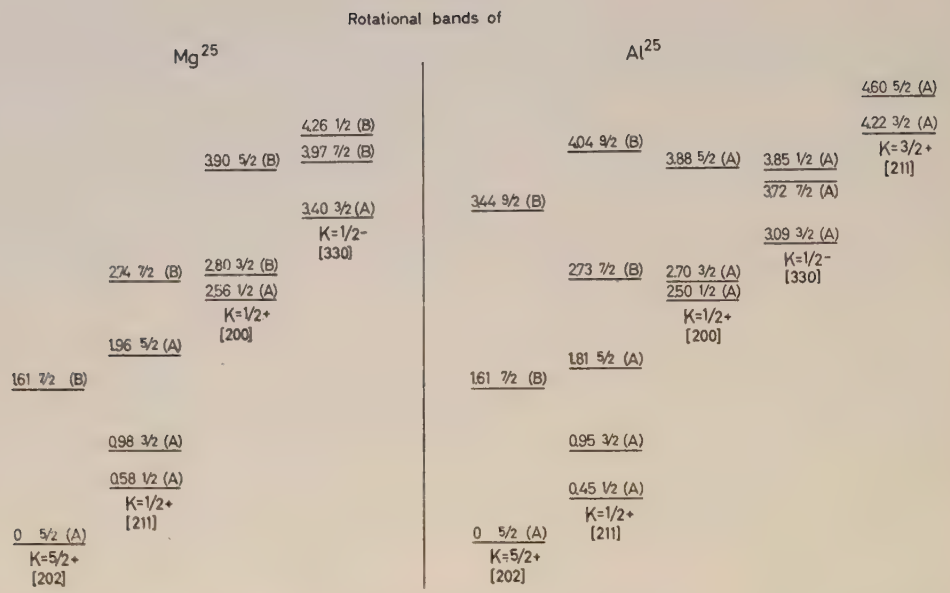

Fig. A = 25 R. The figure contains the same data as Fig. A = 25, except that the rotational bands have been separated from each other.

the relation between the collective and the independent-particle motions in the nucleus (Paul, 1956; Elliot, 1958).

We shall not attempt, in the present section, to retrace the ground covered in the above papers, and shall therefore restrict ourselves to a brief discussion of the

Table III. *Comparison between the spectra of the mirror nuclei* Mg^{25} *and* Al^{25}.

Orbital	Nucleus	Excitation energy of $I = K$ member (MeV)	$\frac{3\hbar^2}{\Im}$ (MeV)	a
[5/2 202]	Mg^{25}	0	1.38	—
	Al^{25}	0	1.38	—
[1 2 211]	Mg^{25}	0.58	0.99	−0.20
	Al^{25}	0.45	1.02	−0.02
[1/2 200]	Mg^{25}	2.56	0.90	−0.42
	Al^{25}	2.50	0.91	−0.56
[1/2 330]	Mg^{25}	4.26	0.69	−3.5
	Al^{25}	3.85	0.68	−3.2

The table gives a comparison between the intrinsic parameters characterizing the different rotational bands occurring in both Mg^{25} and Al^{25}. The orbital assignment of each intrinsic state is given in column one. The excitation energy at which each intrinsic state occurs in the respective spectra is listed in column three in units of MeV. The inertial parameter, $3\hbar^2/\Im$, of each rotational band is listed in column four in units of MeV. Column five exhibits the decoupling factor, characteristic of $K = 1/2$.

spectra for A = 25, which illustrates the type of data and the nature of the classification that is possible in this region of elements. The nuclei with A = 25 provide an especially favourable example, since they lie near the middle of the region and, thus, the coupling scheme should be most applicable to them. In addition, the experimental data are much more complete for these nuclei than they are for any other nuclei in this region.

TABLE IV. *Branching ratios of* M1 *and* E2 *transitions within the ground-state rotational band in* Al^{25}.

	Exp.	Theor.
$\frac{T(E2;\ 9/2\to 7/2)}{T(E2;\ 9/2\to 5/2)}$	0.2 ± 0.1	0.13
$\frac{T(E2;\ 9/2\to 7/2)}{T(M1;\ 9/2\to 7/2)}$	0.02 ± 0.01	0.012
$\frac{T(E2;\ 7/2\to 5/2)}{T(M1;\ 7/2\to 5/2)}$	0.04 ± 0.02	0.015

As was pointed out by ALAGA et al. (1955), the reduced branching ratios of transitions of a certain multipole order, λ, to members of the same rotational band depend only on simple "geometrical" factors involving I and K of initial and final states in addition to λ. The theoretical prediction for $E2$ radiation is compared with the measured ratio in line one of the table (columns two and three give the experimental and theoretical values, respectively). The mixing ratio $E2/M1$ depends in addition on the ratio of the two intrinsic parameters Q_0 and G_{M1} (see, e. g., SGN). The intrinsic quadrupole moment, Q_0, was assumed equal to 0.44 barns (see the text), G_{M1} was calculated = 8.1 on the basis of the wave functions of the present model. Lines two and three of this table exhibit a comparison between experimental and theoretical estimates, the latter based on the above parameters.

The mirror nuclei Al^{25} and Mg^{25} have very similar spectra and we therefore limit ourselves to a detailed discussion of Al^{25} (cf. Fig. A = 25 and Table III for a comparison of the two isobars).

The ground-state configuration of Al^{25} is [202 5/2] (i. e., the intrinsic state of the last odd nucleon corresponds with the orbit $N = 2$, $n_z = 0$, $\Lambda = 2$, $K = 5/2$, cf. Fig. 2 for the calculated single-particle spectrum appropriate to this region) and two excited rotational states associated with this configuration have been identified. Assuming an intrinsic quadrupole moment of 0.4×10^{-24} cm^2 (i. e., $\delta\sim0.3$) as indicated by the hyperfine-structure measurements on Al^{27} and Na^{23} (see STROMINGER, HOLLANDER, and SEABORG, 1958[1], and by the inelastic electron scattering from Mg^{24} (HELM, 1956), one can calculate from the intrinsic wave function the relative intensities and the $M1-E2$ mixtures for the gamme rays within this rotational band; the results are compared with the available data in Table IV.

The orbital [211 1/2] provides a low-lying excited intrinsic state in the Al^{25} spectrum and probably five states of the rotational band have been identified, although

[1] In the following, this reference is denoted by SHS.

TABLE V. *Classification of electromagnetic transitions in* Al^{25} *according to the K selection rule.*

Transition		Multi-polarity	Relative intensity	Reduced rel. intensity	Classification
Initial state	Final state				
3/2 1/2+ [211]	1/2 1/2+ [211]	$M1$	58	91	
	5/2 5/2+ [202]	$M1$	$\leq$ 42	$\leq$ 9	K-forbidden
5/2 1/2+ [211]	3/2 1/2+ [211]	$M1$	30	93	
	1/2 1/2+ [211]	$E2$	50	—	(ii)
	5/2 5/2+ [202]	$M1$	20	7	K-forbidden
1/2 1/2+ [200]	3/2 1/2+ [211]	$M1$	12	25	
	1/2 1/2+ [211]	$M1$	88	75	
	5/2 5/2+ [202]	$E2$	$\leq$ 2	—	
3/2 1/2+ [200]	5/2 1/2+ [211]	$M1$	40	94	(i)
	3/2 1/2+ [211]	$M1$	$\leq$ 2	< 1	(i)
	1/2 1/2+ [211]	$M1$	30	4	(i)
	5/2 5/2+ [202]	$M1$	30	2	K-forbidden
7/2 1/2+ [211]	5/2 1/2+ [211]	$M1$	20	99	
	3/2 1/2+ [211]	$E2$	70	—	(ii)
	7/2 5/2+ [202]	$M1$	not obs.	not obs.	K-forbidden
	5/2 5/2+ [202]	$M1$	10	1	K-forbidden
3/2 1/2− [330]	5/2 1/2+ [211]	$E1$	$\leq$ 2	$\leq$ 15	
	3/2 1/2+ [211]	$E1$	9	14	
	1/2 1/2+ [211]	$E1$	78	65	
	5/2 5/2+ [202]	$E1$	13	7	K-forbidden
7/2 1/2− [330]	5/2 1/2+ [211]	$E1$	70	96	
	7/2 5/2+ [202]	$E1$	not obs.	not obs.	K-forbidden
	5/2 5/2+ [202]	$E1$	30	4	K-forbidden
1/2 1/2− [330]	1/2 1/2+ [200]	$E1$	13	63	
	3/2 1/2+ [211]	$E1$	58	28	(i)
	1/2 1/2+ [211]	$E1$	29	9	(i)
5/2 1/2+ [200]	7/2 1/2+ [211]	$M1$	6	30	(i)
	3/2 1/2+ [200]	$M1$	9	40	
	5/2 1/2+ [211]	$M1$	5	5	(i)
	7/2 5/2+ [202]	$M1$	4	3	K-forbidden
	3/2 1/2+ [211]	$M1$	60	20	(i)
	1/2 1/2+ [211]	$E2$	5	—	
	5/2 5/2+ [202]	$M1$	9	1	K-forbidden

(i) These transitions exhibit considerable variations in intensity despite their interpretation as leading to different states of the same rotational band. In cases such as these with $\lambda \geq K_i + K_f$, such an effect can arise from a cancellation between the transition amplitudes for $K_i \rightarrow K_f$ and for $K_i \rightarrow -K_f$ (cf. ALAGA et al., 1955). LITHERLAND et al. (1958) present a quantitative interpretation of these relative intensities in terms of this effect.

(ii) These very strong $E2$ transitions connect states within the same rotational band.

The table compares the relative intensities of the gamma transitions from the different levels of Al^{25}. The first column gives the classification of the initial state, while the second column shows the classification of each final state that is populated from this level. The multipolarity and relative intensity of the transitions are listed in the next two columns. The fifth column gives the reduced relative intensity obtained from the experimental value of column four by dividing with the theoretical energy dependence $E^{2\lambda+1}$. The last column indicates the transitions which should be K-forbidden according to the classification of columns one and two.

there is some uncertainty about the spin of the 4.04 MeV level. (Recent experiments indicate that the spin of the state in question is either 5/2 or 9/2.) The decoupling parameter calculated for the orbital [211 1/2] and the above eccentricity is $a = 0.0$, while the value obtained from the observed energies of the first three states is $a_{exp} = -0.02$. The calculated value is quite sensitive to the value of the nuclear eccentricity.

Starting at 2.50 MeV, a second rotational band with $K = 1/2+$ is observed. This band corresponds quite well with the orbital [200 1/2] (cf. Fig. 2). The calculated decoupling parameter is $a = -0.2$, while the measured rotational energies determine the value $a_{exp} = -0.56$. Also in this case the calculated value of a is quite sensitive to the eccentricity.

The first odd parity state in Al^{25} occurs at 3.09 MeV and appears to be associated with a rotational band characterized by $K = 1/2-$ and a large negative decoupling parameter. These properties correspond well with the expected configuration [330 1/2]. The calculated value of the decoupling parameter is $a \sim -3$, which can be compared with the value deduced from the observed rotational energies $a_{exp} \sim -3.2$. The dependence of a_{theo} on the assumed eccentricity may be studied in Table VIII. The moment of inertia of this band is considerably greater than that of the lower-lying rotational bands, in agreement with the much greater intrinsic angular momentum associated with this orbital (cf. Table VI).

Above 4 MeV, the spectrum of Al^{25} is not as well studied and, in addition, one must expect in this energy region to encounter intrinsic states which represent the excitation of more than one particle (cf., e. g., the 4.23 MeV state in Mg^{24}). However, it is probable that the levels observed at 4.22 MeV and 4.60 MeV in Al^{25} represent states in a rotational band built on the [211 3/2] orbital. From the spectrum of Na^{23} it is known that the states in this band are considerably perturbed due to the Coriolis coupling to the [220 1/2] band which should lie at an excitation energy about 2 MeV higher; this coupling has the effect of bringing the $I = 3/2$ and $I = 5/2$ members of the band relatively close together followed by a considerable gap to the $I = 7/2$ state (cf. Rakavy, 1957).

Besides the interpretation of the observed spins and parities of these levels, one may employ the classification to interpret the observed gamma-ray transition intensities and the reaction widths. We shall not attempt a detailed discussion of these points since they have recently been treated very systematically (Litherland et al., 1958). It is possible, however, to note immediately a very strong influence of the selection rules associated with the quantum number K. Thus, for example, the 0.95 MeV level decays by $M1$ radiation both to the 0.45 MeV level and to the ground state. The latter transition is, however, K-forbidden (since $\Delta K = 2$) and indeed the reduced transition probability is about a factor of 10 smaller than for the transition to the 0.45 MeV level. The gamma-ray branching ratios are collected in Table V, from which one can conclude that the K-forbidden transitions are systematically a factor of from 10 to 100 weaker than transitions that are not thus forbidden.

b) *Region of elements $150 < A < 190$.*

The sharp increase in the nuclear eccentricity in going from neutron number $N = 88$ to $N = 90$ is a very striking feature of the nuclear systematics in this region of elements (for references to the experimental data, cf. MN). It can be understood in terms of the nuclear shell structure for these configurations, which implies the existence of two minima in the curve of nuclear energy as a function of the eccentricity, δ. (See § IV and also Fig. 12). In passing from $N = 88$ to $N = 90$ the absolute energy minimum shifts from the local minimum associated with the lesser to that associated with the greater eccentricity, probably as a consequence of the filling of the [660 1/2] orbital. This interpretation of the rapid change in the ground-state distortion implies, however, that even for $N = 90$ we may encounter excited intrinsic configurations associated with the minimum at smaller eccentricities. It should be expected that, when this happens, there will be an important effect on transition probabilities; thus transitions involving a major change in the nuclear shape should be slowed down by a mechanism which is the analogue of the Frank-Condon principle known in molecular spectra.

A = 153.

It appears that in $_{63}Eu^{153}$ (with $N = 90$) the ground state ($K = 5/2+$), the 103 keV ($K = 3/2+$), and the 710 keV ($K = 1/2+$) intrinsic states are associated with the larger values of the nuclear eccentricity ($\delta \sim 0.3$), while the 98 keV ($K = 5/2-$) state may have the smaller eccentricity.

The $_{63}Eu^{153}$ ground state spin is measured to be 5/2; from Fig. 3 it can be seen that, for deformations around $\delta \sim 0.3$, one expects the orbital [413 5/2] to represent the ground state for nucleon number 63. This state also accounts reasonably well for the measured magnetic moment of Eu^{153} (see Table VII). The rotational band based on the ground state has levels at 83 keV ($I = 7/2+$) and 190 keV ($I = 9/2+$) which have been especially studied by means of Coulomb excitation.

The first excited intrinsic excitation in Eu^{153} occurs at 98 keV and has been shown to decay to the ground state by an $E1$ transition. One may thus identify this level with the [532 5/2] state which would be the lowest orbital at smaller values of the eccentricity and which is known to be the ground state of Eu^{151}. The $E1$ transition from this level to the ground state should be appreciably retarded as a consequence of the selection rules in the asymptotic quantum numbers as well as the change in the nuclear equilibrium shape.

The other low lying intrinsic state expected for Eu^{153} is [411 3/2] (see Fig. 3) and the available evidence is consistent with assigning the observed level at 103 keV to this configuration. The level at 172 keV is identified as the $I = 5/2+$ member of the rotational band based on this state. The rotational energy parameter is $3\hbar^2/\Im = 83$ keV for this band, compared with $3\hbar^2/\Im = 72$ keV for the ground state band. The identification of the 172 keV level as a rotational partner to the 103 keV level is further supported by the fact that it decays to the latter by an essentially unhindered $M1$

transition, while its $M1$ decay to the ground state is hindered by the factor $H \sim 6 \times 10^3$, which is of the same order of magnitude as the hindrance of the transition from the 103 keV level to ground.

These strong hindrance factors for $M1$ transitions between the intrinsic states

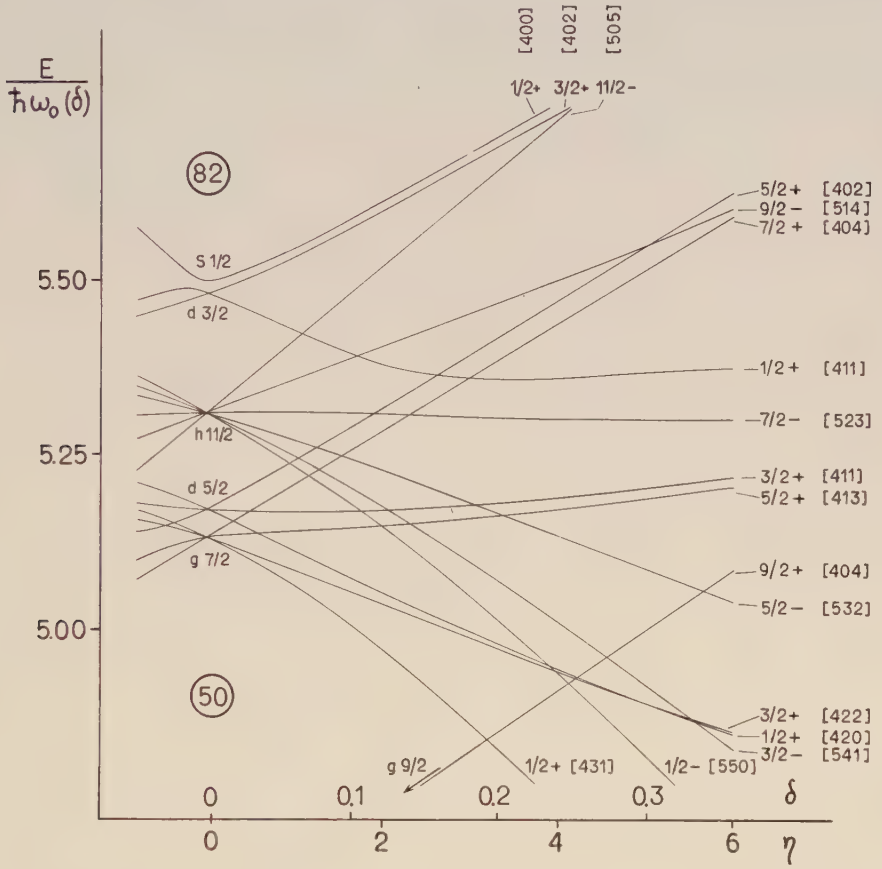

Fig. 3. *Single-particle levels for odd-Z nuclei in the region* $50 < Z < 82$. The corresponding wave functions are found in table I ($N = 5$) and table Ia ($N = 4$) of (SGN). The calculated wave functions correspond to the parameters $\mu = 0.55$ for $N = 4$ and $\mu = 0.45$ for $N = 5$. In comparing with the experimental data, it was found that the high-angular-momentum states of the $N = 5$ shell occurred systematically at lower excitation energies than would correspond to these parameters. Therefore, in constructing the figure, all odd-parity states have been plotted at an energy of approximately 400 keV lower than corresponding to these parameters. This corresponds to using a μ-value approximately equal to 0.50 for the levels belonging to the $N = 5$ shell.

[411 3/2] and [413 5/2] are seen to be in accord with the selection rules associated with the asymptotic quantum numbers.

A level at ~ 710 keV in Eu^{153} has been observed following the beta decay of Sm^{153}. This state is observed to decay by gamma transitions to the 103 and 172 keV levels. The evidence about this state is not very complete, but it may tentatively be

identified as the expected [411 1/2] orbital. If this is correct, there should be two close lying states populated by beta transitions (the $I = 1/2+$ and $I = 3/2+$ members of the rotational band); the energy difference between these two states might be of the order of 10 keV (see A = 169). According to the asymptotic selection rules, these

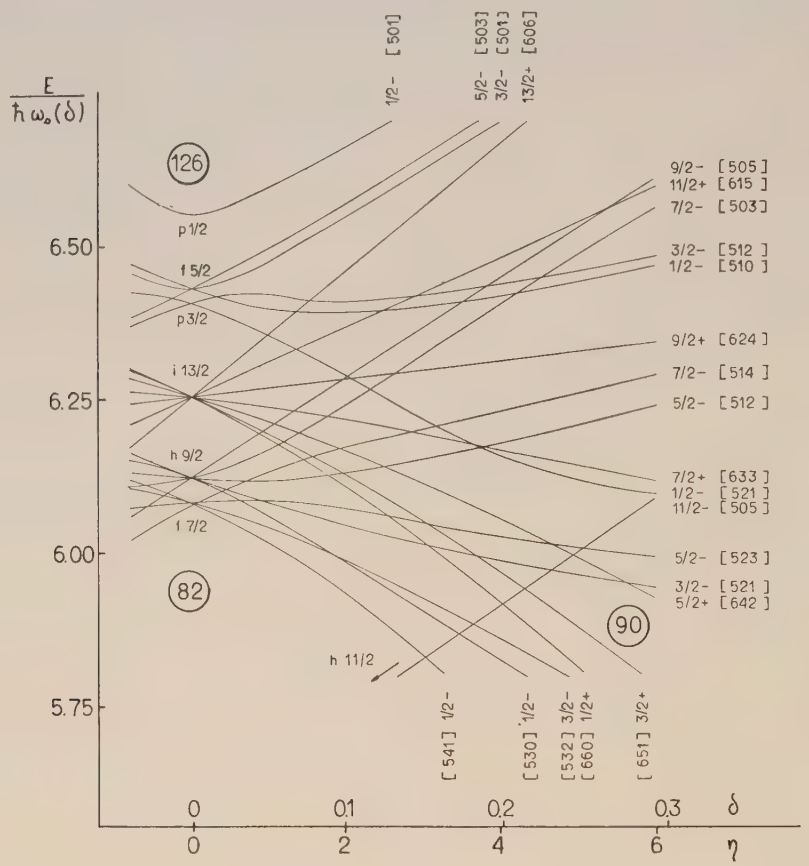

Fig. 4. *Single-particle levels for odd-N nuclei in the region* $82 < N < 126$. The corresponding wave functions are those of table I of (SGN), which corresponds to $\mu = 0.45$ for $N = 5$ and 6. The energy level diagram has been plotted employing $\varkappa = 0.05$, as in fig. 5 of (SGN).

levels should decay strongly by $M1$ radiation to the 103 and 172 keV levels, but not to the ground state.

The one other level in Fig. 3 that might be expected to occur in Eu^{153} below about 500 keV is the [523 7/2] orbital. The fact that it has not been observed so far is not surprising, since it would require a second forbidden beta transition from Sm^{153}, and there is probably not enough energy available to populate it in the Gd^{153} decay.

The decay of $_{62}Sm^{153}$ is found to populate only states in Eu^{153} with spin 5/2 or less, except for the very weak branch leading to the 83 keV 7/2+ level. This is consistent with the assignment of $I = 3/2-$ to Sm^{153}; this state may then be identified

with the orbital [521 3/2], which is the expected ground state for $N = 91$ in the region of deformations $\delta \sim 0.25$. The beta decay to the ground state of Eu^{153} is then classified as $1h$ with an observed log $ft = 7.3$, while the weak transition to the 83 keV member of the ground state rotational band is 1^*h. The transitions to the 103, 172, and 710 keV levels with log ft = 6,8, 6.7 and 6.5, respectively, are all classified as $1u$. The expected transition to the $I = 7/2+$ member of the $K = 3/2+$ rotational band would be 1^*u;

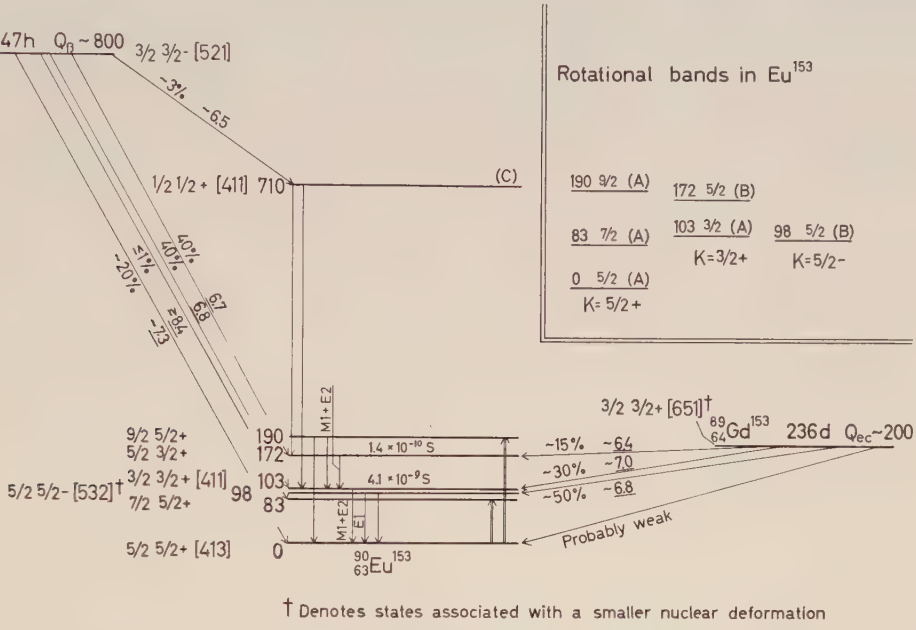

Fig. A = 153.

The Coulomb excitation of Eu^{153}, the beta decay of Sm^{153}, and the electron capture decay of Gd^{153} have been extensively studied in a number of laboratories. The results of these investigations are summarized in *Nuclear Data Cards*, National Research Council, Washington D. C., ed. C. L. McGinnis (in the following referred to as NDC), and in Strominger, Hollander, and Seaborg (1958), Revs. Mod. Phys, **30**, 585, in the following referred to as SHS. There remain, however, considerable disagreement and uncertainty about the properties of the 710 keV level of Eu^{153}.

this level should occur at ~ 269 keV and should thus be populated to the extent of a few tenths per cent of the beta decays. Finally, the 98 keV level is populated very weakly in the Sm^{153} decay, since such a transition involves a considerable change in the nuclear shape.

The Gd^{153} ground state probably has a relatively small eccentricity ($N = 89$) and may therefore not be described too well by the nuclear coupling scheme employed in the present discussion. If, however, we try to use Fig. 3, we would expect the Gd^{153} ground state to have $I = 3/2+$ corresponding to the orbital [651 3/2]. Such a characterization does not account too badly for the observed decay properties. The decay to the 98 keV state in Eu^{153} has log $ft \sim 6.8$ and is classified as $1h$. The transitions to the

ground state, 103 and 173 keV levels are *ah* and in addition very much retarded by the change in the equilibrium shape which is involved. The decay to the 83 keV level is not observed since it would be second forbidden.

A = 155.

The ground state spin of $_{64}Gd^{155}$ has been measured to be $I = 3/2$; both the spin and the magnetic moment are consistent with the assignment of the orbital

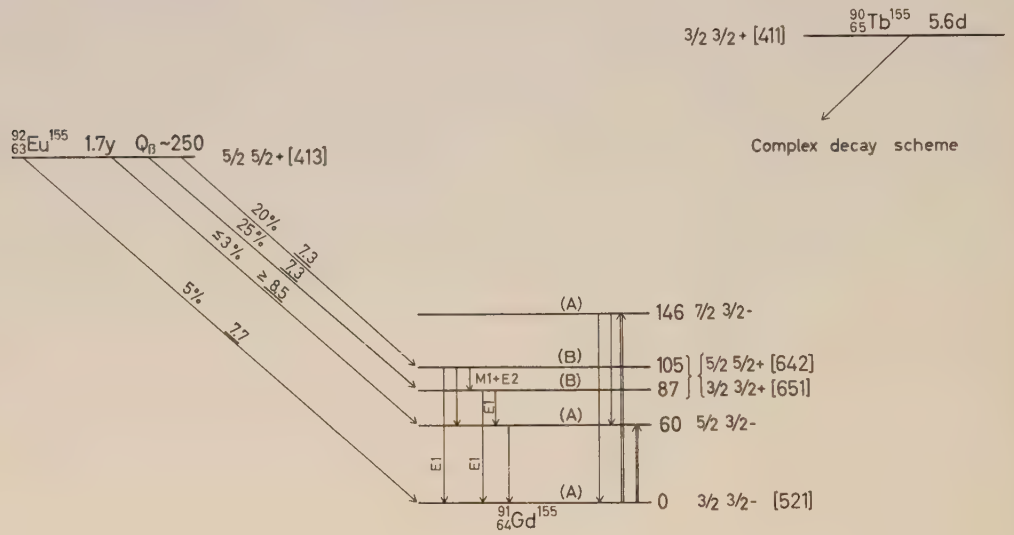

Fig. A = 155.

The decay scheme following the beta decay of Eu^{155} is taken from F. Boehm and E. N. Hatch (1957), Bull. Am. Phys. Soc. **II:2**, 231. For references to earlier work as well as to the Coulomb excitation of Gd^{155}, see NDC. Recently, the Tb^{155} decay has been studied by Mihelich, Harmatz, and Handley (1957), Phys. Rev. **108**, 989; by Ward, Jacob, and Mihelich (1957) Bull. Am. Phys. Soc. **II:2**, 259, and by Djelopov, Preobradjensky, and Sergienko (1958), Izvest. Akad. Nauk. **22**, 791. Note that the log *ft*-value of the ground-state beta branch should be 8.7 and not 7.7!

[521 3/2] which, according to Fig. 4, is the lowest configuration for $N = 91$ and $\delta \sim 0.25$. The $I = 5/2-$ and $I = 7/2-$ rotational states associated with this intrinsic state occur at 60 keV and 146 keV, respectively.

Low-lying even-parity intrinsic excitations occur at 87 and 105 keV in Gd^{155}, and it is probable that these levels correspond to the expected [642 5/2] and [651 3/2] orbitals. However, the available data do not seem able to indicate which of the two orbitals is to be assigned to which of the two levels. According to Fig. 4, the configuration [523 5/2] might also be expected to occur as a fairly low-lying excited state in Gd^{155}.

The ground state of $_{63}Eu^{155}$ should be [413 5/2] in analogy with Eu^{153}. The beta decay from this state to the Gd^{155} ground state rotational band is then classified as 1*h* in agreement with the evidence that the log *ft*-values are ~ 9. The decay to the [642 5/2] and [651 3/2] states would be *ah*, which is not inconsistent with the observed log *ft* = 7.3 for the transitions to the 86 and 105 keV levels.

The $_{65}Tb^{155}$ electron capture decay has recently been studied and found to be very complex. Although the interpretation of this decay is not yet clear, we can on the basis of Figs. 3 and 4 say that we expect the Tb^{155} ground state to be the [411 3/2] orbital and that this state should then decay mainly to the [521 3/2], [642 5/2], and [651 3/2] states in Gd^{155}. It is possible that the [660 1/2] and [521 1/2] states might occur at a somewhat higher excitation energy and might also be populated.

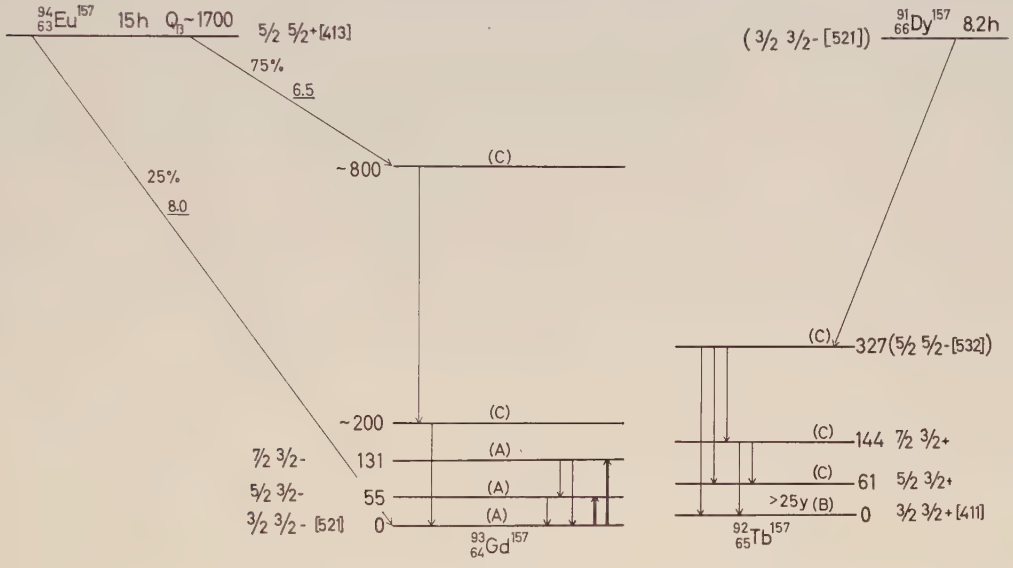

Fig. A = 157.

The Coulomb excitation studies of Gd^{157} are summarized in NDC and SHS. The characteristics of the Eu^{157} decay have been very roughly established by L. Winsberg, *Radiochemical Studies; the Fission Products*, Book II, National Nuclear Energy Series (McGraw Hill, 1951). The levels in Tb^{157}, following the Dy^{157} decay, are based on recent measurements by Mihelich, Harmatz, and Handley (1957), Phys. Rev. **108**, 989.

A = 157.

The ground state of $_{64}Gd^{157}$ is found to have the same spin and approximately the same magnetic moment as Gd^{155}. The orbital [521 3/2] is, therefore, also assigned to Gd^{157}. The identity of the ground state configurations for these nuclei is further supported by the similarity of the excitation energies and branching ratios observed in Coulomb excitation studies of the two isotopes. The fact that the orbit [521 3/2] appears as the ground state for both $N = 91$ and 93 may be associated with the fact that, in Gd^{157}, the eccentricity is known to be somewhat greater and thus the orbitals [521 3/2] and [642 5/2] may have interchanged their relative order in going from one isotope to the next (cf. Fig. 4). Indeed, the three orbits [642 5/2], [521 3/2], and [523 5/2] are all so close together in this region that some irregularity in the order in which they are filled might not be unexpected. One expects, of course, that the configurations [642 5/2] and [523 5/2] will occur as low lying excited states in Gd^{157}.

The evidence on the beta decay of $_{63}Eu^{157}$ is very incomplete. The reported log $ft = 8.0$ for the transition to the Gd^{157} ground state is consistent with the expected [413 5/2] assignment for the Eu^{157} ground state which would imply a $1h$ transition. The transition from Eu^{155} to the Gd^{155} ground state involves the same orbitals and is observed to have log $ft = 8.7$.

The $_{66}Dy^{157}$ electron capture decay populates a level in $_{65}Tb^{157}$ at 327 keV which, from its decay into the levels of the Tb ground state rotational band, appears to have $I = 5/2$. This level is tentatively assigned the configuration [532 5/2] as for the similar excited state observed in Tb^{159}. This assignment receives some further support from the fact that, if we take the Dy^{157} ground state as [521 3/2], as for Gd^{155}, then, according to Fig. 3, the [532 5/2] and [541 3/2] orbitals are expected to be more strongly populated in the Dy^{157} decay than any others available in this region of excitation. At a somewhat higher excitation energy, one might also populate the [411 1/2] state.

The decay of Tb^{157} has not been observed, and it has been established that the half life is either $> 25\ y$ or $< 10\ m$. A short half-life is not expected according to systematics. The experimental data together with the orbital assignments thus suggests that the transition energy is of the order of 20 keV.

A = 159.

The spin of the ground state of $_{65}Tb^{159}$ is measured to be 3/2. This state is identified with the orbital [411 3/2] which is the expected lowest configuration for $Z = 65$ (see Fig. 3) and which also accounts fairly well for the observed magnetic moment. The first two rotational levels associated with this configuration have been found by means of Coulomb excitation at 58 and 138 keV.

An odd-parity intrinsic excitation at 364 keV in Tb^{159} is populated in the $_{64}Gd^{159}$ decay. The decay of the 364 keV level suggests that it has $I = 5/2$ and it is accordingly classified as [532 5/2]. The relative intensities of the gamma rays leading to the different members of the ground state rotational band are in serious disagreement with the simple intensity rules. Thus, the transition to the 3/2, 5/2, and 7/2 states are predicted to have the relative intensities 1 : 0.26 : 0.017, while the observed values are 1 : 0.011 : 0.028. Since these transitions are strongly hindered by the asymptotic selection rules (cf. Table I), such deviations may possibly be interpreted as associated with the expected slowness of the transitions (see § II A).

Besides the states that have so far been identified, we would expect the orbitals [523 7/2] and [413 5/2] to occur as low-lying excited states in Tb^{159}.

On the basis of Fig. 4, it is difficult to tell whether the orbit [642 5/2], [523 5/2] or [521 3/2] should be the ground state of Gd^{159} (see also the spectrum of Dy^{161} where all three of these orbits appear within an interval of 75 keV). The experimental data on the decay of Gd^{159} seem to argue against [523 5/2], but do not conclusively decide between the [642 5/2] or the [521 3/2] assignments. In either case, the observed beta groups with log ft values of about 6.5 are classified as ah and $1u$. The conspicuous weakness of the transition to the 7/2+ member of the ground-state rotational band in Tb^{159} may somewhat favour the assignment [521 3/2].

$_{67}Ho^{159}$ (not shown) has been reported to decay into $_{66}Dy^{159}$ by electron capture with a half life of 33 min (K. Toth and J. Rasmussen, 1957). Even assuming a decay energy of 2.5 MeV, this implies a log *ft* of less than 5 and thus indicates an *au* transition. This is consistent with the expected [523 7/2] assignment for the Ho^{159} ground state (see the other Ho isotopes) and a decay to the orbital [523 5/2] which should be a low lying excited state in Dy^{159}.

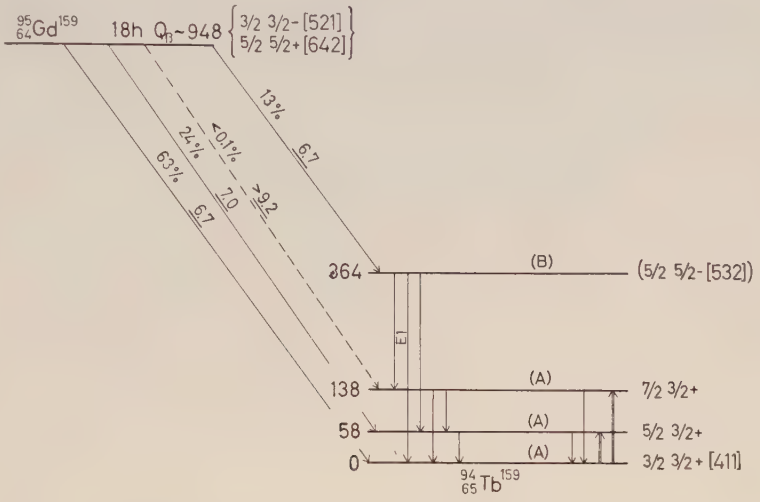

Fig. A = 159.

For references to the experimental data, see NDC and SHS, as well as the recent work by Nielsen, Nielsen, and Skilbreid (1958), Nucl. Phys. **7**, 561.

A = 161.[1]

The ground state spin of $_{66}Dy^{161}$ is 5/2 and, according to Fig. 4, we might assign either the orbit [642 5/2] or [523 5/2]. Coulomb excitation studies of this nucleus have shown that the ground state rotational band has an exceptionally large moment of inertia ($3\hbar^2/\Im$ = 38 keV compared, for example, with $3\hbar^2/\Im$ (Dy^{160}) = 87 keV). This unusually large moment clearly identifies the ground state configuration as [642 5/2] (cf. § III). A further test of this classification would be provided by a measurement of the sign of the magnetic moment, since the assignment [642 5/2] predicts a negative value, while [523 5/2] would imply a positive one.[2]

According to Fig. 4, we would expect the orbitals [523 5/2] and [521 3/2] to provide low lying excited states in Dy^{161}. Indeed, two intrinsic excitations have been identified and both have been shown to have an opposite parity to that of the ground state. The observed properties of these states are quite well accounted for by assigning the orbital [523 5/2] to the rotational band whose lowest state occurs at 26 keV and the orbital [521 3/2] to the intrinsic excitation occuring at 75 keV. Two rotational

[1] An interpretation of the spectrum of Dy^{161} similar to that suggested below has recently been given by Bés (1958). This reference also contains more detailed estimates of the transition matrix elements with inclusion of the Coriolis effect.

[2] *Note added in proof.* A recent measurement by J. G. Park (1958), Proc. Roy. Soc. **245**, 118, has given the value $\mu = -0.4$ for the magnetic moment of Dy^{161}.

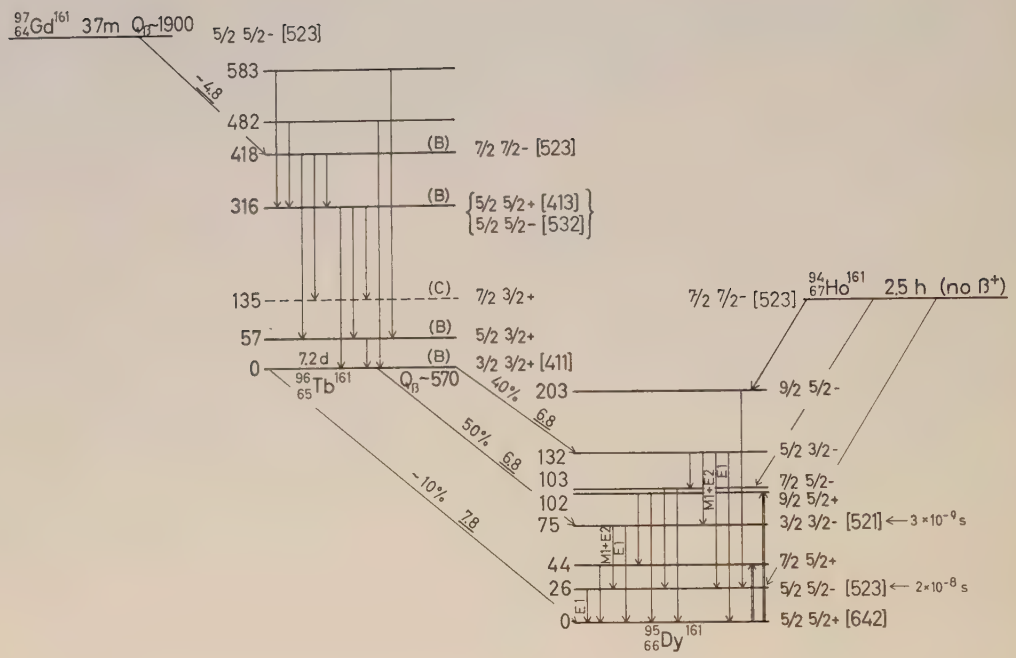

Rotational bands in Dy^{161}

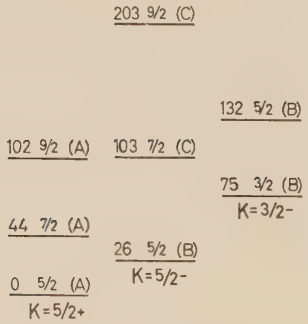

Fig. A = 161.

For the Gd^{161} decay, see L. C. Schmid and S. B. Burson (1957), Bull. Am. Phys. Soc. **II:2**, 341. There exists in the literature conflicting evidence concerning the Tb^{161} decay into Dy^{161} (see SHS and NDC). We have followed here the decay scheme proposed by Cork, Brice, Schmid, and Helmer (1956), Phys. Rev. **104**, 481, M. Vergnes (1958), Journ. Phys. Rad. **18**, 579, Gregers Hansen, Nathan, Nielsen, and Sheline (1958), Nuclear Phys. **6**, 630. References to the Coulomb excitation measurements may be found in NDC. The levels populated in the Ho^{161} decay have been constructed on the basis of the transitions observed by Mihelich, Harmatz, and Handley (1957), Phys. Rev. **108**, 989.

states have been observed associated with the former and one with the latter of these configurations.

Both the [521 3/2] and [523 5/2] orbitals are observed to decay by very hindered $E1$ transitions to the [642 5/2] ground state configuration of Dy^{161} ($H \sim 10^5$ and $H \sim 10^4$ for the former and latter transitions, respectively). The $M1$ transition from the [521 3/2] to the [523 5/2] level is observed to be somewhat retarded ($H \sim 70$), which is also in agreement with the asymptotic selection rules.

Besides the levels that have been identified so far, one might also expect, according to Fig. 4, the orbitals [651 3/2] and [505 11/2] to provide excited configurations in Dy^{161} although, possibly, at somewhat higher excitation energies (for a discussion of the latter configuration, see A = 163).

The Ho^{161} ground state is expected to be [523 7/2] as for the other Ho isotopes and, thus, the electron capture decay should proceed by an *au* transition to the states of the [523 5/2] band in Dy^{161}. This expectation appears to be consistent with the somewhat incomplete data that is available on this decay.[1]

The $_{65}Tb^{161}$ ground state is expected to be [411 3/2] as for the other Tb isotopes. The beta transitions from this state to the [642 5/2] and the [521 3/2] states in Dy^{161} are thus classified as *ah* and 1 *u*, respectively, which is consistent with the observed log *ft* values of 7.8 and 6.8. The transition to the [523 5/2] state has not been observed, which implies log $ft > 8$, which is also consistent with the fact that this transition is classified as 1 *h*.

Besides the ground state rotational band, a number of excited intrinsic states in Tb^{161} have been observed in the beta decay of $_{64}Gd^{161}$. The most striking of these is the state at 418 keV which is populated by a beta transition with log $ft \sim 4.8$. This transition clearly must be classified as *au* and thus identifies the Gd^{161} ground state as [523 5/2] and the 418 keV state in Tb^{161} as the [523 7/2] orbital which is indeed expected at about this excitation energy. The [523 7/2] state in Tb^{161} decays by gamma transitions, partly to excited levels in the ground state rotational band, and partly to a level at 316 keV. We have tentatively assigned this last as either [413 5/2] or [532 5/2] since both these levels are expected in approximately this region of excitation. The latter of these orbitals is indeed observed at about this excitation energy in Tb^{159} and possibly in Tb^{157}. Additional levels at 482 and 583 keV in Tb^{161} have been reported, but so little is known about them that it does not seem possible as yet to make a classification.

A = 163.

The $_{66}Dy^{163}$ ground state spin has been measured to be 5/2 and one again has the two possibilities [523 5/2] and [642 5/2] as width Dy^{161}. In Dy^{163}, however, the moment of inertia of the ground state rotational band is much smaller than in Dy^{161}

[1] *Note added in proof:* Mihelich, Harmatz, and Handley (1958, Bull. Am. Phys. Soc. **II:3**, 358) have recently found an isomeric state at 211 keV in Ho^{161}. Indeed, the [411 1/2] orbital is expected as a low-lying configuration and should give rise to isomerism just as in Ho^{163} and possibly Ho^{165}. The transition is thus expected to be E3.

($3\hbar^2/\Im$ (Dy^{163}) = 66 keV; $3\hbar^2/\Im$ (Dy^{161}) = 38 keV) and the gamma-ray branching ratios within the rotational band are very different from those of Dy^{161}. It thus appears that the Dy^{163} ground-state configuration is [523 5/2].[1]

The Ho^{163} ground state is expected to be [523 7/2] as for the other Ho isotopes. Thus, the electron capture decay to the Dy^{163} ground state should be *au*.

The $_{67}Ho^{163}$ half life has been reported as 5 *d*, which would be consistent with this assignment if the disintegration energy were about ~ 200 keV. Such a low value might not be unexpected from the systematics of nuclear masses in this region. It is also expected that the 74 keV state in Dy^{163} will be populated in the Ho^{163} decay.

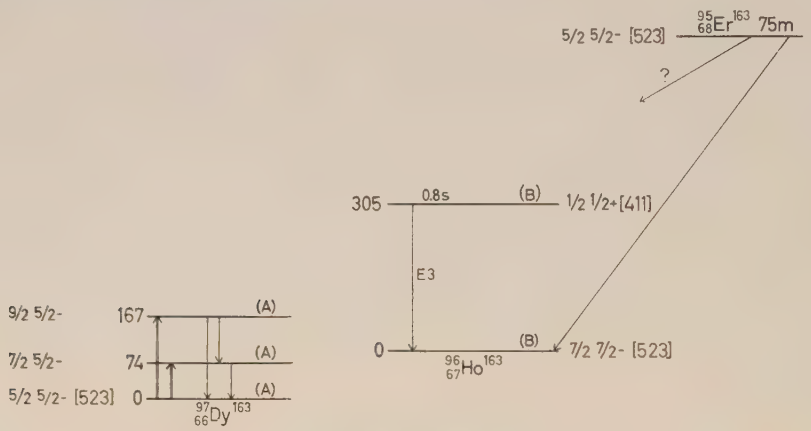

Fig. A = 163.
For references to the experimental data, see NDC and SHS. The Ho^{163} decay has not been observed. For limits on the lifetime of this decay, see T. H. Handley (1954), Phys. Rev. **94**, 945.

A 0.8 s. *E*3 isomer in Ho^{163} has been produced in the Ho^{165} (γ, $2n$) reaction. This state, at 305 keV, thus corresponds well with the [411 1/2] orbital which, according to Fig. 3, is indeed expected in just this region. The transition is rather hindered (H ~ 10^4), which is consistent with the selection rules implied by the asymptotic quantum numbers.

The $_{68}Er^{163}$ lifetime has been reported as 75 m, which probably implies an *au* transition. This would in turn require the assignment [523 5/2] also to the Er^{163} ground state.

It is interesting that the low energy spectra of the odd-neutron nuclei with $N = 91$ to 95 are all quite nicely accounted for by the rotational bands associated with the expected orbits [521 3/2], [523 5/2], and [642 5/2]. However, according to Fig. 4, one might also expect the orbit [505 11/2] in this region. This orbit has not so far been observed, which is perhaps not unexpected, since its high spin implies that it would not usually be populated in the beta-decay process. Its identification none the less remains an interesting problem, especially since the interpretation of the strong

[1] *Note added in proof:* The value of the magnetic moment has recently been determined as $\mu = 0.5$ (J. G. Park, 1958, Proc. Roy. Soc. **245**, 118), which strongly supports the suggested classification (see the discussion on Dy^{161}).

discontinuity in the nuclear eccentricity at $N = 90$ depends in such an important way on this orbit. It is possible that one might observe the [505 11/2] configuration as a short lived isomer following a reaction such as (γ, xn) on some isotope in this region.

A = 165.

The ground-state spin of $_{67}Ho^{165}$ has been measured to be 7/2. This is in agreement with what one would expect from Fig. 3 which predicts the [523 7/2] state as

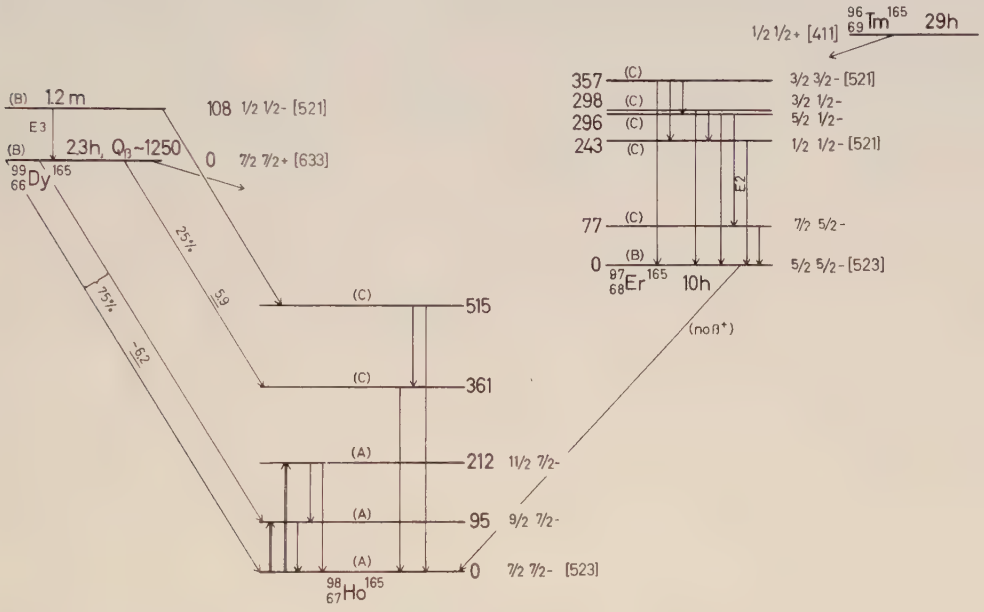

Fig. A = 165.

The Coulomb excitation data is reviewed in Alder, Bohr, Huus, Mottelson, and Winther (1956), Revs. Mod. Phys. **28**, 432, hereafter referred to as ABH. The properties of the levels populated by the decay of Dy^{165} and Dy^{165m} are uncertain to some extent. The available data come mainly from the work of Jordan, Cork, and Burson (1953), Phys. Rev. **92**, 1218, see also SHS. The levels in Er^{165} populated in the decay of Tm^{165} are constructed from the transitions recently observed by Mihelich, Harmatz, and Handley (1957), Phys. Rev. **108**, 989.

the lowest configuration for $Z = 67$. The rotational band based on this configuration has states at 95 keV and 212 keV which have been studied by Coulomb excitation. The rotational energy parameter for this band is $3\hbar^2/\Im = 63$ keV, which is somewhat smaller than for neighbouring odd-proton configurations (compare, e. g., Tb^{159} with $3\hbar^2/\Im = 70$ keV for the ground state band and Tm^{169} with $3\hbar^2/\Im = 74$ keV). This difference is a consequence of the large intrinsic angular momentum associated with particle motion in this orbit (i. e., the wave function contains a very large component of $j = 11/2$, see § III for further discussion of this point).

Fig. 4 is apparently in error in predicting the [521 1/2] level to be below the [633 7/2] level. In every case where clear-cut experimental evidence is available, the

latter level is found to lie somewhat below the former (see, for example, the low levels of $^{99}_{66}Dy^{165}$, or the ground state spins of $^{99}_{69}Er^{167}$ and $^{101}_{70}Yb^{171}$).

Thus, the ground state of $_{66}Dy^{165}$ corresponds well with the expected properties of the orbital [633 7/2]. The beta decay to the ground state of Ho^{165} is classified as $1u$ and is observed to have log $ft \sim 6.2$. The Dy^{165} ground state also appears to populate a number of higher-lying excited states in Ho^{165}. Not enough is known about these states, however, to make possible a classification at the present time. The configurations which might be expected according to Fig. 3 and which should be populated directly in the Dy^{165} ground state decay are [413 5/2], and at a somewhat higher excitation energy [404 7/2] and [532 5/2].

The 108 keV, 1.2 min isomeric level of Dy^{165} corresponds well with the [521 1/2] orbital. It decays by a hindered $E3$ transition ($H \sim 10^3$) to the [633 7/2] ground state configuration.

According to Fig. 3 and the known spectra of neighbouring odd-proton nuclei, one would expect the [411 1/2] and [411 3/2] orbitals to occur as excited states in Ho^{165} at about 400 keV. The beta transitions to these states from the Dy^{165} isomer would be $1u$ and thus might be expected to occur in about 0.1 % of the decays of the isomer. Beta transitions from 1.2 min Dy^{165} have been reported, leading to levels in this region, but again not enough is known as yet about the decay scheme to make further identification possible.

One might expect the $_{68}Er^{165}$ ground-state configuration to be represented by the [523 5/2] orbital (just as for the Dy^{163} and Gd^{161} ground states). In this case, the electron-capture decay to Ho should go entirely to the ground state by an *au* transition. In order to be consistent with log $ft \lesssim 5$, the 10 hr half-life would imply a disintegration energy of less than 0.5 MeV.

The electron-capture decay of $_{69}Tm^{165}$ has been studied, and a number of gamma transitions have been reported. In the figure (A = 165), these transitions have been tentatively arranged in a manner consistent with the expectations of the present model. Thus, the Tm^{165} ground state is expected to be [411 1/2] as for the other Tm isotopes, and the levels directly populated in Er^{165} should have low spin. According to Fig. 4, the low spin orbitals available are [521 1/2] and [521 3/2]. A sequence of three levels, beginning at 243 keV in Er^{165}, resemble very closely the rotational band expected for the former of these configurations (compare the ground-state rotational band of $_{70}Yb^{171}$). In addition, a level at 357 keV has been tentatively classified as the [521 3/2] orbital.

A = 167.

The ground-state spin of $_{68}Er^{167}$ has been measured to be 7/2 and the magnetic moment is also fairly well accounted for by the assignment [633 7/2] which is found to be the lowest configuration for all nuclei with $N = 99$ (see the comments in connection with Dy^{165}).

The rotational band based on the ground-state configuration has been studied

by Coulomb excitation. It is found that the moment of inertia is somewhat greater than in neighbouring odd-neutron nuclei, ($3\hbar^2/\Im$ (Er^{167}) = 52 keV, compared, for example, with $3\hbar^2/\Im$ (Yb^{171}) = 73 keV), which is consistent with the assigned configuration (cf. § III).

The first intrinsic excitation in Er^{167} occurs at 208 keV and is an isomeric level with 2.5 sec. half-life. This level corresponds with the [521 1/2] orbital which is also

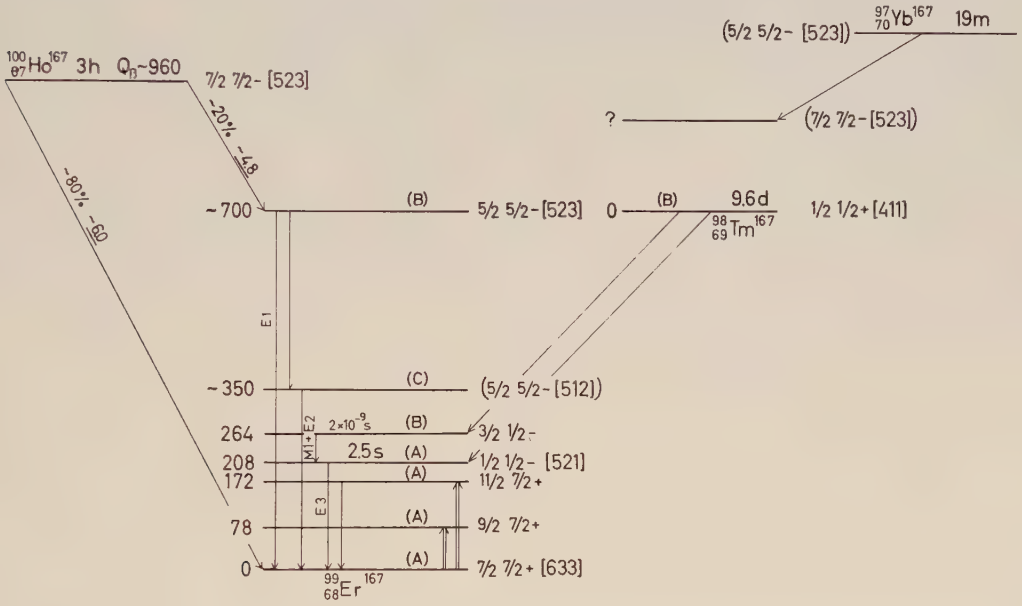

Fig. A = 167.

For references to the experimental data, see SHS and NDC. Many parts of the decay scheme are as yet quite uncertain. The most well-established features are the ground-state rotational band of Er^{167}, which is studied by Coulomb excitation, and the 208 keV isomeric level, which is populated in the decay of Tm^{167} in the Er(γn) reaction, C. L. Hammer and M. G. Stewart (1957), Phys. Rev. **106**, 1001, and Er($n\gamma$) reaction, Campbell, Kahn, and Goodrich (1951), ONRL — 1164. The lifetime of the 264 keV level of Er^{167} has been measured by Berlovich, Grotovsky, Bonits, and Gorodinsky (1958), Journ. Exper. Theor. Phys. **34**, 264.

responsible for isomerism in Dy^{165} (E_γ = 108 keV, $T_{1/2}$ = 1.2 m.) and possibly in Yb^{169} (E_γ = 200 keV, $T_{1/2}$ = 6 sec.). In all of these cases, the $E3$ decay is retarded by a similar factor ($H \sim 10^3$). The slowness of these transitions is consistent with the selection rules appropriate to the asymptotic quantum numbers.

The expected configuration for the $_{67}Ho^{167}$ ground state is [523 7/2] (as for all the other Ho isotopes) and the beta decay to the Er ground state is thus 1 *u*, consistent with the observed log *ft* = 6.0. It should be expected that the first rotational state in Er^{167} at 78 keV would also be populated in this decay.

There is also a lower energy beta group populating a level in Er^{167} at about 700 keV. The very small *ft*-value (log *ft* = 4.8) identifies this level as the [523 5/2] orbital. This is the same *au* beta transition which is seen consistently in all the decay

schemes with $N = 97$. It is expected that the rotational states with $I = 7/2$ and $I = 9/2$, based on the [523 5/2] orbital in Er^{167}, would also be populated in this decay.

The 700 keV level appears to decay, partly, by a direct transition to the Er^{167} ground state (according to the above classification of the levels this is a hindered $E1$ transition) and, partly, by a cascade through a level at about 350 keV. Very little is known about the latter level, but, according to Fig. 4, one might expect the orbital [512 5/2] at about this region of excitation.

The ground-state configuration of $_{69}Tm^{167}$ should be [411 1/2], as for the other Tm isotopes. This assignment is consistent with the fact that the electron-capture decay of Tm^{167} is observed to populate the [521 1/2] isomeric state of Er^{167} and also a level which is probably the $I = 3/2$ member of the rotational band based on this configuration. These transitions are thus classified as $1u$.

The $_{70}Yb^{167}$ ground state is expected to be [523 5/2] and thus it may decay by an au electron-capture transition to the [523 7/2] excited state in Tm^{167} which is expected at about 400 keV (see the level schemes of Tm^{169} and Tm^{171}). Indeed, Yb^{167} does have a very short half-life. The observed half-life would be consistent with the expected $\log ft \lesssim 5$, if the transition energy were of the order of $\lesssim 2$ MeV.

A = 169.

The $_{69}Tm^{169}$ spin has been measured to be 1/2. The ground state is identified with the [411 1/2] orbital which, according to Fig. 3, should be the lowest configuration for $Z = 69$. Rotational levels associated with this intrinsic state have been observed at 8, 118, 139, and 336 keV, corresponding to a decoupling factor $a = -0.77$ and $3\hbar^2/\Im = 74$ keV. Both the decoupling factor and the experimental magnetic moment, as well as the branching ratios within the rotational band, are excellently accounted for by the assigned orbital[1] (cf. Mottelson and Nilsson, 1955b, and Tables VII and VIII of the present paper).

The first excited intrinsic state occurs at 316 keV. The multipolarities of the observed gamma transitions from this state to the levels of the ground rotational band strongly suggest that it has $I = 7/2+$ and should be identified with the orbital [404 7/2]. The $M1$ transitions to the 118 and 139 keV levels are strongly hindered ($H \sim 5 \times 10^5$ for both transitions), which is consistent with their being K-forbidden. The other near-lying orbital according to Fig. 3 should be [523 7/2]. The next intrinsic excitation, which occurs at 379 keV, is indeed of different parity from the two previous intrinsic states, as evidenced by its observed $E1$ decay. These transitions are strongly hindered ($H \sim 1 \times 10^5$ for the transition to the 316 keV level and $H \sim 2 \times 10^7$ and 2×10^8 for the transition to the 138 and 118 keV levels, respectively), in agreement with the K-forbiddenness of the transitions to the ground-state band and the selection rules in the asymptotic quantum numbers applying to the transition to the 316 keV level. Finally, an excited state observed at 473 keV agrees well in energy and decay characteristics with the expected $I = 9/2-$ rotational state based on the [523 7/2] con-

figuration[1]. (The rotational-energy parameter would thus be $3\hbar^2/\Im = 63$ keV, which is the same as for the corresponding rotational band in Ho^{165}).

The ground state of $_{68}Er^{169}$ with $N = 101$ is expected to correspond with the [521 1/2] orbital (see the discussion in connection with Dy^{165}) and the observed beta

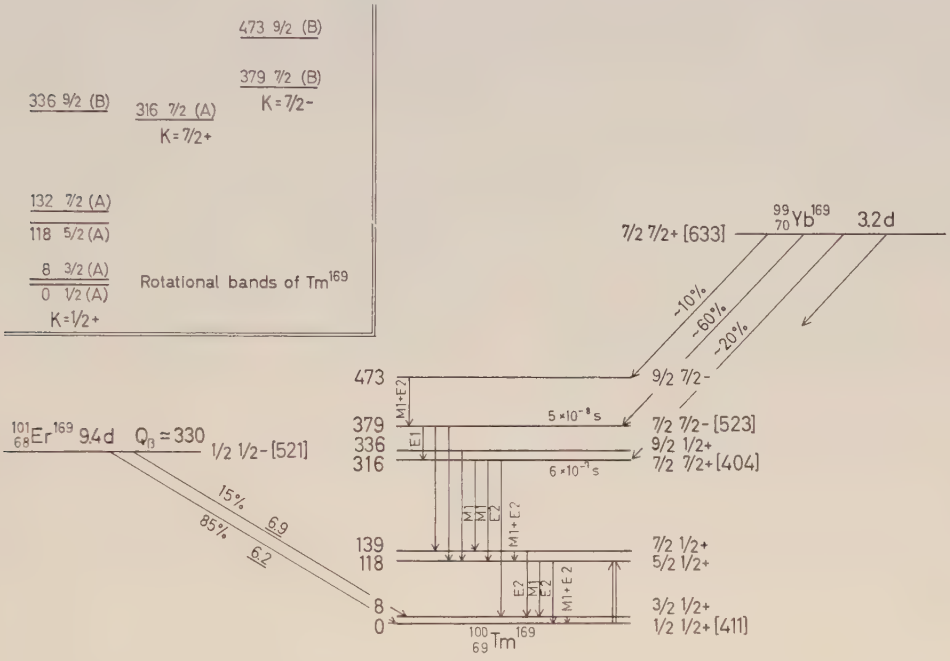

Fig. A = 169.

The Coulomb excitation data on Tm^{169} is reviewed in ABH. The decay of Yb^{169} has been extensively studied, and the decay scheme seems to be quite well established (see SHS and NDC). The data for the beta decay of Er^{169} are taken from E. N. Hatch and F. Boehm (1956), Bull. Am. Phys. Soc. **II:1**, 390. *Added in proof:* The half-life of the 8 keV state in Tm^{169} has recently been measured to be $4 \times 10-7$ *s* (H. Beckhuis and H. de Waard, 1958, Physica **24**, 767).

decay to the ground state and 8 keV level in Tm^{169} is consistent with this classification. Thus, the beta transitions are expected to be $1u$ and are observed to have log ft 6.2 and 6.9, respectively.

The ground state of $_{70}Yb^{169}$ is expected to be [633 7/2], which is consistent with the evidence that the electron capture takes place almost entirely to the [404 7/2] and [523 7/2] configurations of Tm^{169}. These transitions are classified as ah and $1u$, respectively.

A 6 sec. isomer ($E_\gamma = 200$ keV), which has been observed in Yb($n\gamma$), might tentatively be assigned to Yb^{169}, since an $E3$ isomeric level very similar to those ob-

[1] A previously reported lifetime of 4×10^{-7} sec for this level would have been in serious disagreement with the expectation of the present model. It is thus important that more recent measurements have shown that this state has indeed a very short half-life ($T_{1/2} < 3 \times 10^{-9}$ sec), as was to be expected (E. W. Hatch and D. E. Alburger, 1958, Phys. Rev. **110**, 413; O. Nathan and I. Marklund, 1958, Nuclear Phys. **6**, 102).

served in Dy^{165} and Er^{167} is expected. This level would correspond to the orbital [521 1/2].

A = 171.

The ground-state spin of $_{70}Yb^{171}$ has been measured to be 1/2 and the magnetic moment is in agreement with the classification of this orbital as [521 1/2] which, as discussed above, is found as the ground state for all nuclei with $N = 101$. The rotational band built on the ground state has been studied by Coulomb excitation and is found to have a decoupling factor $a = +0.87$, which also agrees with the orbital assignment [521 1/2] (cf. Table VIII).

Recently, the decay of $_{71}Lu^{171}$ has been studied and it has been found that this decay leads to a 75 keV $E3$ isomeric transition in Yb^{171}. This level thus corresponds well with the expected [633 7/2] orbital, and the isomeric transition is just the inverse of the transition responsible for isomerism in the nuclei with $N = 99$. The Lu^{171} ground state should be [404 7/2] as for the other Lu isotopes, and the electron capture transition is thus classified as ah. An additional level in Yb^{171} is also populated in this decay, and this level has very tentatively been assigned as [514 7/2], since this configuration should be populated by a $1u$ electron-capture transition.

The ground state of $_{69}Tm^{171}$ should correspond to the [411 1/2] orbital just as for Tm^{169}. The beta decay to Yb^{171} would thus be $1u$, in agreement with the observed $\log ft = 6.2$. The lowest excited states of Tm^{171} are found to be very similar to those observed in Tm^{169}. Thus, the ground state rotational band in the former is described by $3\hbar^2/\Im = 72$ keV and the decoupling constant $a = -0.86$ compared with $3\hbar^2/\Im = 74$ keV and $a = -0.76$ for Tm^{169}.

The first excited intrinsic state in Tm^{171} occurs at 425 keV and appears to correspond with the [523 7/2] orbital which occurs in Tm^{169} at 379 keV. In both nuclei, this configuration decays by very retarded $E1$ gamma transitions to the ground-state rotational levels. These transitions are classified as K-forbidden.

According to Fig. 4, the ground state for $N = 103$ should be [512 5/2]. Thus, one expects the beta transition to the Tm^{171} ground state to be 1^*u, while the first forbidden transitions to the levels at 5, 117 and 129 keV are K-forbidden. These classifications are consistent with the observed $\log ft = 8.6$ for the beta groups to the ground state and ~ 120 keV levels. The beta transition to the 425 keV level should be ah and is observed to have $\log ft = 6.3$.

Recently, a detailed study of the $_{68}Er^{171}$ decay has revealed a very complex spectrum above the 425 keV level in Tm^{171}. Although the interpretation of this high-energy part of the spectrum must still be considered very tentative, we have provisionally attempted to interpret these levels in terms of the levels expected according to Fig. 3[1]. Thus, the orbitals [411 3/2], [413 5/2], and [402 5/2] are expected in Tm^{171} in this region of excitation and should be populated by $1u$ beta transitions. These orbitals have therefore been tentatively suggested as possible assignments for the ob-

[1] The state assignments suggested here for these highly excited levels are the same as those proposed by Cranston, Bunker, and Starner (1958), Phys. Rev. **110**, 1427.

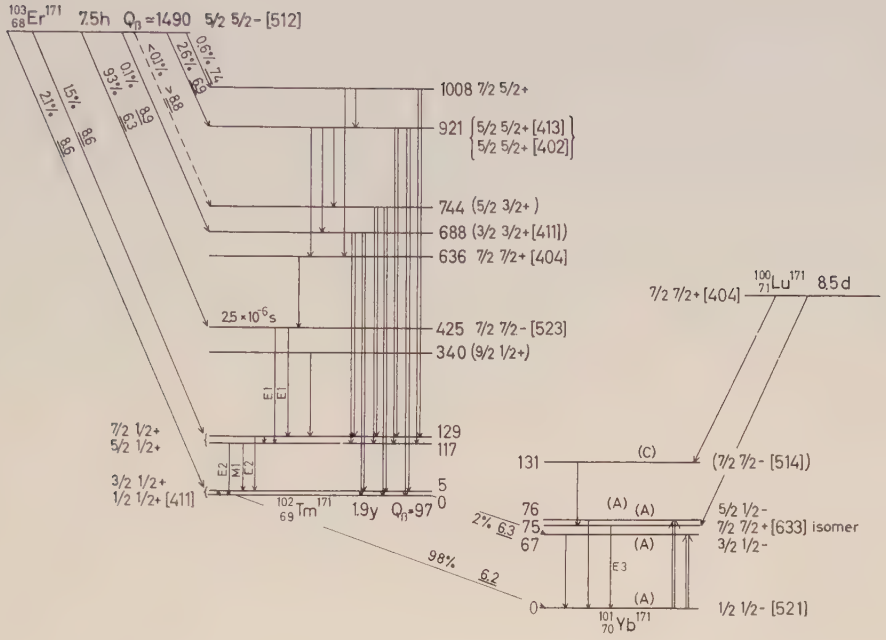

Rotational bands of Tm^{171}

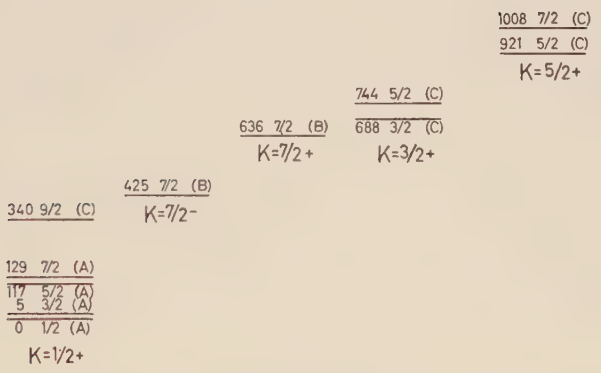

Fig. A — 171.

The Coulomb excitation of Yb^{171} has been studied by Elbek, Nielsen, and Olesen (1957), Phys. Rev. **108**, 406. The Yb^{171} isomer has been found by J. W. Mihelich and B. Harmatz (1957), Phys. Rev. **106**, 1232. The other levels populated in the Lu^{171} decay have been constructed on the basis of transitions observed by Mihelich, Harmatz, and Handley (1957), Phys. Rev. **108**, 989. The data on the decay of Tm^{171} are taken from Smith, Robinson, Hamilton, and Langer (1957), Phys. Rev. **107**, 1314. The levels in Tm^{171} up to 425 keV populated in the decay of Er^{171} have been extensively studied (for references see SHS and NDC). The higher energy part of this decay scheme has recently been investigated by Cranston, Bunker, and Starner (1958), Phys. Rev. **110**, 1427.

served levels at 688 and 921 keV. The orbital [404 7/2] is also expected, but would only be populated by a 1 *h* transition. Therefore, this orbit might correspond to the level at 636 keV which is not directly populated in the Er^{171} decay. The orbital [514 9/2] is also expected, but would not be populated directly. All of these classifications must be considered as somewhat speculative, since so little is known about these highly excited states. Especially the rather high log *ft* for the transition to the 688 keV state does not agree with the suggested classification.

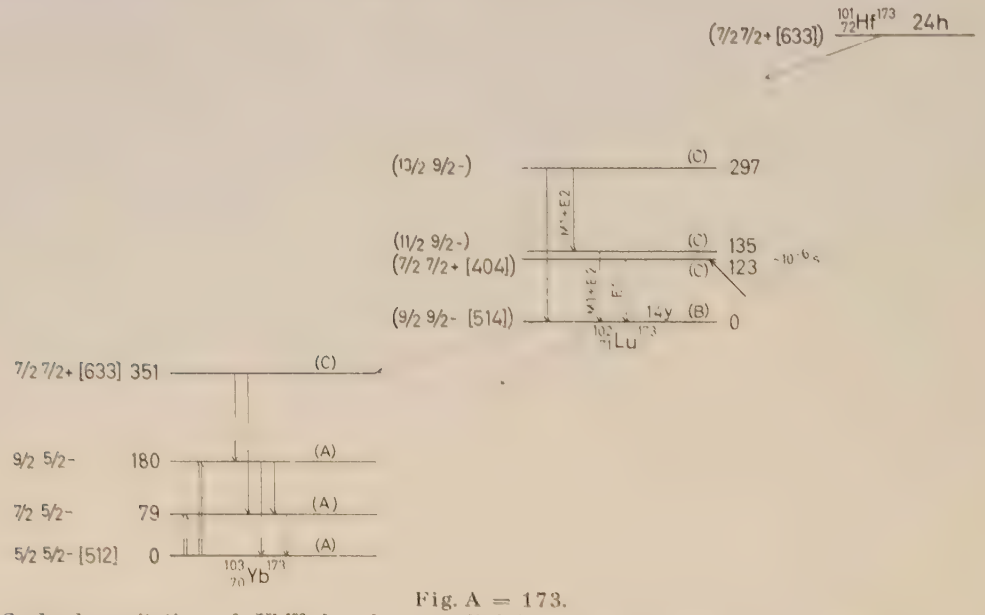

Fig. A = 173.

The Coulomb excitation of Yb^{173} has been studied by Elbek, Nielsen, and Olesen (1957), Phys. Rev. **108**, 406. The rest of the experimental data is taken from Mihelich, Harmatz, and Handley (1957), Phys. Rev. **108**, 989, and Ward, Mihelich, Harmatz, and Handley (1957), Bull. Am. Phys. Soc. **II:2**, 341.

A = 173.

The ground-state spin of $_{70}Yb^{173}$ is 5/2. According to Fig. 4, the lowest configuration for $N = 103$ is expected to be [512 5/2] and this orbital also accounts well for the observed magnetic moment (see Table VII). The rotational band built on the ground-state configuration has been studied by Coulomb excitation.

Except for the ground-state rotational band of Yb^{173}, most of the spectra of the A = 173 nuclei are still somewhat uncertain.

The long lifetime of the $_{71}Lu^{173}$ decay may possibly suggest that the ground state of Lu^{173} corresponds to the orbital [514 9/2] rather than to [404 7/2] which is found for the other Lu isotopes.[1] These orbits are known to be very close to each other in

[1] *Note added in proof:* The existence of a direct ground state to ground state transition in the decay of Lu^{173}, as suggested by recent measurements of Djelepov, Preobrajensky, and Sergienko (1958), Izvest. Akad. Nauk. **22**, 795, would imply that the ground state of Lu^{173} should be identified with the [404 7/2] orbital, as in the case of the other Lu isotopes. Additional evidence on this decay scheme has recently been obtained by Richard, Mihelich, and Harmatz (1958), Bull. Am. Phys. Soc. **II:3**, 358. Besides the transitions indicated in the figure, these authors find a level at 636 keV in Lu^{173}, to which they assign the orbital [514 7/2].

this region of elements. The Lu^{173} decay also populates a level at 351 keV in Yb^{173}, which may possibly correspond with the orbital [633 7/2] which is expected at roughly this excitation.

A level at 123 keV in Lu^{173} has been reported to decay by an $E1$ transition to the ground state. The 123 keV level may thus correspond to the [404 7/2] configuration which, as mentioned above, is expected as a low lying excited state in Lu^{173}.

If the tentative classification given in the diagram for the low lying Lu^{173} states is correct, the spin for the Hf^{173} ground state must be fairly large. We have therefore provisionally assigned the orbital [633 7/2] for the Hf^{173} ground state. In any case, the [633 7/2] and [521 1/2] orbitals are expected to be very close together in Hf^{173} and probably to give rise to isomerism just as in Yb^{171} and in the nuclei with $N = 99$.

A = 175.

The ground-state spin of ${}_{71}Lu^{175}$ has been determined to be $I = 7/2$ and thus corresponds with what one would expect from Fig. 3, according to which the [404 7/2] orbital should provide the ground state for $Z = 71$[1]. Until recently, there existed a rather large discrepancy between the measured magnetic moment of Lu^{175} and the value predicted for this orbit. However, the recent redetermination of the moment brings the measured value much closer to that expected (cf. Table VII).

The rotational band associated with the Lu^{175} ground state configuration has levels at 114 keV ($I = 9/2$) and 251 keV ($I = 11/2$), as found in Coulomb excitation experiments.

The first excited intrinsic state is found at 343 keV and corresponds well with the [402 5/2] configuration. In ${}_{73}Ta^{181}$, one encounters a similar pattern with the [404 7/2] ground state and the [402 5/2] excited configuration at 480 keV. In Ta it is found that the latter state has a lifetime of 10^{-8} sec. However, attempts to measure the lifetime of the 343 keV level in Lu^{175} indicate that it is at least an order of magnitude shorter than this value. This apparently indicates that the extremely large hindrance of the $M1$ part of the gamma transition observed in Ta^{181} ($H = 3 \times 10^6$) is a consequence of a somewhat fortuitous cancellation which is not reproduced in Lu^{175}. The limit on the lifetime observed in Lu^{175} still permits the transition to be considerably hindered, as would be expected from the asymptotic quantum numbers. According to this interpretation of the difference between these transitions in Lu^{175} and Ta^{181}, we would expect the percentage of $E2$ radiation to be much smaller in the Lu^{175} transition than in Ta^{181}, and this seems consistent with the available data. The first rotational excitation ($I = 7/2$) built on the [402 5/2] configuration occurs at 433 keV in Lu^{175} and thus determines $3\hbar^2/\Im = 77$ keV for this band. Almost the same value is obtained for the ground-state rotational band.

[1] In the classification of nuclear ground states by K. Gottfried (1956), this nucleus has been assigned the [523 7/2] configuration (i. e., the same orbital as assigned to the ${}_{67}Ho^{165}$ ground state). However, according to Fig. 3, it is strongly suggested that the Lu ground state should be [404 7/2] and, as discussed below, there seems to be considerable evidence in the Lu^{175} decay scheme to support this assignment according to which the parity of Lu^{175} is even. The classification employed here has also been discussed by Chase and Wilets (1956).

A second excited intrinsic state in Lu^{175} occurs at 396 keV. The observed $E1$ and $M2$ decays from this state to the lower lying levels indicate that it corresponds with the [514 9/2] configuration. The large admixture of $M2$ with the $E1$ transitions (20 % $M2$ in the decay to the ground state and 4% $M2$ in the decay to the 113 keV level) corresponds with the fact that the $E1$ radiation would be forbidden by the asymptotic quantum numbers, while the $M2$ is allowed according to these selection rules.

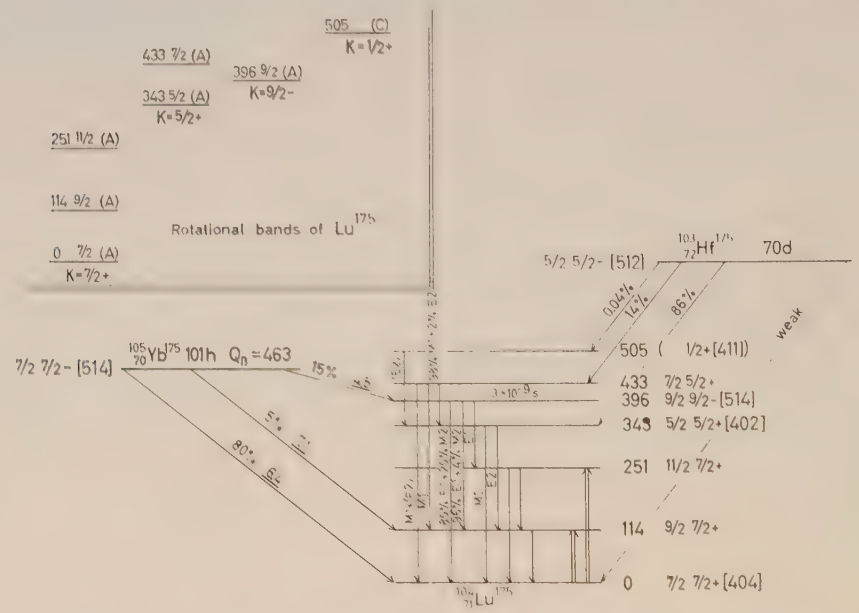

Fig. A = 175.
Both the Hf^{175} and the Yb^{175} decay have been extensively studied in a number of different experiments which are in essential agreement. The references may be found in SHS and NDC.

Finally, a level in Lu^{175} at 505 keV has been found to be very weakly populated in the $_{72}Hf^{175}$ decay. The observed properties of this level correspond fairly well with those expected for the [411 1/2] configuration. If this classification is correct, one might expect the 505 keV level to have a lifetime in the neighbourhood of 10^{-5} sec. as for the corresponding transition in Ta^{181}. However, it is probable (cf. below) that the Hf^{175} decay populates the $I = 3/2$ member of the rotational band which would be much less delayed. Thus, the delay would not be observed in the Hf^{175} decay, although it might be seen in some process such as Lu^{175} $(\gamma\gamma')$ or Lu^{176} (γn).

The ground state of Hf^{175} should be [512 5/2] as for the $_{70}Yb^{173}$ ground state. The observed electron-capture decay of this nucleus is consistent with such an assignment; the decay goes mainly to the 5/2+ and 7/2+ members of the [402 5/2] rotational band by transitions that are classified as $1u$. The transition to the Lu^{175} ground state which would be classified as $1h$ is very weak. The extremely weak transition to the [411 1/2] level is consistent with its classification as 1^*u, provided the available electron-capture energy is very small.

According to Fig. 4, we expect the orbital [514 7/2] to provide the ground state

for $N = 105$. The decay of $_{70}Yb^{175}$ accords well with such an interpretation. Thus, the transition to the Lu^{175} ground state is classified as $1u$ and is observed to have $\log ft = 6.4$, while the strikingly low $\log ft = 4.5$ for the transition to the 395 keV level in Lu^{175} is classified as *au*. The observation of this *au* beta transition provides very strong support for the assumed classification; however, the recently measured magnetic moment of Yb^{175} disagrees quite badly with the value computed for this orbital.

A = 177.

The spin of $_{72}Hf^{177}$ is measured to be 7/2, which is in agreement with Fig. 4, according to which the orbital [514 7/2] should be the ground-state configuration for $N = 105$. The observed magnetic moment is also reasonably well accounted for by this state (cf. Table VII). Rotational levels associated with this intrinsic configuration have been observed at 113 keV ($I = 9/2$) and 250 keV ($I = 11/2$).

An intrinsic excitation has been observed at 321 keV in Hf^{177}; its spin has been determined from angular correlation (Steffen, 1957) as 9/2; it decays by $E1$ transitions to the members of the ground-state rotational band, and the configuration is clearly identified as [624 9/2].[1]

The $_{73}Ta^{177}$ ground state is probably [404 7/2] as for the other Ta isotopes. This classification is consistent with the observed electron-capture transitions to the Hf^{177} ground-state rotational band ($\log ft = 6.6$ and 6.9 for the transitions to the $I = 7/2$ and $I = 9/2$ members; both transitions are classified as $1u$) and to the 321 keV level ($\log ft = 8.3$ for this transition which is classified as *ah*). Recently, a number of higher excited levels of Hf^{177} have been identified in the Ta^{177} decay. Although the interpretation of these levels is still quite tentative, one might provisionally attempt a classification on the basis of Fig. 4. Thus, the orbital [633 7/2] could correspond to the intrinsic excitation found at 748 keV and possibly [503 7/2] to the level at 1070 keV. The capture transition to the 748 keV level with $\log ft = 7.8$ is thus classified as *ah*, while the transition to the 1070 keV level with $\log ft = 6.5$ would be $1u$. According to Fig. 4, we should also expect the orbital [512 5/2] to occur at an excitation energy somewhat lower than these last two. However, the transition from Ta^{177} would be $1h$ and apparently has not yet been seen. In addition, the [521 1/2] orbital may occur at a few hundred keV of excitation in Hf^{177} and give rise to a long-lived isomer if it can be populated.

The $_{71}Lu^{177}$ ground state should correspond with the orbital [404 7/2], as is the case for all the Lu isotopes (except perhaps Lu^{173}, cf. A = 173), and the observed beta decay is consistent with this assignment, i. e., $\log ft = 6.7$, 7.7, and 6.3 for the transitions to the ground state ($1u$), first rotational state, and 326 keV state (*ah*), respectively.

The first rotational state built on the Lu^{177} ground state has been observed at 119 keV. A second excited state in Lu^{177} occurs at 147 keV and is found to decay to

[1] *Note added in proof:* The recent observation of a 0.1 % admixture of M2 radiation in the ground-state transition (E. Klema, 1958, Phys. Rev. **108**, 1652) is consistent with the fact that the E1 transition is classified as hindered according to the asymptotic quantum numbers, while the M2 radiation is unhindered.

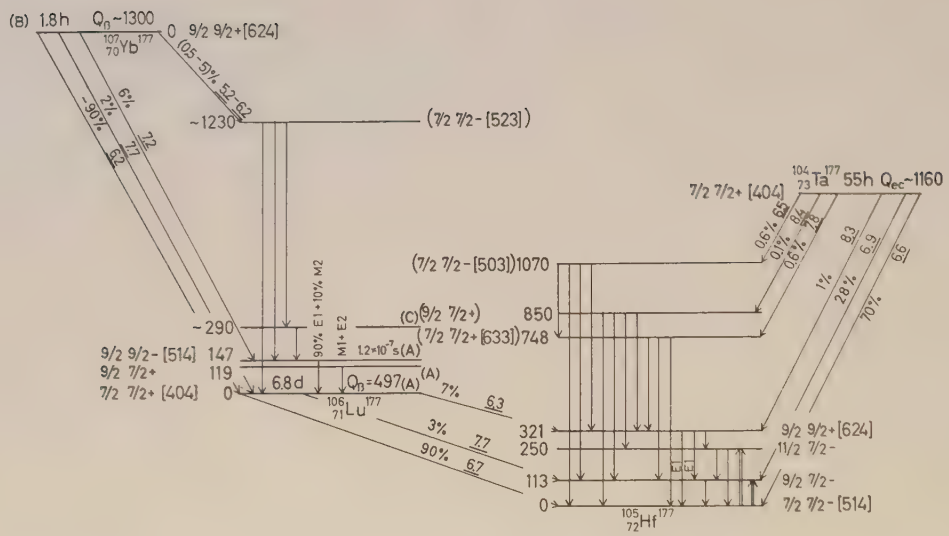

Rotational bands of Hf^{177}

1070 7/2 (C)
K=7/2-

850 9/2 (C)
748 7/2 (C)
K=7/2+

250 11/2 (A)
113 9/2 (A)
0 7/2 (A)
K=7/2-

326 9/2 (A)
K=9/2+

Fig. A = 177.

The decay of Lu^{177} into Hf^{177} as well as the Coulomb excitation of this latter nuclide have been studied in a number of different laboratories and the resulting decay scheme seems well established (see SHS, ABH, and NDC). The data on the Ta^{177} decay have been taken from the recent study by Mann, Nagle, and West (1957), Bull. Am. Phys. Soc. **II:2**, 231, L. G. Mann, private communication; see also F. Felber (1956), University of California Radiation Laboratory Report UCRL — 3618. The three lowest states in Lu^{177} populated in the Yb^{177} decay have been known for some time (cf. SHS and NDC), higher levels have recently been found by Cork, Brice, Martin, Schmid, and Helmer (1956), Phys. Rev. **101**, 1042, and by Mize, Bunker, and Starner (1956), Phys. Rev. **103**, 182. Note that in the decay of Yb^{177} the 2 % branch should terminate at the 119 keV level!

the ground state by a mixed $E1 + M2$ gamma transition. This level thus corresponds with the orbital [514 9/2]. The $E1$ decay is strongly hindered ($H = 5 \times 10^6$), while the $M2$ radiation is unhindered. This corresponds nicely with the fact that, according to the asymptotic selection rules, the $E1$ transition should be forbidden while the $M2$ is not.

The ground-state configuration for $N = 107$ should be [624 9/2] and the beta decay of $_{70}Yb^{177}$ corresponds well with such a classification. Thus, the transitions to the ground state and first rotational state of Lu^{177} are classified as *ah* and are found to have log *ft* = 6.2 and 7.7, respectively, while the transition to the 147 keV level is $1u$ and has log *ft* = 7.2.

The orbitals [402 5/2] and [411 1/2] are expected to occur in Lu^{177} at excitation energies of a few hundred keV (cf., e. g., Lu^{175}). However, the beta transition to the rotational states based on these configurations are expected to be very weak as a result of the *K*-forbiddenness.

Still higher energy gamma rays have recently been reported in the Yb^{177} decay. Very tentatively, it might be suggested that these could be associated with the orbital [523 7/2] which might occur in this general region of excitation and be populated by a $1u$ beta transition from Yb^{177}.

It is probable that Yb^{177} will have an isomer associated with the configuration [510 1/2], as is also observed in Hf^{179} and Os^{183}.

A = 179.

The ground-state spin of $_{72}Hf^{179}$ has been measured to be 9/2 and accords well with the orbital [624 9/2] which should occur as the ground state for $N = 107$, ac-

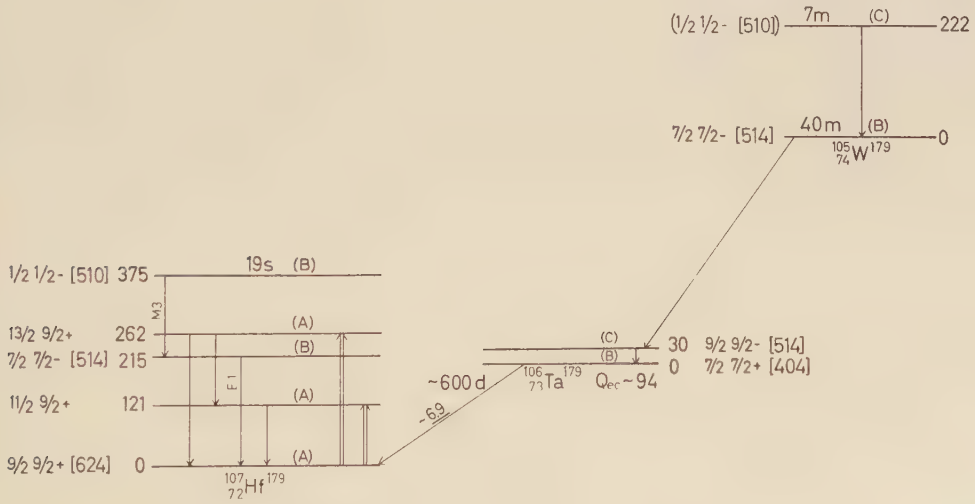

Fig. A = 179.

For references to the experimental data on Hf^{179}, see SHS, ABH, and NDC. The W^{179} isomer and the decay of W^{179} into Ta^{179} have been studied by T. J. Rock (1956), Proc. Roy. Soc. Canada **50**, 28 A.

cording to Fig. 4. The rotational band built on this configuration is found to have levels at 121 keV ($I = 11/2$) and at 262 keV ($I = 13/2$). The moment of inertia for this band is somewhat greater than in neighbouring odd-A nuclei (i. e., compare $3h^2/\Im = 66$ keV for Hf^{179} with $3h^2/\Im = 75$ keV for the Hf^{177} ground-state band and $3h^2/\Im = 91$ keV for the Ta^{181} ground-state band). This difference can be accounted for in terms of the especially large intrinsic angular momenta involved in the orbital [624 9/2] (cf. Table VI).

Besides the rotational levels, two intrinsic levels have been observed in Hf^{179} associated with a 19 sec. isomeric transition. It appears that the first level (at 215 keV) represents the [514 7/2] configuration, while the second (at 375 keV) is the isomer and corresponds with the [510 1/2] orbital. According to this interpretation, the 160 keV transition should be $M3$ and the 215 keV radiation should be $E1$. The $M3$ transition is considerably hindered ($H \sim 10^3$), in agreement with the proposed classification according to which it should be forbidden by the asymptotic quantum numbers. Similarly, the 215 keV $E1$ transition is forbidden by the asymptotic quantum numbers and it may therefore contain an appreciable admixture of $M2$ radiation which is not forbidden by the selection rules.

The $_{73}Ta^{179}$ ground state probably corresponds to the [404 7/2] orbital as for Ta^{181}. The decay to the Hf^{179} ground state is thus classified as *ah*, which is in agreement with the observed log $ft \sim 6.9$. A 30 keV level in Ta^{179} is populated in the W^{179} decay. The [514 9/2] orbital is expected to provide a quite low lying excited state in Ta^{179} (cf. also Ta^{181}) and so this configuration has been assigned to the 30 keV level.

The $_{74}W^{179}$ ground state should correspond to the orbital [514 7/2] as for the Hf^{177} and $_{70}Yb^{175}$ ground states. This assignment is consistent with the observation that the W^{179} electron-capture decay populates the 30 keV level in Ta^{179}. This transition is classified as *au*; the observed 40 m half-life of W^{179} is consistent with this interpretation if the transition energy is about 1 MeV or less. In addition, a 7 m isomeric transition of 222 keV is found in W^{179}. This level may correspond either with the orbital [510 1/2] or with [521 1/2] which, according to Fig. 4, might occur in about this region of excitation. The $M3$ transition is strongly hindered ($H = 7 \times 10^4$) in agreement with the selection rules on the asymptotic quantum numbers.

A = 181.

The spin of the $_{73}Ta^{181}$ ground state is measured to be 7/2. This is a very clear-cut exception to the orderly filling of the levels of Fig. 3, according to which the [404 7/2] orbital occurs as the ground state for $Z = 71$ (and is indeed observed for $_{71}Lu^{175}$ and $_{71}Lu^{177}$) and the [402 5/2] or [514 9/2] orbital should provide the lowest configuration for $Z = 73$. It appears that the near-lying orbital [514 9/2] is filled pairwise in going from Lu to Ta, and thus the orbital [404 7/2] occurs as a ground-state configuration a second time in the Ta isotopes. The configuration [514 9/2] is not observed as a ground state in any stable nucleus. This irregularity in the filling of the single-particle states may possibly be a consequence of differences in the pairing

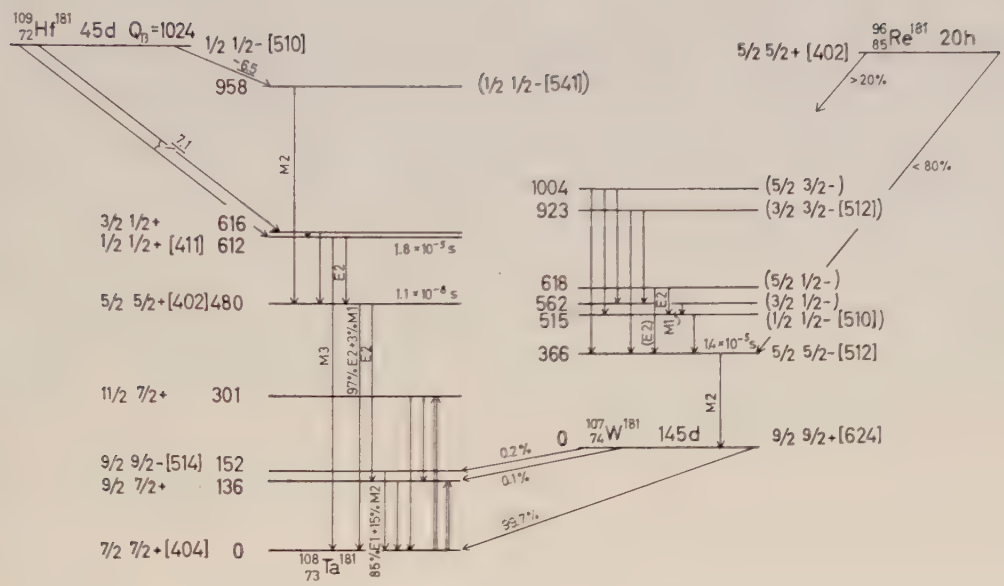

Rotational bands of

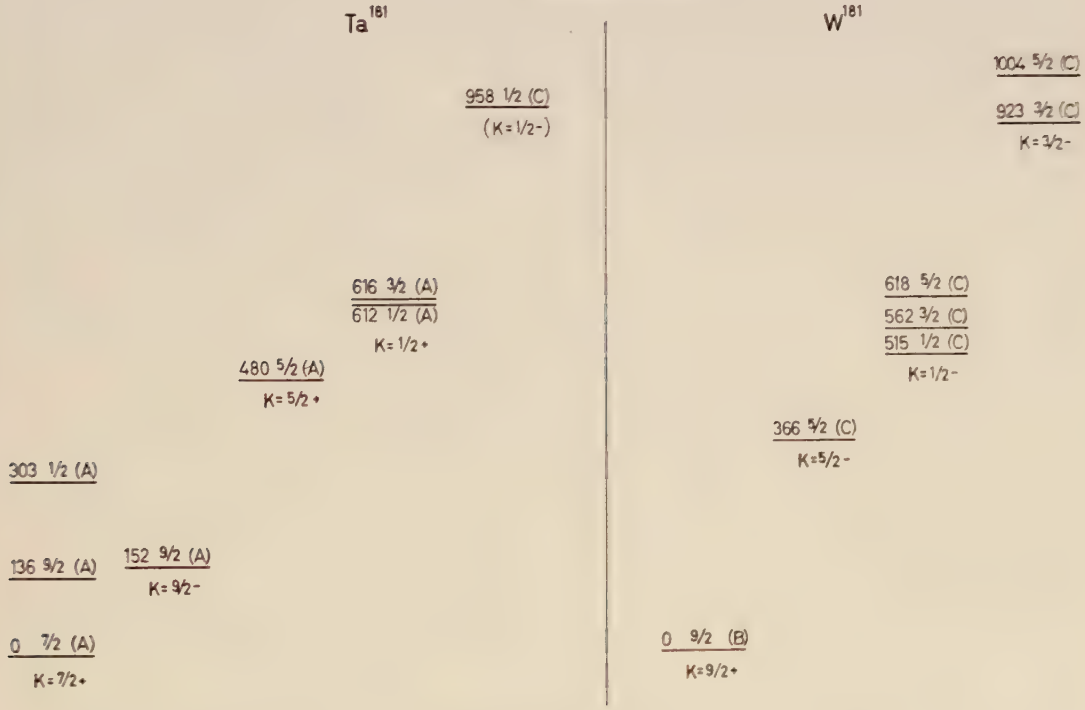

Fig. A = 181.

A large number of experimenters have come to essential agreement on the Ta^{181} level scheme as populated in the Hf^{181}, in the W^{181} decay, and by Coulomb excitation (see SHS, ABH, and NDC). The level scheme of W^{181} following the decay of Re^{181} has been constructed on the basis of the data of C. J. Gallagher (1957), University of California Radiation Laboratory Report UCRL-3928; Gallagher, Sweeney and Rasmussen (1957), Phys. Rev. **108**, 108. The W^{181} isomer has also been found in the $W(\gamma n)$ reaction, see A. J. Bureau and C. L. Hammer (1957), Phys. Rev. **105**, 1006; and S. H. Vegors and P. Axel (1956), Phys. Rev **101**, 1067.

energy for pairs of nucleons in the different orbitals. The rotational band built on the Ta^{181} ground state has levels at 136 keV ($I = 9/2$) and 301 keV ($I = 11/2$).

The configuration [402 5/2] which, as mentioned above, might have been expected as the Ta^{181} ground state in the absence of pairing effects, occurs at 480 keV as an excited configuration. The $M1$ transition from this level to the ground state is very strongly hindered ($H = 3 \times 10^6$), while the $E2$ decay is also hindered but much less ($H = 30$). These hindrances are in accord with the asymptotic selection rules. The magnetic moment of the 480 keV state has been measured and is in accord with that calculated from the [402 5/2] orbital (cf. Table VII). The 480 keV transition has a very anomalous $M1$ conversion coefficient which has been interpreted in terms of the configurations employed in the present classification (Stelson and McGowan, 1956; Reiner, 1958; Nilsson and Rasmussen, 1958).

At 612 keV, the [411 1/2] configuration is found and the characteristic close-lying $I = 3/2+$ rotational state associated with this configuration is at 616 keV. The 612 keV state decays by a hindered $E2$ transition to the 480 keV level ($H = 4 \times 10^2$) and an essentially unhindered $M3$ transition to the ground state ($H = 7$). These hindrances are in agreement with the asymptotic selection rules (see Table X).

The $_{72}Hf^{181}$ ground state should correspond to the [510 1/2] orbital just as the $_{74}W^{183}$ ground state. The beta decay to Ta^{181} thus takes place almost entirely to the $I = 1/2+$ and $I = 3/2+$ members of the rotational band associated with the [411 1/2] configuration. The transition is thus classified as $1u$ and has log $ft = 7.1$.

An additional $M2$ gamma ray of 478 keV has been reported in the Hf^{181} decay and apparently represents a transition from a level at 958 keV. It is possible that this level corresponds to the orbital [541 1/2] which is really a member of the next shell ($Z > 82$), but which is brought into this region of excitation as a consequence of the nuclear deformation. If this is correct, additional information about this level would be very interesting. It should tend to increase the nuclear deformation considerably, and thus the moment of inertia associated with its rotational band should be especially great. Its decay to the lower lying [411 1/2] and [402 5/2] configurations should be appreciably retarded both as a consequence of the asymptotic selection rules and of the change in the equilibrium shape.

The $_{74}W^{181}$ ground state should correspond with the [624 9/2] configuration just as for Hf^{179}. The electron-capture decay to Ta^{181} populates the ground state and 136 keV level by ah transitions and in addition populates an odd-parity level at 152 keV. This level thus corresponds with the [514 9/2] orbital, which, as discussed above, is expected as a low-lying configuration in Ta. The observation of an appreciable admixture of $M2$ radiation in the decay of this level to the ground state is consistent with the fact that, according to the asymptotic quantum numbers, the $E1$ decay should be hindered, but $M2$ should be unhindered. The transition from W^{181} to the 152 keV state of Ta^{181} is classified as $1u$.

The spectrum of W^{181} has recently been studied in the W^{182} (γn) reaction and in the decay of Re^{181}. An isomeric level ($t_{1/2} = 1.4 \times 10^{-5}$ sec.) is found at 366 keV

in W^{181}. The most simple interpretation of this level might be to assign it to the configuration [514 7/2] which is known to occur in this region (cf., e. g., Hf^{179}). However, this assignment would imply a hindrance of $H \sim 10^{10}$ for the $E1$ decay to the ground state. Since such a large hindrance is not usually encountered for this type of transition, we have preferred the assignment [512 5/2] for the 366 keV level[1]. The interpretation of the transition as pure $M2$ does not seem inconsistent with the available information on the radiation. The hindrance is then $H = 7 \times 10^2$. According to the asymptotic selection rules for protons, this transition would be unhindered. However, the matrix element vanishes for a neutron transition and this may explain the moderate hindrance observed. The assignment [512 5/2] for the 366 keV level seems also to be in better agreement with the observation that an appreciable fraction of the Re^{181} electron-capture decay feeds this level directly. Thus, the Re^{181} ground state is probably [402 5/2], as for the other Re isotopes, and the decay to the [512 5/2] level would be $1u$, while that to the [514 7/2] level would be $1h$. However, the assignment adopted for the W^{181} isomer raises the question of why the [514 7/2] orbital is not seen in the W^{181} spectrum and why the [512 5/2] orbital does not also appear in the spectrum of Hf^{179}.

Above 366 keV in W^{181}, a number of levels are populated in the Re^{181} decay, but the level scheme in this region is very uncertain. We have tentatively attempted to interpret the available data in terms of the states of Fig. 4 and the known systematics of levels in this region. Thus, the 512, 562, and 618 keV levels might correspond to a rotational band built on the [510 1/2] configuration. This band would thus correspond to the ground-state rotational band of W^{183} which it resembles very closely. Similarly, the 923 and 1004 keV levels might correspond to a rotational band built on the [512 3/2] orbital which is found at 209 keV in W^{183}. The decay of Re^{181} to the latter configuration is $1u$.

A = 183.

The ground-state spin of $_{74}W^{183}$ has been determined experimentally to be 1/2. One may then identify this ground state with the orbital [510 1/2] which, according to Fig. 4, should be the lowest configuration for $N = 109$, assuming an eccentricity $\delta \approx 0.2$ (see Fig. 9). Excited rotational states associated with this configuration have been identified at 46 keV ($I = 3/2$), 99 keV ($I = 5/2$), 207 keV ($I = 7/2$), and 309 keV ($I = 9/2$). The observed magnetic moment and decoupling parameter agree very roughly with those calculated from the assigned orbital (see Tables VII and VIII).

Besides the ground-state configuration, one can see from Fig. 4 that the orbitals [512 3/2] and [503 7/2] are expected as low-lying intrinsic states in W^{183}. Indeed, one finds a $K = 3/2$ band with levels at 209 keV ($I = 3/2$), 292 keV ($I = 5/2$), and 412 keV ($I = 7/2$). This intrinsic excitation thus corresponds well with the expected [512 3/2] orbital. The [503 7/2] configuration occurs at 453 keV.

The accurate energy measurements as well as the relative gamma-ray intensities

[1] This assignment has also been suggested by Gallagher et al. (1957).

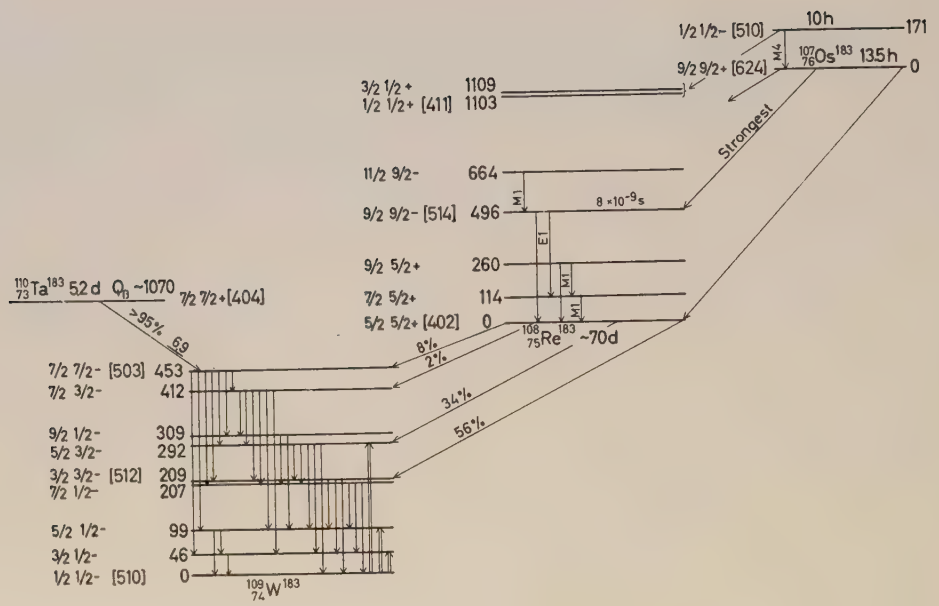

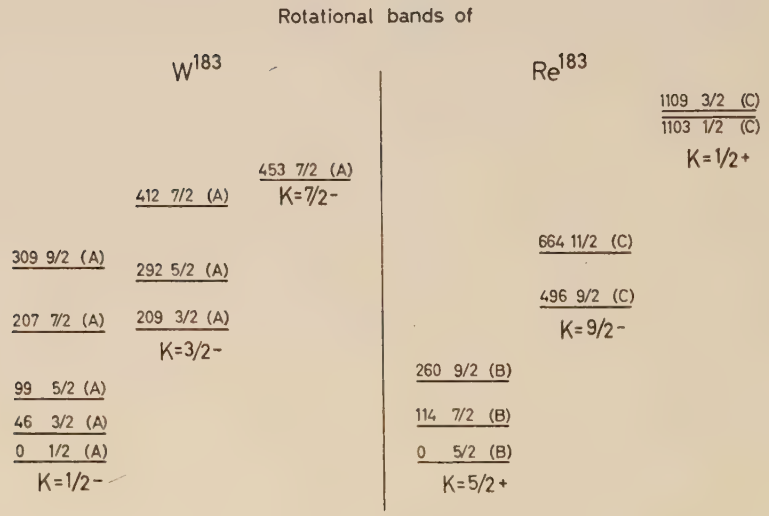

Fig. A = 183.

The decay of Ta^{183} has been studied in great detail by Murray, Boehm, Marmier, and DuMond (1955), Phys. Rev. **97**, 1007. The Re^{183} has been similarly studied by Thulin, Rasmussen, Gallagher, Smith, and Hollander (1956), Phys. Rev. **104**, 471. The decay scheme of Os^{183} and Os^{183m} has been taken from a recent study by J. O. Newton and V. S. Shirley (1957), Bull. Am. Phys. Soc. **II:2**, 395 and private communication. For a review of the Coulomb excitation experiments on W^{183}, see ABH.

in W^{183} have been analyzed in considerable detail by KERMAN (1955) who has taken into account the deviations from the simple rotational wave functions that are induced by the Coriolis coupling between the [512 3/2] and [510 1/2] orbitals. In this analysis, the observed spectrum is fitted by adjusting the value of the matrix element, $\langle K = 3/2 \,|\, j_+ \,|\, K = 1/2 \rangle$, which determines the magnitude of the Coriolis effect. The value for this matrix element which is thus determined is 1.5, while from the assigned orbitals one calculates the value 0.9.

The beta decay of $_{73}Ta^{183}$ populates directly only the 453 keV level ($I = K = 7/2$), which is consistent with the assignment of the orbital [404 7/2] to the Ta^{183} ground state as for all the other Ta isotopes. The decay is classified as $1u$ and has log $ft = 6.9$. The decay to the 209 keV level would be 1^*h, and the evidence from the observed beta spectrum indicates that log $ft > 8.7$.

The electron-capture transitions from $_{75}Re^{183}$ go to levels in W^{183} with spins 3/2, 5/2, and 7/2, which suggests the spin 5/2 for the Re^{183} ground state; this state thus appears to correspond with the [402 5/2] orbital which is also found as the ground state of Re^{185} and Re^{187}. The observed Re^{183} decays are all classified as $1u$.

Recently, the Os^{183} decay into Re^{183} has been studied[1]. An $M4$ isomer (10 h.) of Os^{183} has been found which corresponds well to the transition between the [510 1/2] and [624 9/2] configurations which are known to be very close together in this region (cf. W^{181} and Hf^{179}). The [624 9/2] configuration seems to provide the ground state as in W^{181} and Hf^{179}. This state decays mainly to an odd-parity level at 496 keV in Re^{183}. This last level can then be classified as the expected [514 9/2] configuration. The electron-capture transition is classified as $1u$.

The 10 h $_{76}Os^{183}$ isomer decays to a pair of levels at about 1100 keV in Re^{183}. These states must have low spin and they appear to correspond to the characteristic doublet representing the first two rotational states associated with the [411 1/2] configuration (cf. the Tm isotopes, Ta^{181} etc.). It might be expected that the orbital [402 3/2] should occur in this region of excitation, but it would be much less populated in the Os^{183m} decay, since the transition would be $1h$ compared with the $1u$ transition to the [411 1/2] orbital.

A = 185.

The ground state spin of $_{75}Re^{185}$ is 5/2; this value and the observed magnetic moment are both consistent with the assignment of the orbital [402 5/2] as the ground state configuration. Rotational states associated with this configuration have been studied by Coulomb excitation.

The $_{76}Os^{185}$ ground state appears to be represented by the [510 1/2] configuration as for W^{183} and Hf^{181}. The decay to the Re^{185} ground state would thus be 1^*h and is indeed observed to be very weak. The dominant mode of the Os^{185} electron-capture decay populates a state at 646 keV in Re^{185}. According to Fig. 3, one might expect either the [402 3/2] or [400 1/2] configuration in this region. The $E2$ decay of this level to

[1] J. O. NEWTON (private communication) has suggested a classification of the Re^{183} spectrum which is the same as that employed here.

the Re ground state as well as the asymptotic selection rules for the electron capture transition both suggest that [400 1/2] is the proper assignment. It appears that the [402 3/2] configuration, requiring a $1h$ transition has not been seen in the Os^{185} decay.

A state at 717 keV in Re^{185} is also populated in the Os^{185} decay. It is probable that this state corresponds to the $I = 3/2$ rotational state built on the [400 1/2] orbital. A small decoupling parameter is expected for this band.

Finally, a pair of states at 872 and 879 keV in Re^{185} are populated in the Os^{185} decay. These states appear to represent the characteristic $I = 1/2$ and $I = 3/2$ doublet associated with the [411 1/2] configuration.

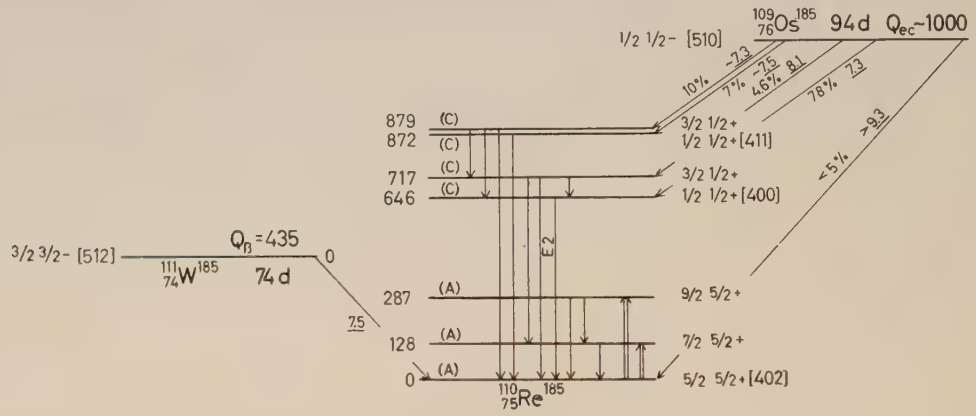

Fig. A = 185.

A number of different investigations are in essential agreement on the decay scheme given here; for references, see SHS and NDC.

In the figure, the log *ft*-values for the different Os^{185} electron-capture transitions have been calculated, assuming a decay energy of 1 MeV. A comparison of these values with those expected according to the classification of the transitions (cf. § V) indicates that the assumed transition energy may be slightly too high.

According to Fig. 4, one might expect either [510 1/2], [512 3/2] or [503 7/2] as the ground state of $_{74}W^{185}$. On the basis of the observed beta decay directly to the Re^{185} ground state, we have adopted the assignment [512 3/2].

It should be mentioned that the available means of populating the low-lying states of Re^{185} ensures that only the low spin states could have been seen so far. According to Fig. 3, one expects the configurations [404 7/2] and [514 9/2] also to occur in the low-energy spectrum of Re^{185}, but they could not have been populated in the experiments that have been reported.

c. Region of the heavy elements.[1]

The spectra of the even-even nuclei beyond Pb begin to exhibit well-defined rotational patterns starting at about $A \sim 224$. It is thus expected that the coupling

[1] *Note added in proof:* A discussion of the heavy element odd-A spectra on the basis of Figs. 5 and 6 has also been given recently by Stephens, Asaro, and Perlman (to be published).

scheme of the present article should also be appropriate for the interpretation of the odd-A nuclei starting at about the same point. There is not, however, sufficient data to make possible a unique classification of the odd-proton spectra for $Z < 93$ or for the odd-neutron nuclei with $N \lesssim 139$, and at the present time we shall not attempt any detailed interpretation of the configurations of the nuclei lighter than these. One may notice, however, that, according to Fig. 5, the orbitals [651 3/2] and [530 1/2] might be expected for the ground states of $Z = 91$ or $Z = 89$ and that possibly [532 3/2] and [660 1/2] might also be expected as low-lying excited configurations in this region.

Similarly, for the odd-neutron configurations, one expects to find the orbitals [631 3/2] and [752 5/2] appearing in the region around $N = 137$ (see Fig. 6).

There is one particularly important piece of experimental evidence in the region $225 < A < 233$ which requires special mention, and this is the ground-state spin, $I_0 = 3/2$, and negative quadrupole moment ($Q = -1.7 \times 10^{-24}$ cm^2) reported for $_{89}Ac^{227}$ (Fred et al., 1955). As discussed in Section IV, the calculations based on the level schemes of Figs. 5 and 6 clearly indicate a prolate intrinsic shape for Ac^{227} (see especially Fig. 12). This prediction also receives support from the observed regularity in the rotational patterns of the even-even nuclei ranging from $_{88}Ra^{224}$ to the region of U and Am, where the measured quadrupole moments are found to be positive. One possible explanation of the Ac^{227} moment could be that the ground-state configuration has $K = 1/2$ and, e. g., the expected orbital [530 1/2] with a decoupling constant $a \sim -2$. The ground state would then have $I_0 = 3/2$ and a negative quadrupole moment. This is indeed the same configuration which appears to provide the ground state configuration of $_{91}Pa^{231}$ and Pa^{233} (see below). If this is correct, one also expects a negative spectroscopic quadrupole moment for the Pa isotopes.

We begin the more detailed discussion of the heavy-element spectra with A = 233.

A = 233.

The ground-state spin of $_{92}U^{233}$ is 5/2; both the spin and magnetic moment (cf. Table VII) of this state agree well with the odd-neutron configuration [633 5/2] expected, according to Fig. 6, for $N = 141$. The ground-state rotational band has been studied by Coulomb excitation.

An excited intrinsic state at 313 keV in U^{233} is populated in the $_{91}Pa^{233}$ decay; this excited state appears to have $K = 3/2$ and the same parity as the ground state and may thus correspond with the orbital [631 3/2]. In addition, the close-lying levels at 400 and 413 keV appear to represent the two lowest states in a $K = 1/2$ rotational band which may be identified with the configuration [631 1/2] (cf. the same orbital appearing in the spectra of U^{235} and Pu^{239}).

The favoured alpha decay of $_{94}Pu^{237}$ is found to populate an excited state at about 295 keV in U^{233}. This level is thus identified with the [743 7/2] orbital (see the discussion of Pu^{237} below).

Besides the levels which have so far been observed in U^{233} one should expect,

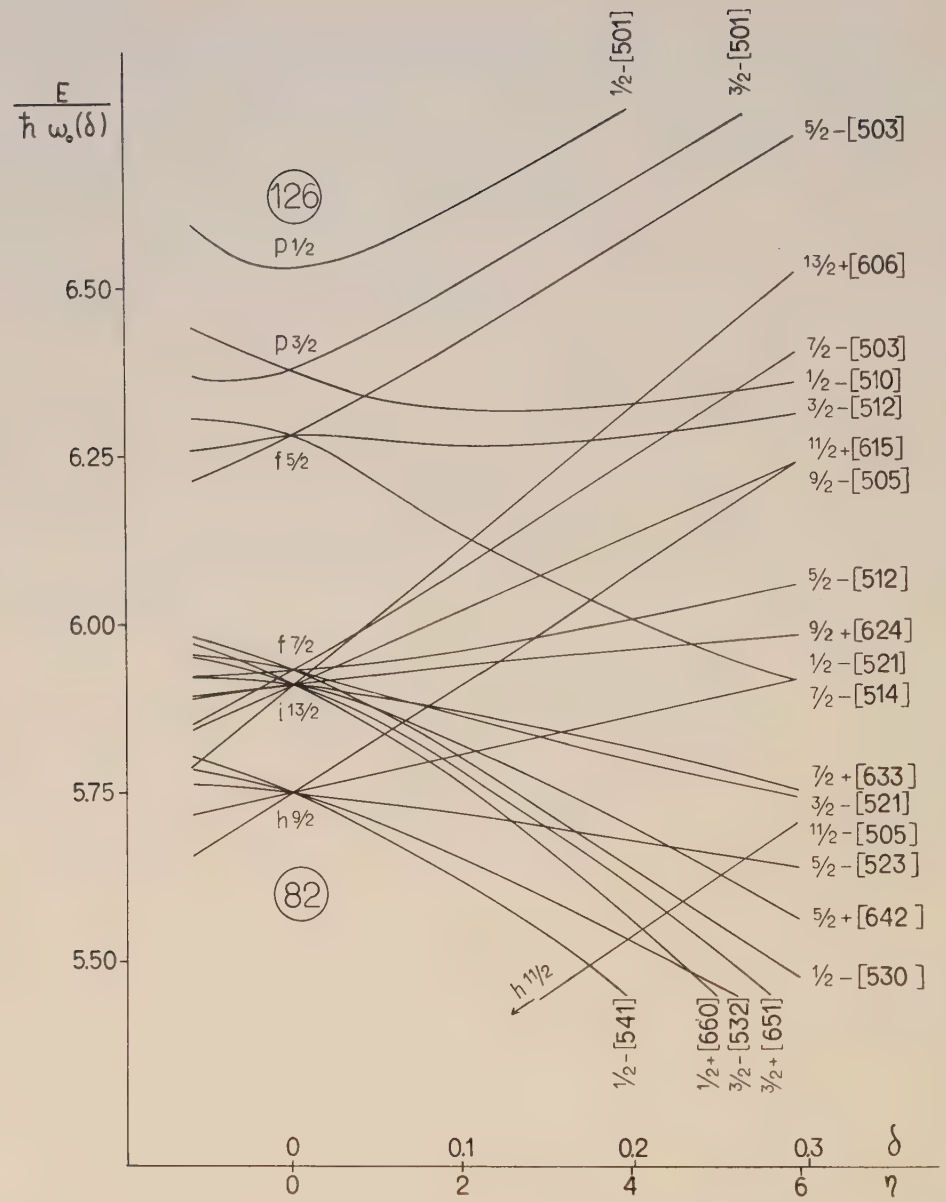

Fig. 5. *Single-particle levels for odd-Z nuclei in the "heavy element" region* ($Z > 82$). The corresponding wave functions are found in table I of (SGN) for states having $N = 6$ and in Appendix I of the present paper for the $N = 5$ states. The wave functions have been calculated using $\mu = 0.45$ for the $N = 6$ states and $\mu = 0.70$ for $N = 5$ states. In comparing with the experimental data, it was found that the high-angular-momentum states of the $N = 6$ shell occurred systematically lower than would correspond to these parameters. (Cf. the similar situation encountered in Fig. 3.) In drawing the figure, the states of the $N = 6$ shell have been consistently plotted at an energy 2.4 MeV lower than corresponding to these parameters. This corresponds to using a μ-value of approximately 0.62 for the $N = 6$ states in this diagram.

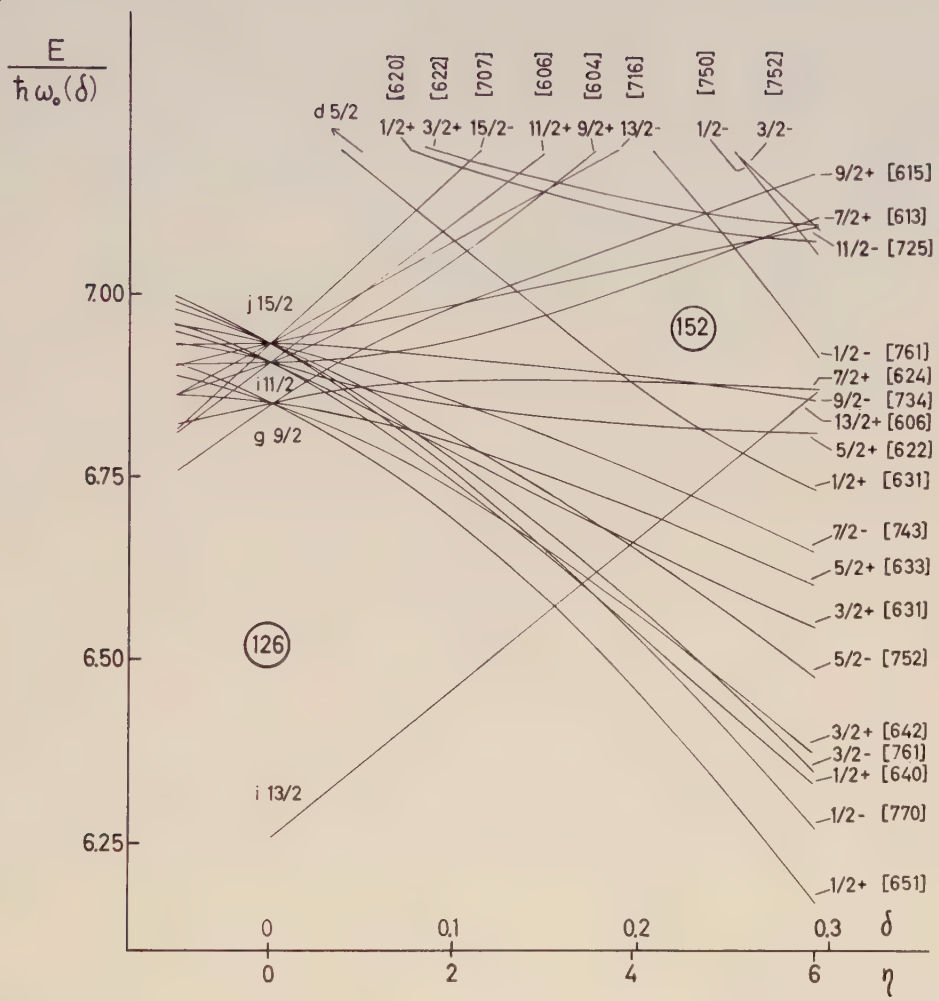

Fig. 6. *Single-particle levels for odd-N nuclei in the "heavy element" region* ($N > 126$). The corresponding wave functions for $N = 6$ states are found in table I of (SGN) and for $N = 7$ states in Appendix I of the present paper. The calculated wave functions correspond to the parameters $\mu = 0.45$ for $N = 6$ and $\mu = 0.40$ for $N = 7$. In comparing with the experimental data, it was found that the high-angular-momentum states of the $N = 7$ shell occurred systematically lower than would correspond to these parameters. (Cf. the similar situation discussed in the caption to Figs. 3 and 5.) Therefore, in constructing the figure, all odd-parity states ($N = 7$) have been plotted at an energy approximately 700 keV lower than corresponding to these parameters. This effectively amounts to using a μ-value of 0.44 for the $N = 7$ states (i. e., the effective μ is very nearly the same as that used for $N = 6$). In plotting Fig. 6 we have employed, as in Figs. 4 and 5, $\varkappa = 0.05$.

according to Fig. 6, that the orbital [752 5/2] will also occur as a fairly low-lying excited configuration.

The ground-state transition energy for the electron-capture decay of $_{93}Np^{233}$ (not shown in the figure) has been estimated on the basis of closed cycles to be 1.0 MeV (see SHS). The 35 min. half-life thus implies log $ft = 5.0$, assuming the ground-state transition to predominate, and a somewhat smaller log ft-value if the transition goes

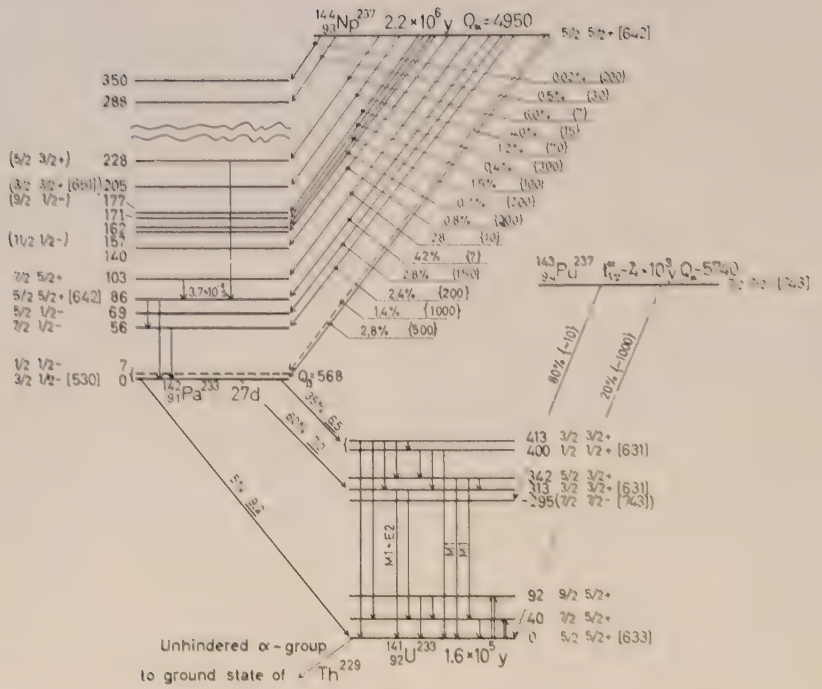

Fig. A = 233.

The level scheme of U^{233} has been studied by Coulomb excitation – J. O. Newton (1957), Nuclear Phys. **5**, 218 – and in the beta decay of Pa^{233} (for references, see SHS and NDC). The Pu^{237} alpha-decay to U^{233} has been investigated by Thomas, Van den Bosch, Glass, and Seaborg (1957), Phys. Rev. **106**, 1228. The level scheme of Pa^{233} populated in the alpha decay of Np^{237} has been given by Asaro, Perlman, and Stephens, private communication. For references to previous work on this decay scheme, see I. Perlman and J. O. Rasmussen (1957), Chapter on Alpha Radioactivity in *Handbuch der Physik*, Vol. **42** (Springer Verlag, Berlin), hereafter referred to as PR.

mainly to an excited state. Such a fast transition is indeed expected if we assign the orbital $\lfloor 642\ 5/2 \rfloor$ to the Np^{233} ground state, as for all the other Np isotopes, and assume the transition to go to the configuration $\lfloor 642\ 3/2 \rfloor$ in U^{233}. More detailed experimental information on this decay would thus be of considerable interest. This configuration might be expected to occur at an excitation energy of the order of 1–2 MeV in U^{233}.

The favoured alpha decay of U^{233} is somewhat different from that of most odd-A nuclei in that it populates the ground-state rotational band in the $_{90}Th^{229}$ daughter. The Th^{229} ground state should thus be assigned the same configuration, $\lfloor 633\ 5/2 \rfloor$, as the U^{233} ground state. This implies that there is either a crossing of levels or an important effect of the pairing energy in going from $N = 139$ to $N = 141$. Additional information on the low configurations of other nuclei with these neutron numbers would thus be of interest in studying these effects.

Although the experimental evidence on the Pa^{233} spectrum still leaves considerable uncertainty about many of the levels, we have tentatively attempted a classification of the available data.

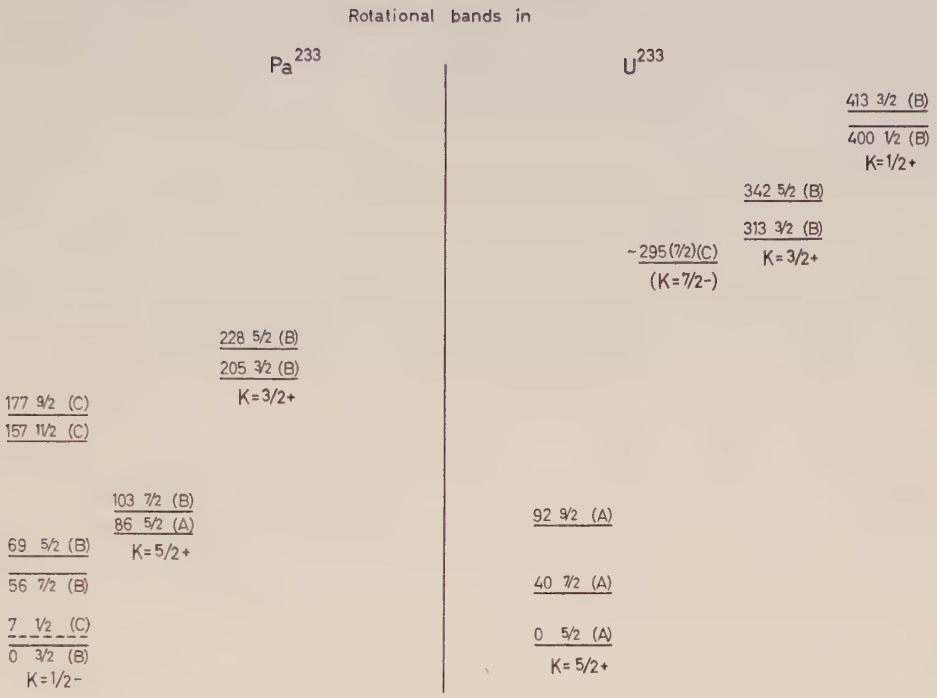

The lowest levels of Pa^{233} and Pa^{231} exhibit a very great similarity and we have assumed that the orbitals are the same in the two nuclei. The Pa^{231} ground-state spin of $I = 3/2$ is therefore also assumed for Pa^{233}. This is in agreement with the evidence on the Pa^{233} beta decay.

The similarity in the alpha-decay hindrance factors for the transition from Np^{237} to the ground state, 56 and 69 keV level of Pa^{233}, might suggest that these levels form a rotational band (Asaro, Perlman, and Stephens, 1957). There is also preliminary evidence from the Coulomb excitation of Pa^{231} which suggests the same conclusion (Newton, 1957b). If this is the case, the irregularity of the spacings indicates that we are dealing with a $K = 1/2$ band which has a negative decoupling constant. The ground state, 56, 69, 157 and 177 keV levels, are fitted quite well by assuming $3\hbar^2/\Im = 36$ keV and $a = -1.3$. These parameters imply that the $I = 1/2$ member of the band should occur at about 6 keV. Indeed, there is evidence in the Pa^{231} spectrum for a level at about this energy and preliminary evidence in the alpha decay of Np^{237} for such a level in Pa^{233}.

Essentially unhindered alpha transitions from Np^{237} populate states in Pa^{233} at 86 and 103 keV. These levels are accordingly identified with the configuration [642 5/2] which is found as the ground-state configuration in all the Np isotopes. The very close spacing of these two levels (as compared, for example, with the spacing of the corresponding two rotational states in Np^{237}) may reflect a strong perturbation of this

rotational band caused by the presence of the near-lying [651 3/2] configuration (see below).

There are also very strong alpha transitions to levels at 205 and 228 keV in Pa^{233}. These levels have been tentatively assigned the orbital [651 3/2] since, according to Fig. 5, this orbital should occur in this region. It is expected to be strongly coupled to the [642 5/2] orbital through the Coriolis forces. Such a coupling would imply a considerable perturbation of the rotational band associated with the latter configuration and would also lead to relatively strong alpha transitions populating the [651 3/2] levels.

Besides these levels there are also excited states in Pa^{233} at 140, 162, 171, 288, and 350 keV which are populated in the Np^{237} alpha decay. As yet not enough is known about these levels to make configuration assignments possible.

A = 235.

The ground state spin of $_{92}U^{235}$ is $I_0 = 7/2$; this as well as the negative value of the magnetic moment agree with the configuration [743 7/2] suggested by Fig. 6. The rotational band associated with this configuration has been studied by Coulomb excitation. The unusually large moment of inertia for this rotational band lends further support to this classification (see Section III).

The favoured alpha decay of $_{94}Pu^{239}$ populates a rotational band characterized by $K = 1/2$. Rotational states ranging from the lowest member $I = 1/2$ up to the $I = 9/2$ member have been observed. It has quite recently been shown that the lowest state of this band decays to the U^{235} ground state by an $E3$ transition of 0.08 keV and $T_{1/2} = 26$ min. This very low lying intrinsic state corresponds well with the configuration [631 1/2] (see the discussion of Pu^{239}).

Very weak alpha transitions also populate a number of higher-lying excited states in U^{235}, starting at 172 keV. Little is as yet known about these states, but it might be suggested that the orbitals [633 5/2] and [622 5/2] occur as fairly low-lying configurations in U^{235}.

The $_{93}Np^{235}$ ground state is classified as [642 5/2] as for the other Np isotopes. The electron-capture decay energy estimated from closed cycles leads to $\log ft \sim 7.5$ for the transition to the U^{235} ground state. This ft-value is somewhat greater than is usually encountered for a $1u$ transition.

The favoured alpha decay of $_{95}Am^{239}$ populates a level at 48 keV in Np^{235} which in turn decays to the ground state by an $E1$ transition. This pattern is observed in all the odd Am alpha decays (Am^{239}, Am^{241}, and Am^{243}) and corresponds well with the assignment of [523 5/2] as the excited configuration in Np (see especially the spectrum of Np^{237}).

The transition energy for the electron-capture decay of Pu^{235} into Np^{235} has been estimated on the basis of closed cycles to be about 1.1 MeV (see SHS). The observed lifetime thus implies $\log ft < 5$ for the main transition. The au transition implied by this low value would result from assigning the configuration [633 5/2] to the

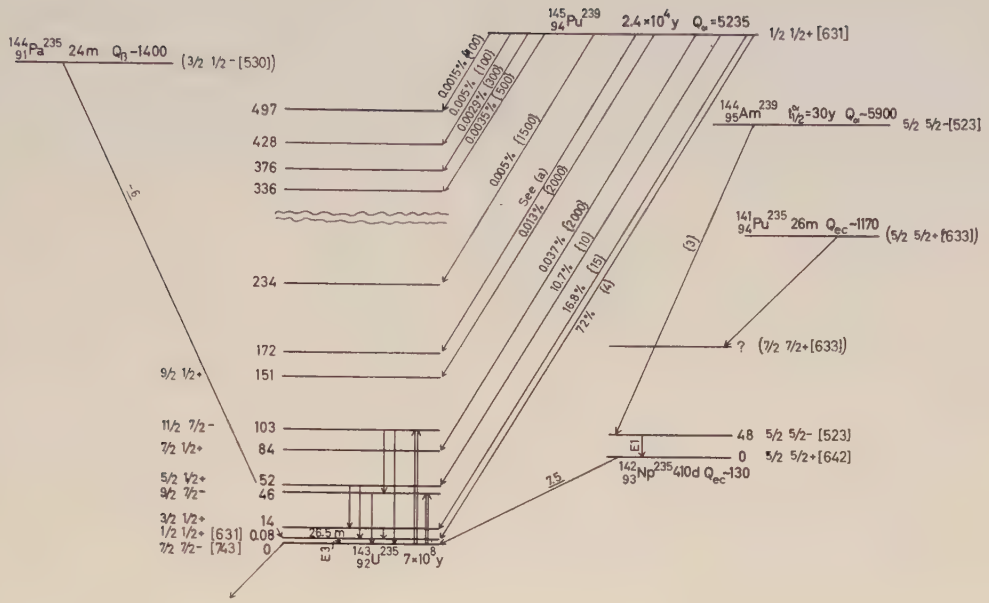

Rotational bands in U^{235}

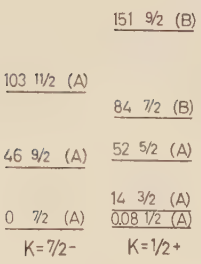

Fig. A — 235.

The Coulomb excitation of U^{235} has been studied by J. O. Newton (1957), Nuclear Phys. **3**, 345. The data on the alpha decay of Pu^{239} are taken from PR and from the recent work of Novikova, Kondiatev, Sobolev, and Goldin (1957), Journ. Exper. Theor. Phys. **32**, 1018. The U^{235} isomer has recently been found by F. Asaro and I. Perlman (1957), Phys. Rev. **107**, 318, Huizenga, Rao, and Engelkemeir (1957), Phys. Rev. **107**, 319; cf. also Michel, Asaro, and Perlman (1957), Bull. Am. Phys. Soc. **II:2**, 394. The Np^{235} electron-capture decay has been studied by Hoff, Olsen, and Mann (1956), Phys. Rev. **102**, 805, and Gindler, Huizenga, and Engelkemeir (1958), Phys. Rev. **109**, 1263. References to the Am^{239} alpha decay may be found in PR. The Pu^{235} electron-capture decay has been studied by Thomas, Van den Bosch, Glass, and Seaborg (1957), Phys. Rev. **106**, 1228.

Pu^{235} ground state (as also for U^{233} and Th^{231}) and assuming the decay to go to the state [633 7/2] expected as an excited configuration in Np^{235}.

If we assume the $_{91}Pa^{235}$ ground state to be [530 1/2] $I = 3/2$, as is tentatively suggested for Pa^{231} and Pa^{233}, then the beta decay to U^{235} should go predominantly to the 26 min. isomeric level.

A = 237[1].

The spin, the very roughly known magnetic moment, and the exceptionally large moment of inertia associated with the $_{93}Np^{237}$ ground state configuration all support the classification [642 5/2] for this orbital (see Tables VII and VI). The two lowest rotational excitations associated with this configuration have been studied by Coulomb excitation.

An intrinsic excitation with $K = 5/2$ and opposite parity from the ground state is found at 60 keV. This level which is populated in the favoured alpha decay of $_{95}Am^{241}$ is identified with the [523 5/2] configuration. The measured magnetic moment of this state also supports this interpretation (Table VII). The $E1$ decay of this level is strongly hindered ($H \sim 3 \times 10^5$) as required by this classification. Rotational states built on this configuration have been found at 103, 160, and 225 keV.

Another intrinsic excitation is found at 267 keV in Np^{237} and appears to have $K = 3/2-$. This state may thus be associated with the expected configuration [521 3/2].

Finally, there are weakly populated states at 332 keV, 368 keV, and possibly 371 keV. These states appear to have even parity and may form a rotational band with $K = 1/2$ (Rasmussen et al., 1957). According to Fig. 5, such a state is not expected in this region and the interpretation of these levels is difficult (see Rasmussen et al., 1957, for a discussion of these levels and suggestions concerning their classification.)

The $_{94}Pu^{237}$ electron-capture decay populates the ground-state rotational band in Np^{237} and the 60 keV excited state with log $ft \sim 7$ in each transition. Assigning the Pu^{237} ground-state configuration as [743 7/2] (as for $_{92}U^{235}$) these transitions are classified as $1u$ and ah, respectively.

The favoured alpha decay of $_{96}Cm^{241}$ has recently been shown to populate a 0.18 s $E3$ isomer in Pu^{237}. The Cm^{241} ground state should be [631 1/2] as for Pu^{239} and the favoured alpha decay should thus populate this same configuration in Pu^{237}. This assignment accounts well for the spin and parity of the isomeric level. The $E3$ transition is thus classified as hindered according to the asymptotic quantum numbers and is observed to have $H \sim 10^2$.

The U^{237} beta decay goes predominantly to the [521 3/2] configuration in Np^{237} (log $ft = 6.0$) and not at all to the levels associated with the ground state or first excited configuration. This behaviour is consistent with the assignment [631 1/2] to the U^{237} ground state (as for the Pu^{239} ground state); the dominant beta transition is thus

[1] The theoretical classification of the Np^{237} levels has been discussed previously on a number of occasions, see especially Rasmussen, Canavan, and Hollander (1957).

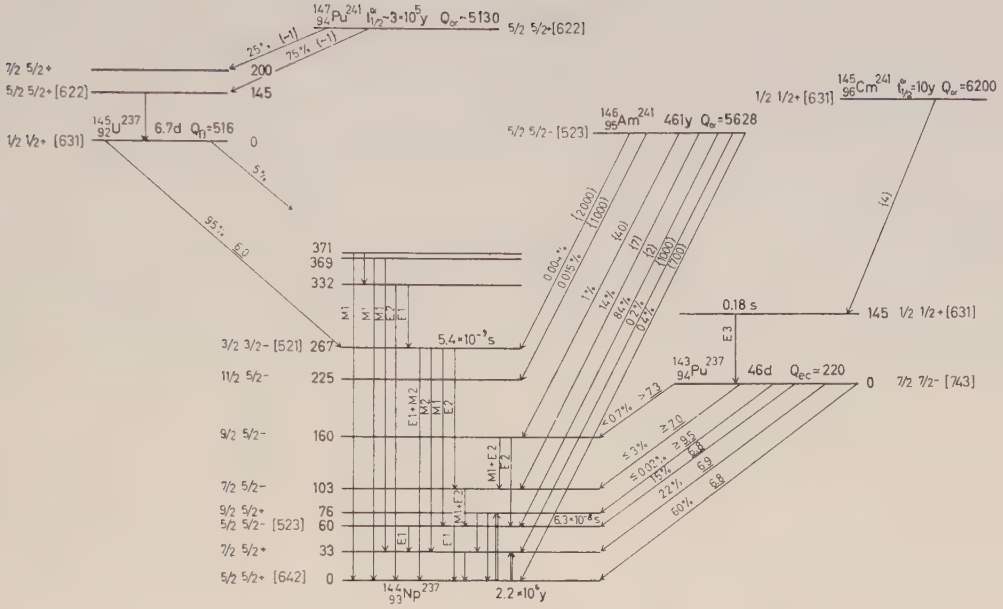

Rotational bands in Np^{237}

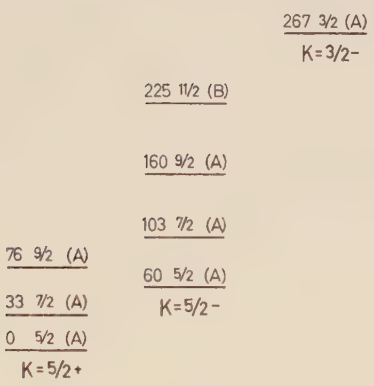

Fig. A = 237.

For detailed references of the level scheme of Np^{237} as populated both by the beta decay of U^{237} and the alpha decay of Am^{241}, see SHS (cf. also PR). New data on the Pu^{237} electron-capture decay are provided by D. C. Hoffman and B. J. Dropesky (1958), Phys. Rev. **109**, 1282, and private communication. The 145 keV 0.18 s isomeric transition in Pu^{237} has been found recently by Stephens, Asaro, Amiel, and Perlman (1957), Phys. Rev. **107**, 1456. Concerning references to the alpha decay of Cm^{241} and Pu^{241}, see SHS and PR.

classified as $1u$, while the higher energy transitions would be second forbidden and 1^*h. The ground-state rotational band of U^{237} should resemble that of Pu^{239}.

The favoured alpha decay of Pu^{241} populates an excited intrinsic state in U^{237}, which is accordingly assigned the orbital [622 5/2] (see A = 241).

A = 239[1].

The ground state of $_{94}Pu^{239}$ has $I_0 = 1/2$ and the corresponding rotational band has a decoupling parameter $a = -0.58$. The orbital [631 1/2] accounts well for these properties and for the measured magnetic moment (see Fig. 6, Tables VII and VIII).

The first excited intrinsic state in Pu^{239} occurs at at 286 keV and has been shown to have $K = 5/2+$. This state can thus be identified with the orbital [622 5/2] which is expected in this region of excitation. The $M1$ transitions from this level to the ground-state band are K-forbidden and observed to be strongly hindered ($H \sim 10^4 - 10^5$); the $E2$ components in these transitions are hindered by the asymptotic quantum numbers and are observed to be slowed down by factors $\sim 10^2$ compared to a single-proton transition. The favoured alpha transition from $_{96}Cm^{243}$ is found to lead to the 286 keV level in Pu^{239} and thus to imply the classification [622 5/2] for the Cm^{243} ground state.

A second excited intrinsic configuration is found at 392 keV (almost coincident in energy with the $I = 9/2$ member of the [622 5/2] rotational band). This new level decays by very hindered $E1$ radiation ($H \sim 10^6$) to the [622 5/2] levels and is accordingly identified with the [743 7/2] orbital.

Finally, a level at 512 keV in Pu^{239} has been observed in the $_{93}Np^{239}$ and $_{95}Am^{239}$ decays. This level may correspond with the [633 5/2] configuration.

The Np^{239} ground state has been assigned the orbital [642 5/2] as for all the other Np isotopes. This interpretation accounts well for the Np^{239} spectrum observed in the Am^{243} decay and for the Np^{239} decay into Pu^{239} (see below). However, it does not agree with the value $I_0 = 1/2$ reported for the ground-state spin in several earlier investigations of the Np^{239} hyperfine structure. For the present classification it is therefore of decisive importance that a recent redetermination of the Np^{239} spin has given the value $I_0 = 5/2$ (Hubbs and Marrus, 1958).

The Np^{239} ground state decays to all the low lying configurations in Pu^{239} with log $ft = \sim 9$, 6.9, 6.5, and 6.8 for transitions to the orbitals [631 1/2] (probably the $I = 3/2$ and 5/2 members of the rotational band based on this orbital are mainly populated) [622 5/2], [743 7/2] and [633 5/2], respectively. These transitions are classified as 1 (K-forbidden), ah, $1u$, ah, respectively.

The favoured alpha transition from Am^{243} populates an excited configuration in Np^{239} at 74 keV. This configuration is classified as [523 5/2] (see the discussion on the spectra of the Am isotopes). This level is observed to decay by an $E1$ transition

[1] The theoretical classification of the Pu^{239} levels has been considered by Hollander (1957) with conclusions essentially the same as those obtained here.

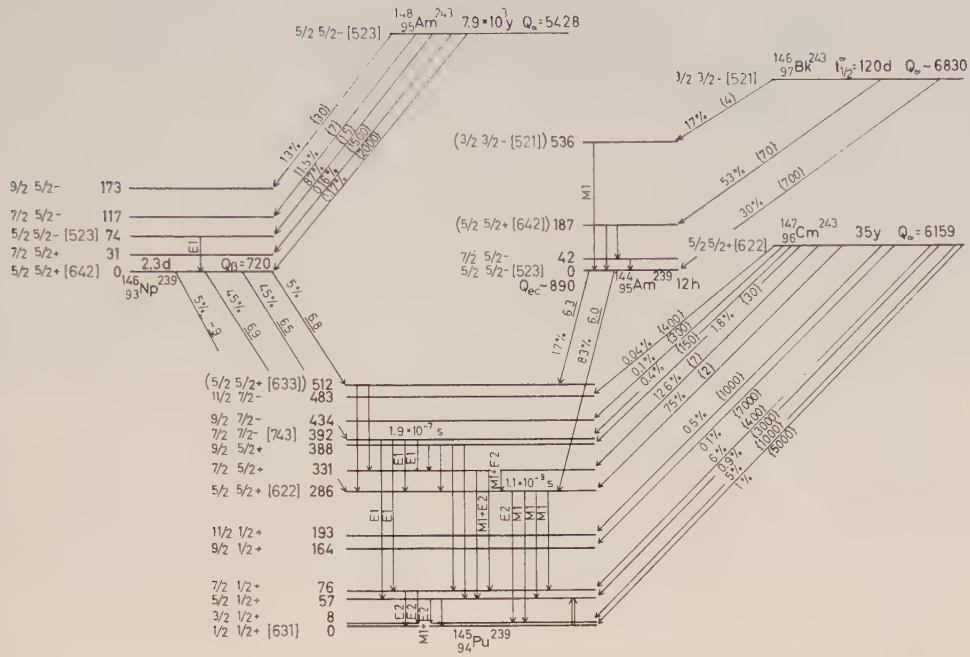

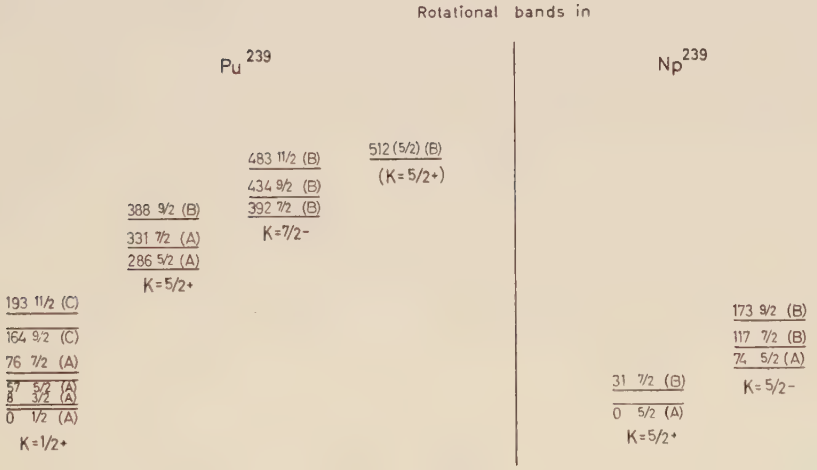

Fig. A – 239.

The complex spectrum of Pu^{239} was first illucidated by a detailed study of the Np^{239} beta decay, Hollander, Smith, and Mihelich (1956), Phys. Rev. **102**, 740. The decay scheme has been further clarified and substantiated by experiments involving the Cm^{243} alpha decay, the Am^{239} electron-capture decay, Coulomb excitation, as well as further study of the Np^{239} decay (for references and decay schemes, see SHS). For references to the alpha-decay spectrum of Am^{243}, see also SHS. The Bk^{243} decay scheme has recently been studied by A. Chetham-Strode (1956), University of California Radiation Laboratory Report UCRL-3322.

to the Np^{239} ground state, in agreement with the adopted classification (cf. also the very similar situation in the spectra of Np^{235} and Np^{237}).

The $_{92}U^{239}$ decay (not shown) is reported to go predominantly through the 74 keV level of Np^{239} with log $ft \sim 6$. This is to be expected if we assign the orbital [622 5/2] to the U^{239} ground state (as to $_{94}Pu^{241}$). The observed decay is then classified as $1u$; the intensity of the ah transition to the ground state may be estimated on the basis of the corresponding transition in $Np^{239} \rightarrow Pu^{239}$ and is expected to be about ten times weaker. In addition, one might expect some branching to the 117 keV level.

The Am^{239} electron-capture decay goes to the [622 5/2] configuration in Np^{239} with log $ft \sim 6$ and to [633 5/2] also with log $ft \sim 6$. Assuming [523 5/2] for the Am^{239} ground state, as for all the other Am isotopes, these transitions are classified as $1u$. The unobserved transitions to the ground state and 392 keV level would be classified as 1^*h and ah, respectively.

The favoured alpha transition from $_{97}Bk^{243}$ populates a state in Am^{239} at $\sim$ 540 keV, and a somewhat hindered transition leads to a state in Am at $\sim$ 190 keV. Not enough is known about the Bk^{243} spectrum nor of the transitions between these states in Am to make a unique classification, but from Fig. 5 one may conclude that [521 3/2] is not an unlikely choice for the Bk ground state (and thus also for the 540 keV state in Am) and that the orbitals [633 7/2] and [642 5/2] should also provide low lying excited states in Am.

A = 241

There is as yet not enough experimental evidence about the spectra of nuclei with A > 239 to make possible a unique assignment of configurations, and we therefore confine ourselves to a discussion of a few of the best studied levels.

The experimental evidence, both from the alpha decay and the measured spins and magnetic moments, supports the assignment of the orbital [523 5/2] to the ground state of both $_{95}Am^{241}$ and Am^{243} (for the alpha decay, see the level schemes of $_{93}Np^{237}$ and Np^{239}; the magnetic moments are summarized in Table VII). In analogy to the Np spectra, one expects the configuration [642 5/2] to occur fairly close to [523 5/2] also in Am. As discussed in the following paragraph, it is probable that the $_{97}Bk^{245}$ ground state corresponds with the orbital [521 3/2]; if this is the case, the alpha decay of Bk^{245} implies that the same assignment, [521 3/2], should be made for the 480 keV level in Am^{241}.

The $_{96}Cm^{241}$ ground state is expected to be the same as that of $_{94}Pu^{239}$, i. e., [631 1/2], and indeed the electron capture decay of this level goes to the low spin [521 3/2] state in Am^{241} and to a level at 640 keV which may possibly be [651 3/2] or [530 1/2].

The measured spin and magnetic moment of the Pu^{241} ground state are in agreement with the orbital [622 5/2] expected according to Fig. 6. Further, the clas-

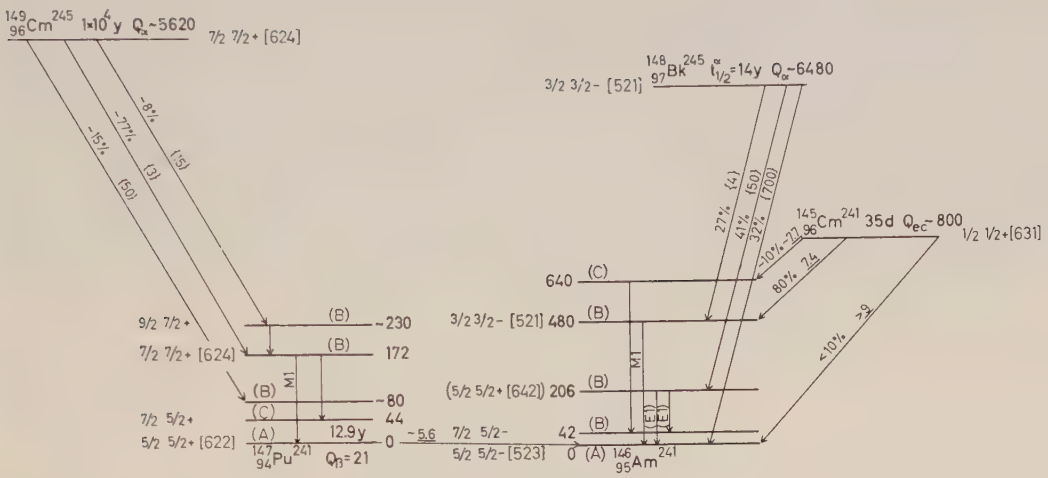

Fig. A = 241.

The Bk^{245} alpha decay has been studied by A. Chetham-Strode (1956), University of California Radiation Laboratory Report UCRL-3322. The decay scheme of Cm^{241} is based on the recent work of Asaro and F. Stephens (private communication). We are also indebted to these investigators for informing us of their additional results on the Bk^{245} decay. For references to the Pu^{241} beta decay and to the Cm^{245} alpha decay, see SHS and PR.

sification of the Cm^{245} ground state made in the next paragraph, together with the observed alpha decay of Cm^{245} into Pu^{241}, implies that the 172 keV level in Pu^{241} corresponds with the configuration [624 7/2].

A = 243.

(No decay scheme is drawn).

As mentioned above, the ground state of Am^{243} may be classified as [523 5/2]. The ground state of Pu^{243} should be the same as that of Cm^{245} and may thus be tentatively classified as [624 7/2]. This assignment is consistent with the observed electron-capture decay to the [523 5/2] ground state of Am^{243} and to a 84 keV level, which may correspond to the [642 5/2] configuration.

Finally, the ground state of Cm^{243} should correspond with that of Pu^{241} and may accordingly be assigned the configuration [622 5/2]. This assignment is strongly supported by the observed alpha decay to Pu^{239} (see the level scheme of Pu^{239}).

A = 245[1].

Although the available evidence does not yet test nor define uniquely most of the spin and parity assignments suggested in the decay schemes of Fig. A = 245,

[1] The theoretical classification of the Cm^{245} levels has been discussed by Stephens, Asaro, Thompson, and Perlman (1957), Bull. Am. Phys. Soc. **II:2**, 394, with conclusions in agreement with those suggested below.

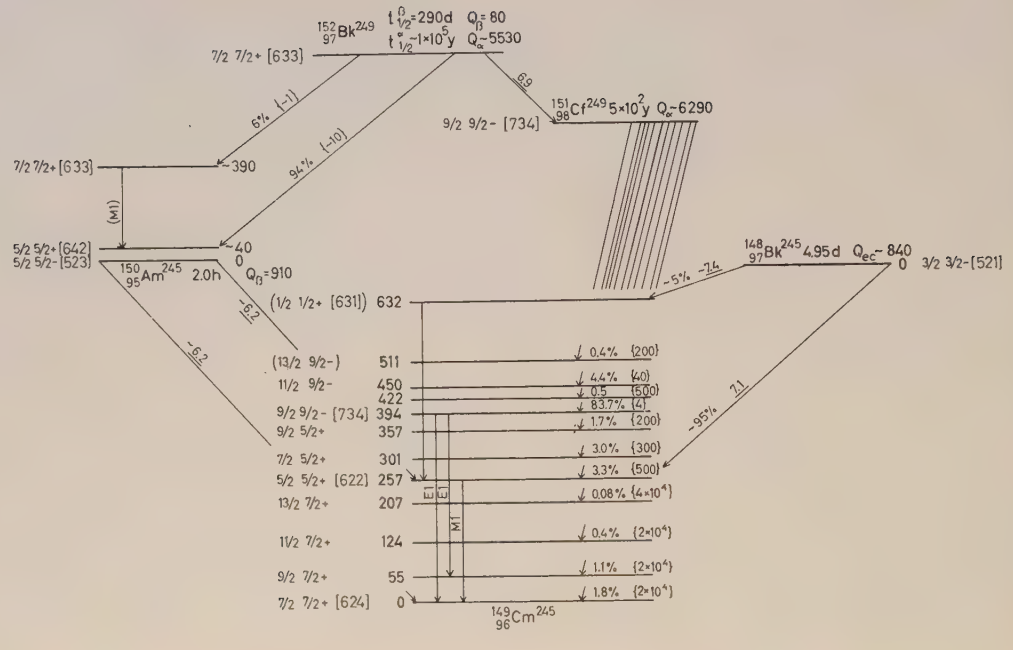

Rotational bands in Cm^{245}

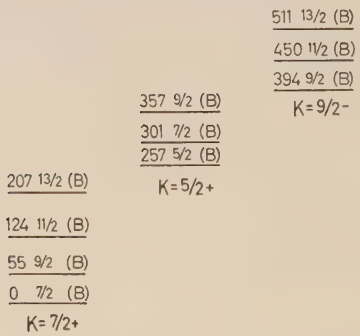

Fig. A = 245.

The level scheme of Cm^{245} populated by alpha decay of Cf^{249} has been given by Stephens, Asaro, Thompson, and Perlman (1957), Bull. Am. Phys. Soc. **II:2**, 394. Supporting evidence on the level scheme is provided by the recent Bk^{245} electron-capture decay studies by A. Chetham-Strode (1956), University of California Radiation Laboratory Report UCRL-3322; cf. also Magnusson, Friedman, Engelkemeir, Fields, and Wagner, (1956), Phys. Rev. **102**, 1097. The beta decay of Am^{245} has been studied by several groups; for references, see SHS. A complex spectrum of gamma rays (not shown) has been observed in this decay scheme by C. I. Brown et al. (1955), J. Inorg. Nucl. Chem. **1**, 254. The data on the alpha decay of Bk^{249} may be found in PR. This nuclide also decays by emission of beta rays to Cf^{249}, Diamond, Magnusson, Mech, Stevens, Friedman, Studier, Fields, and Huizenga (1955), Phys. Rev. **94**, 1083 and Phys. Rev. **96**, 1576.

we shall attempt a classification on the basis of the theoretical spectra of Figs. 5 and 6. In such a situation, many of the assignments must be considered rather tentative.

The $_{96}Cm^{245}$ ground state might be expected to be either [624 7/2] or [734 9/2]. The evidence for a ground-state beta transition from $_{95}Am^{245}$ (assumed to be [523 5/2] as for all the other Am isotopes) suggests that it is the former. This assignment is further supported by the evidence from the Cm^{245} alpha decay; the favoured transition proceeds to a level at 172 keV in $_{94}Pu^{241}$ which then decays by an $M1$ gamma transition to the 5/2+ Pu^{241} ground state (see A = 241).

The Am^{245} beta decay also populates a level in Cm^{245} at 257 keV, which has the same parity as the Cm^{245} ground state; this excited state may tentatively be identified with the orbital [622 5/2].

Since the [624 7/2] orbit occurs as the ground state of Cm^{245}, one might expect the orbital [734 9/2] to occur as a low-lying excited configuration in Cm^{245} and to provide the ground state of $_{98}Cf^{249}$. Indeed, the favoured alpha decay of Cf^{249} populates a state in Cm^{245} which decays by $E1$ transitions to the ground-state rotational band. This level, at 394 keV, is thus identified with the [734 9/2] configuration. The detailed study of the Cf^{249} alpha-decay fine structure has revealed a large number of low-lying states in Cm^{245} which have been tentatively associated with the expected rotational excitations built on the three lowest intrinsic states.

As discussed in connection with the Am^{241} level scheme, the alpha decay of $_{97}Bk^{245}$ is consistent with the assignment [521 3/2] for the Bk^{245} ground state. This assignment is also consistent with the fact that the electron-capture decay of Bk^{245} does not go to the higher spin states, but rather populates the 257 keV 5/2+ state and another excited configuration at 632 keV in Cm^{245}. This latter state might tentatively be classified as [631 1/2]. Such a classification is consistent with the fact that it is observed to decay only to the 257 keV level.

The observed pattern of the alpha decay of Bk^{249} (and probably Bk^{247}) differs considerably from that of Bk^{245} and Bk^{243}. This probably implies that the ground-state configuration of the heavier Bk isotopes is different from that of the lighter ones. This possibility is further suggested by the favoured alpha decay of $_{99}E^{253}$ which appears to populate the ground-state rotational band in Bk^{249}. From the observed energy intervals it appears that the ground-state spin of Bk^{249} (and of E^{253}) is 7/2. Accordingly, we have assigned the orbital [633 7/2] to the Bk^{249} ground state. The favoured alpha decay of Bk^{249} populates a level at about 400 keV in Am^{245} and this level is thus also assigned the configuration [633 7/2].

Finally, a slightly hindered alpha group from Bk^{249} populates a level at $\sim$ 40 keV in Am^{245}. This level is most probably the [642 5/2] configuration which is known from the Np spectra to lie very close to the orbital [523 5/2].

The beta decay from Bk^{249} to the Cf^{249} ground state with log ft = 6.9 further supports the assumed classification of Bk^{249}. This classification assigns the decay a $1u$ character.

A > 245.

Evidence from the spectra of the even-even nuclei indicates that the heaviest known nuclides continue to exhibit the simple rotational spectra characteristic of strongly deformed, axially symmetric systems. This fact can also be understood in terms of the calculation of equilibrium shapes discussed in § IV. One thus expects that, for a considerable distance beyond A = 245, the odd-A nuclei may still be described quite well by means of the coupling scheme employed in the present article and in particular in terms of the single-particle level spectra of Figs. 5 and 6. There is not at the present time sufficient data available to warrant an extension of the analysis into this region.

In this region, there is, however, one very striking experimental fact which seems to fit in well with these theoretical ideas. It has been observed that there is a marked discontinuity in the nuclear binding energies associated with the neutron number $N = 152$ (Ghiorso et al., 1954). Thus, the alpha-decay energy of nuclei with $N = 154$ is unusually great. Further, the spontaneous fission half-lives of the nuclei with $N > 152$ are unusually short and have been interpreted in terms of an especially low binding energy for these isotopes. The data are consistent with the assumption that there is a gap of about 300 keV between the orbital of the 151st and 153rd neutron. This discontinuity in the binding energy is not accompanied by any noticeable discontinuity in the nuclear moment of inertia or in the intensities of the alpha-decay fine structure populating states in a rotational band. These facts can be understood in terms of Fig. 6, according to which there is a considerable energy gap between the filling of the orbitals [624 7/2] and [734 9/2] (filled at $N = 152$) and the orbitals [725 11 2], [613 7 2], and [620 1/2] which are expected to start filling at $N = 153$.

Since the new orbits that come after $N = 152$ have about the same general structure and the same polarizing effect on the nuclear shape (i. e., the same slope in Fig. 6 as a function of δ) as the orbits filled before $N = 152$, one does not expect any great change in the nuclear eccentricity, in the moment of inertia, or in the alpha fine structure intensities.

III. MOMENTS OF INERTIA

The moments of inertia corresponding to the rotational bands in the spectra discussed in § II are found to vary considerably in going from one intrinsic state to another and are also systematically larger than the moments of inertia corresponding to the ground state rotational bands in neighbouring even-even nuclei (cf. Table VI). In this section, we shall attempt an analysis of this effect on the basis of a simplified model in which we treat the last odd nucleon in terms of an independent-particle description, but assume that an appreciable energy is required to excite a pair of nucleons from the even-even core into a state in which they are no longer paired.

The nuclear rotational energy represents the additional kinetic energy which the nucleons must have in order to follow the rotation of the nuclear field. Thus, the moment of inertia, $\Im_a$, for rotation about the intrinsic x-axis and associated with the intrinsic configuration a, may be expressed as (Inglis, 1954; cf. also Bohr and Mottelson, 1955a)

$$\Im_a = 2\hbar^2 \sum_i \frac{|<i|J_x|a>|^2}{E_i - E_a}, \tag{5}$$

where J_x is the x-component of the total intrinsic angular momentum of all the nucleons. The sum in (5) extends over all the intrinsic states i.

If the whole of the intrinsic motion were described in terms of an independent-particle model, the expression (5) would yield the rigid moment of inertia for all intrinsic configurations (Bohr and Mottelson, 1955a). Thus, in this approximation, the calculated moments of inertia are systematically larger than those observed, and there is no significant difference between odd and even nuclei. However, correlations in the intrinsic motion of the type implied by short-range attractive forces tend to reduce the value of $\Im$.

In a rough approximation, we may describe the effect of these forces in terms of a pairing energy. Thus, in the lowest configuration of an even-even nucleus (total $K = 0$), each nucleon in an orbit $+K_p$ is paired with a nucleon with $-K_p$. These two nucleons will interact especially strongly with each other, both because of the similarity of their wave functions and because of the many near-lying pairs of states with total $K = 0$ into which they may scatter. In order to obtain an excited intrinsic state with $K = 1$, as required for the states i in the sum (1), at least one such pair must be broken, and so the excitation energy of the states i will be appreciably greater than would have been estimated from an independent-particle model.

We may thus obtain a very rough estimate[1] of the expression (5) by replacing the matrix elements and energies E_i by values obtained from an independent-particle description, but increasing the value of the denominators by the pairing energy Δ whenever the state i has more unpaired nucleons than the state a. The observed magnitude of the moments of inertia of the even-even nuclei indicate that $\Delta \sim 2$ MeV. In this approximation, the difference in $\Im$ between an even-even nucleus and the next odd-A nucleus is

$$\delta\Im_a = 2\hbar^2 \sum_i \frac{<i|j_x|a>^2}{|\varepsilon_i - \varepsilon_a|} - 4\hbar^2 \sum_{\varepsilon_i < \varepsilon_a} \frac{<i|j_x|a>^2}{\varepsilon_a + \Delta - \varepsilon_i}, \tag{6}$$

where j_x is the x-component of the angular momentum of the last odd nucleon, and the energies ε_i and ε_a are the energies of the intrinsic states i and a of this particle.

[1] This method of estimating the effect of the pairing forces has been considered in connection with the calculations of the total moment of inertia by Bohr and Mottelson (1955a) and by Moszkowski (1956).

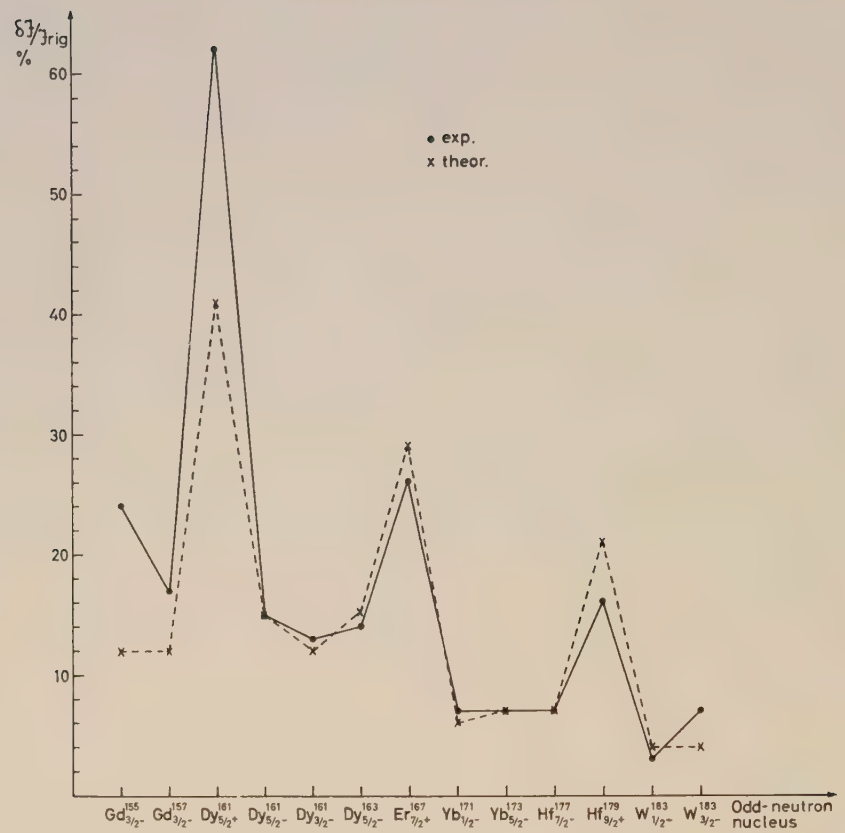

Fig. 7. *Variations in the moments of inertia of odd-N nuclei in the region* $155 \leq A < 183$. The figure is based on the material contained in Table VI:a. The abscissa gives the nuclide together with the K-value and parity which characterize the intrinsic state. The ordinate corresponds to the difference in the moment of inertia of the rotational band in the odd-A nucleus and the moment of the ground state rotational band of the adjacent even-even nucleus. The theoretical values in the figure are calculated from Eq. (6). This figure is reproduced from the article by O. Prior, Ark. f. Fysik (in press), which may also be consulted for similar figures for odd-Z nuclei.

In evaluating (6) we have neglected the contribution of the last term which is usually quite small and therefore probably not significant within the accuracy of the approximation involved in obtaining this expression.

The contribution of the last odd nucleon has been calculated, using the wave functions and classification of the intrinsic states given in § II. The results are compared with the experimental moments in Table VI and in Figs. 7 and 8[1]. It is seen that the simple expression (6) and the one-particle wave functions reproduce quite well the main variations in the moments of inertia. It has already been mentioned

[1] The evaluation of (6) has been performed by Mr. O. Prior, and we wish to thank him for permission to include his results in the present paper. For further details of these calculations, see O. Prior (1958, in press). The expression (6) has also been used by D. Bés (1958) in his discussion of the exceptionally great moment of inertia of the ground-state rotational band of Dy^{161}.

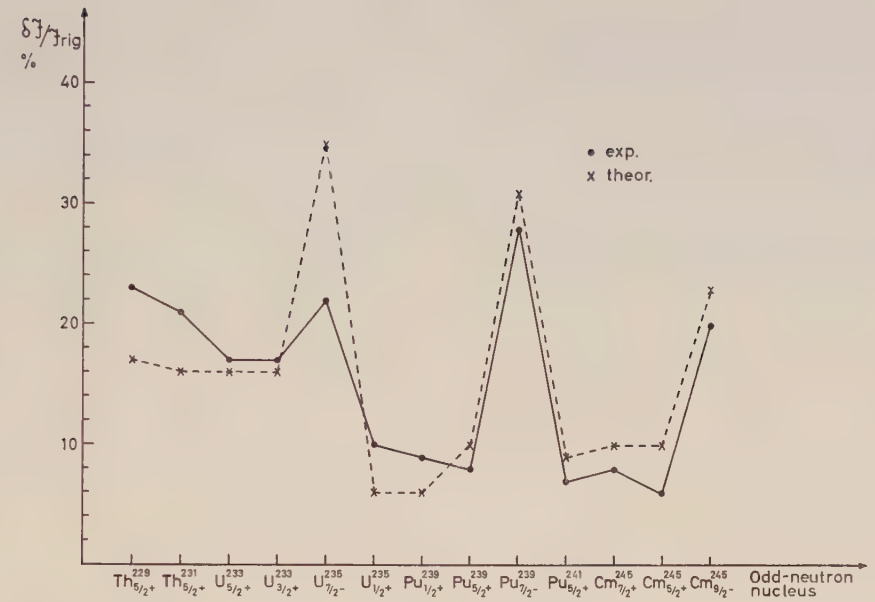

Fig. 8. *Variations in the moments of inertia of odd-N nuclei in the region 229 < A < 245.* See caption to Fig. 7.

several times in § II that the configurations with large intrinsic angular momenta stand out clearly because of the exceptionally large moments of inertia which characterize their rotational bands[1].

IV. CALCULATION OF THE EQUILIBRIUM SHAPE

In the previous section, we have considered the interpretation of a large number of nuclear properties all of which were associated with the state of the last odd particle. In the present section, we shall attempt a discussion of a collective property, the nuclear equilibrium shape, in terms of the independent-particle model. Thus, we obtain an estimate of the total nuclear energy as a function of the deformation δ by summing the one-particle energies of Figs. 2—6. According to this model, the nuclear equilibrium shape should correspond with that value of δ which makes the total energy a minimum, subject to the constraint that the volume contained within the equipotential surfaces is independent of δ (cf. SGN for the details of this calculation).

The most simple calculation of this type corresponds to assuming a definite orbital assignment for each nucleon. The equilibrium deformations calculated in this way for the nuclear ground-state configurations are shown in Fig. 9. The experimental deformations, deduced from the measured intrinsic quadrupole moments by means of (1), are also shown in this figure. It is seen that the theoretical estimates reproduce quite well the observed nuclear distortions. The sharp rise in the distortion at $N = 90$

[1] This effect has been previously noted in Np^{237} by Hollander, Smith, and Rasmussen (1956), Phys. Rev. **102**, 1372.

TABLE VI. *Contribution to the moment of inertia from the last odd particle.* a) odd-N nuclei.

Nucleus	Assigned orbital	Levels in rotational band (keV)	a_{exp}	δ	$\left(\frac{3\hbar^2}{\Im}\right)_{odd}$ (keV)	$\left(\frac{3\hbar^2}{\Im}\right)_{e-e}$ (keV)	$\frac{\delta\Im_{exp}}{\Im_{rig}}$ %	$\frac{\delta\Im_{orb}}{\Im_{rig}}$ %
$^{91}_{64}Gd^{155}$	[521 3/2]	$7/2 \frac{(A)}{} 146$ $5/2 \frac{(A)}{} 60$ $3/2 \frac{(A)}{} 0$	..	0.31	72	123	26 (i)	12
$^{93}_{64}Gd^{157}$	[521 3/2]	$7/2 \frac{(A)}{} 131$ $5/2 \frac{(A)}{} 55$ $3/2 \frac{(A)}{} 0$	..	0.31	66	89	17	12
$^{95}_{66}Dy^{161}$	[642 5/2]	$9/2 \frac{(A)}{} 102$ $7/2 \frac{(A)}{} 44$ $5/2 \frac{(A)}{} 0$	..	0.30	38	87	62	41
$^{95}_{66}Dy^{161}$	[523 5/2]	$9/2 \frac{(C)}{} 203$ $7/2 \frac{(C)}{} 103$ $5/2 \frac{(B)}{} 26$	..	0.30	66	87	15	15
$^{95}_{66}Dy^{161}$	[521 3/2]	$5/2 \frac{(B)}{} 132$ $3/2 \frac{(B)}{} 75$	..	0.30	68	87	13	12
$^{97}_{66}Dy^{163}$	[523 5/2]	$9/2 \frac{(A)}{} 167$ $7/2 \frac{(A)}{} 74$ $5/2 \frac{(A)}{} 0$	..	0.30	63	81	14	15
$^{99}_{68}Er^{167}$	[633 7/2]	$11/2 \frac{(A)}{} 172$ $9/2 \frac{(A)}{} 78$ $7/2 \frac{(A)}{} 0$	..	0.29	52	81	27	29
$^{101}_{70}Yb^{171}$	[521 1/2]	$5/2 \frac{(A)}{} 76$ $3/2 \frac{(A)}{} 67$ $1/2 \frac{(A)}{} 0$	0.87	0.28	73	84	7	6

Column one gives the nuclide, column two the orbital assignment of the intrinsic state characterizing each band, column three the experimentally identified members of the rotational band. Columns six and seven list the experimental values of the inertial parameter, $3\hbar^2/\Im$, characterizing the rotational band on each intrinsic state and the same parameter for the neighbouring even-even nucleus of mass A-1. Column eight exhibits the observed contribution of the last odd particle to the moment of inertia; this quantity is obtained from the difference of columns six and seven, and is expressed in units of the rigid moment of inertia (see ABH). This value, $\frac{\delta\Im_{exp}}{\Im_{rig}}$, is to be compared with the values $\frac{\delta\Im_{orb}}{\Im_{rig}}$ calculated from the wave functions of the present model and listed in column nine.

TABLE VI (continued).

Nucleus	Assigned orbital	Levels in rotational band (keV)	a_{exp}	δ	$\left(\frac{3h^2}{\Im}\right)_{odd}$ (keV)	$\left(\frac{3h^2}{\Im}\right)_{e-e}$ (keV)	$\frac{\delta\Im_{exp}}{\Im_{rig}}$ %	$\frac{\delta\Im_{orb}}{\Im_{rig}}$ %
$^{103}_{70}Yb^{173}$	[512 5/2]	$9/2\frac{(A)}{}180$ $7/2\frac{(A)}{}79$ $5/2\frac{(A)}{}0$	..	0.28	68	79	7	7
$^{105}_{72}Hf^{177}$	[514 7/2]	$11/2\frac{(A)}{}250$ $9/2\frac{(A)}{}113$ $7/2\frac{(A)}{}0$	..	0.27	75	88	7	7
$^{107}_{72}Hf^{179}$	[624 9/2]	$13/2\frac{(A)}{}262$ $11/2\frac{(A)}{}121$ $9/2\frac{(A)}{}0$	..	0.26	66	93	16	21
$^{109}_{74}W^{183}$	[510 1/2]	$7/2\frac{(A)}{}207$ $5/2\frac{(A)}{}99.1$ $3/2\frac{(A)}{}46.5$ $1/2\frac{(A)}{}0$	0.19	0.21	78.1 (95.1)	100	10 (3) (ii)	7 (4)
$^{109}_{74}W^{183}$	[512 3/2]	$7/2\frac{(A)}{}412.1$ $5/2\frac{(A)}{}291.7$ $3/2\frac{(A)}{}208.8$	..	0.21	99.5 (84.3)	100	0 (7) (ii)	8 (4)
$^{139}_{90}Th^{229}$	[633 5/2]	$9/2\frac{(B)}{}99$ $7/2\frac{(B)}{}43$ $5/2\frac{(B)}{}0$	..	0.22	37	58	23 (i)	17
$^{141}_{90}Th^{231}$	[633 5/2]	$7/2\frac{(B)}{}42$ $5/2\frac{(B)}{}0$	..	0.23	36	53	21 (i)	16
$^{141}_{92}U^{233}$	[633 5/2]	$9/2\frac{(A)}{}92$ $7/2\frac{(A)}{}40$ $5/2\frac{(A)}{}0$	..	0.24	34	47	17	16
$^{141}_{92}U^{233}$	[631 3/2]	$5/2\frac{(B)}{}342$ $3/2\frac{(B)}{}313$	..	0.24	35	47	17	16

TABLE VI (continued).

Nucleus	Assigned orbital	Levels in rotational band (keV)	a_{exp}	δ	$\left(\frac{3\hbar^2}{\Im}\right)_{odd}$ (keV)	$\left(\frac{3\hbar^2}{\Im}\right)_{e-e}$ (keV)	$\frac{\delta\Im_{exp}}{\Im_{rig}}$ %	$\frac{\delta\Im_{orb}}{\Im_{rig}}$ %
$^{143}_{92}U^{235}$	[743 7/2]	$11/2 \overset{(A)}{\text{---}} 103$ $9/2 \overset{(A)}{\text{---}} 46$ $7/2 \overset{(A)}{\text{---}} 0$	..	0.24	31	43	21	35
$^{143}_{92}U^{235}$	[631 1/2]	$7/2 \overset{(B)}{\text{---}} 84$ $5/2 \overset{(A)}{\text{---}} 52$ $3/2 \overset{(A)}{\text{---}} 14$ $1/2 \overset{(A)}{\text{---}} 0.08$	..	0.24	37	43	9	6
$^{145}_{94}Pu^{239}$	[631 1/2]	$7/2 \overset{(A)}{\text{---}} 76$ $5/2 \overset{(A)}{\text{---}} 57$ $3/2 \overset{(A)}{\text{---}} 8$ $1/2 \overset{(A)}{\text{---}} 0$	..	0.26	37	44	9	6
$^{145}_{94}Pu^{239}$	[622 5/2]	$9/2 \overset{(B)}{\text{---}} 388$ $7/2 \overset{(A)}{\text{---}} 331$ $5/2 \overset{(A)}{\text{---}} 286$	..	0.26	39	44	8	10
$^{145}_{94}Pu^{239}$	[743 7/2]	$11/2 \overset{(B)}{\text{---}} 483$ $9/2 \overset{(B)}{\text{---}} 434$ $7/2 \overset{(B)}{\text{---}} 392$	..	0.26	28	44	28	31
$^{147}_{94}Pu^{241}$	[622 5/2]	$7/2 \overset{(C)}{\text{---}} 44$ $5/2 \overset{(A)}{\text{---}} 0$		0.27	38	43	7	9
$^{149}_{96}Cm^{245}$	[624 7/2]	$11/2 \overset{(B)}{\text{---}} 124$ $9/2 \overset{(B)}{\text{---}} 55$ $7/2 \overset{(B)}{\text{---}} 0$	..	0.26	37	43	8	10
$^{149}_{96}Cm^{245}$	[622 5/2]	$9/2 \overset{(B)}{\text{---}} 357$ $7/2 \overset{(B)}{\text{---}} 301$ $5/2 \overset{(B)}{\text{---}} 257$	..	0.26	38	43	6	10
$^{149}_{6}Cm^{245}$	[734 9/2]	$13/2 \overset{(B)}{\text{---}} 511$ $11/2 \overset{(B)}{\text{---}} 450$ $9/2 \overset{(B)}{\text{---}} 394$	..	0.26	31	43	19	23

b) odd-Z nuclei.

Nucleus	Assigned orbital	Levels in rotational band (keV)	a_{exp}	δ	$\left(\frac{3\hbar^2}{\Im}\right)_{odd}$ (keV)	$\left(\frac{3\hbar^2}{\Im}\right)_{e-e}$ (keV)	$\frac{\delta\Im_{exp}}{\Im_{rig}}$ %	$\frac{\delta\Im_{orb}}{\Im_{rig}}$ %
$^{90}_{63}Eu^{153}$	[413 5/2]	$9/2 \xrightarrow{(A)} 190$ $7/2 \xrightarrow{(A)} 83$ $5/2 \xrightarrow{(A)} 0$		0.30	71	122	26 (i)	8
$^{90}_{63}Eu^{153}$	[411 3/2]	$5/2 \xrightarrow{(B)} 172$ $3/2 \xrightarrow{(A)} 103$	..	0.30	83	122	18 (i)	8
$^{92}_{65}Tb^{157}$	[411 3/2]	$7/2 \xrightarrow{(C)} 144$ $5/2 \xrightarrow{(C)} 61$ $3/2 \xrightarrow{(B)} 0$	..	0.31	73	89	11	7
$^{95}_{65}Tb^{159}$	[411 3/2]	$7/2 \xrightarrow{(A)} 138$ $5/2 \xrightarrow{(A)} 58$ $3/2 \xrightarrow{(A)} 0$	..	0.31	70	79	8	8
$^{96}_{65}Tb^{161}$	[411 3/2]	$5/2 \xrightarrow{(B)} 57$ $3/2 \xrightarrow{(B)} 0$	..	0.31	68	76	6	7
$^{98}_{67}Ho^{165}$	[523 7/2]	$11/2 \xrightarrow{(A)} 212$ $9/2 \xrightarrow{(A)} 95$ $7/2 \xrightarrow{(A)} 0$	..	0.30	63	73	8	17
$^{100}_{69}Tm^{169}$	[411 1/2]	$7/2 \xrightarrow{(A)} 139.0$ $5/2 \xrightarrow{(A)} 118.2$ $3/2 \xrightarrow{(A)} 8.4$ $1/2 \xrightarrow{(A)} 0$	−0.76	0.28	74	80	4	3
$^{100}_{69}Tm^{169}$	[523 7/2]	$9/2 \xrightarrow{(B)} 473$ $7/2 \xrightarrow{(B)} 379$	..	0.28	63	80	13	18
$^{102}_{69}Tm^{171}$	[411 1/2]	$7/2 \xrightarrow{(A)} 129.1$ $5/2 \xrightarrow{(A)} 116.7$ $3/2 \xrightarrow{(A)} 5.1$ $1/2 \xrightarrow{(A)} 0$	−0.86	0.28	72	80	5	3
$^{102}_{69}Tm^{171}$	[411 3/2]	$5/2 \xrightarrow{(C)} 744$ $3/2 \xrightarrow{(C)} 688$	..	0.28	67	80	9	7

TABLE VI (continued).

Nucleus	Assigned orbital	Levels in rotational band (keV)	a_{exp}	δ	$\left(\frac{3\hbar^2}{\Im}\right)_{odd}$ (keV)	$\left(\frac{3\hbar^2}{\Im}\right)_{e-e}$ (keV)	$\frac{\delta\Im_{exp}}{\Im_{rig}}$ %	$\frac{\delta\Im_{orb}}{\Im_{rig}}$ %
$^{104}_{17}Lu^{175}$	[404 7/2]	$11/2 \overset{(A)}{\text{——}} 251$ $9/2 \overset{(A)}{\text{——}} 114$ $7/2 \overset{(A)}{\text{——}} 0$	..	0.28	76	77	0	3
$^{104}_{71}Lu^{175}$	[402 5/2]	$7/2 \overset{(A)}{\text{——}} 433$ $5/2 \overset{(A)}{\text{——}} 343$	..	0.28	77	77	0	2
$^{106}_{71}Lu^{177}$	[404 7/2]	$9/2 \overset{(A)}{\text{——}} 119$ $7/2 \overset{(A)}{\text{——}} 0$	..	0.26	79	78	−1	3
$^{108}_{73}Ta^{181}$	[404 7/2]	$11/2 \overset{(A)}{\text{——}} 301$ $9/2 \overset{(A)}{\text{——}} 136$ $7/2 \overset{(A)}{\text{——}} 0$	..	0.23	91	93	1	3
$^{108}_{75}Re^{183}$	[402 5/2]	$9/2 \overset{(B)}{\text{——}} 260$ $7/2 \overset{(B)}{\text{——}} 114$ $5/2 \overset{(B)}{\text{——}} 0$	..	0.21	98	100	1	3
$^{108}_{75}Re^{183}$	[514 9/2]	$11/2 \overset{(C)}{\text{——}} 664$ $9/2 \overset{(C)}{\text{——}} 496$	..	0.21	92	100	3	13
$^{110}_{75}Re^{185}$	[402 5/2]	$9/2 \overset{(A)}{\text{——}} 286$ $7/2 \overset{(A)}{\text{——}} 125$ $5/2 \overset{(A)}{\text{——}} 0$	..	0.19	107	112	1	2
$^{112}_{75}Re^{187}$	[402 5/2]	$9/2 \overset{(A)}{\text{——}} 300$ $7/2 \overset{(A)}{\text{——}} 134$ $5/2 \overset{(A)}{\text{——}} 0$	..	0.19	115	124	2	2
$^{12}_{13}Al^{25}$	[202 5/2]	$9/2 \overset{(B)}{\text{——}} 3440$ $7/2 \overset{(B)}{\text{——}} 1610$ $5/2 \overset{(A)}{\text{——}} 0$	..	0.35	1380	1380	0 (i)	15
$^{12}_{13}Al^{25}$	[211 1/2]	$5/2 \overset{(A)}{\text{——}} 1810$ $3/2 \overset{(A)}{\text{——}} 950$ $1/2 \overset{(A)}{\text{——}} 450$	..	0.41	1020	1380	23 (i)	24

TABLE VI (continued).

Nucleus	Assigned orbital	Levels in rotational band (keV)	a_{exp}	δ	$\left(\frac{3\hbar^2}{\Im}\right)_{odd}$ (keV)	$\left(\frac{3\hbar^2}{\Im}\right)_{e-e}$ (keV)	$\frac{\delta\Im_{exp}}{\Im_{rig}}$ %	$\frac{\delta\Im_{orb}}{\Im_{rig}}$ %
$^{12}_{13}Al^{25}$	[200 1/2]	$5/2\overset{(A)}{—}3880$ $3/2\overset{(A)}{—}2700$ $1/2\overset{(A)}{—}2500$	−0.02	0.37	910	1380	34 (i)	17
$^{12}_{13}Al^{25}$	[330 1/2]	$1/2\overset{(A)}{—}3850$ $7/2\overset{(A)}{—}3720$ $3/2\overset{(A)}{—}3090$	−0.56	0.55	680	1380	63 (i)	39
$^{12}_{13}Al^{25}$	[211 3/2]	$5/2\overset{(A)}{—}4600$ $3/2\overset{(A)}{—}4220$	−3.2	0.39	460	1380	130 (i)	47
$^{142}_{91}Pa^{233}$	[530 1/2]	$5/2\overset{(B)}{—}69$ $7/2\overset{(B)}{—}56$ $1/2\overset{(C)}{—}7$ $3/2\overset{(B)}{—}0$	−1.31	0.24	36	52	20 (i)	5
$^{142}_{91}Pa^{233}$	[642 5/2]	$7/2\overset{(B)}{—}103$ $5/2\overset{(A)}{—}86$	..	0.24	15	52	112 (i)	35
$^{144}_{93}Np^{237}$	[642 5/2]	$9/2\overset{(A)}{—}76$ $7/2\overset{(A)}{—}33$ $5/2\overset{(A)}{—}0$	..	0.25	28	45	29	32
$^{144}_{93}Np^{237}$	[523 5/2]	$9/2\overset{(A)}{—}160$ $7/2\overset{(A)}{—}103$ $5/2\overset{(A)}{—}60$	..	0.25	37	45	11	9
$^{146}_{93}Np^{239}$	[642 5/2]	$7/2\overset{(B)}{—}31$ $5/2\overset{(A)}{—}0$	..	0.26	27	45	33	29
$^{146}_{93}Np^{239}$	[523 5/2]	$9/2\overset{(B)}{—}173$ $7/2\overset{(B)}{—}117$ $5/2\overset{(A)}{—}74$	..	0.26	37	45	10	8
$^{146}_{95}Am^{241}$	[523 5/2]	$7/2\overset{(B)}{—}42$ $5/2\overset{(A)}{—}0$	..	0.27	36	43	10	8

TABLE VI (continued).

Nucleus	Assigned orbital	Levels in rotational band (keV)	a_{exp}	δ	$\left(\frac{3\hbar^2}{\Im}\right)_{odd}$ (keV)	$\left(\frac{3\hbar^2}{\Im}\right)_{e-e}$ (keV)	$\frac{\delta\Im_{exp}}{\Im_{rig}}$ %	$\frac{\delta\Im_{orb}}{\Im_{rig}}$ %
$^{148}_{95}Am^{243}$	[523 5/2]	$7/2\frac{(C)}{}126$ $5/2\frac{(B)}{}84$	..	0.27	36	45	11	8

(i) The estimate of the contribution of the last odd particle to the observed moment of inertia is somewhat obscured by the rapid variation of the deformation and moment of inertia observed for the even-even isotopes in this region of elements.

(ii) The values in parenthesis indicate that the effect of the Coriolis couplings to the especially close-lying states have been subtracted both from the observed and the calculated moments (see A. KERMAN, 1955).

is found to reflect a rather unusual situation in which the closed shell at $N = 82$ is partially broken as a result of the deformation (cf. the discussion in § II, A = 153, and in MN). In the heavy element region, the calculations have been carried to A = 243. Beyond this point, it is expected that the distortion will gradually decrease with increasing A.

Calculations have also been made in the light-element region around A = 25

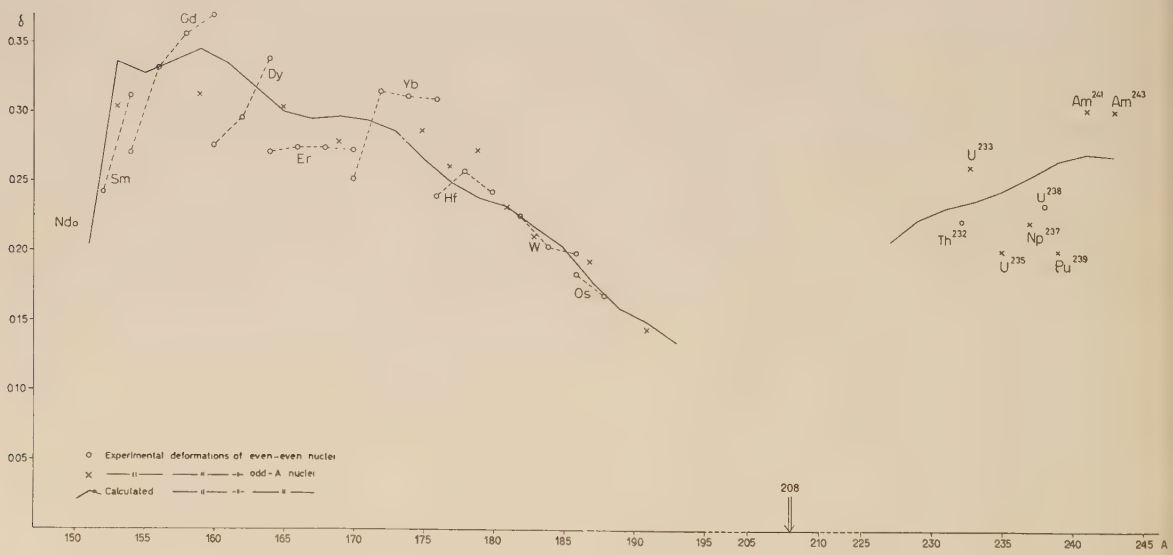

Fig. 9. *Nuclear deformations.* The solid line represents calculated values of the equilibrium deformation for odd-A nuclides along the valley of beta stability. The experimental data corresponds to δ-values obtained by means of Eq. (1) from measured Q_0 values. These latter are based on observed $E2$ transition probabilities and their experimental uncertainty is usually of the order 10–20 %. Values of δ corresponding to odd-A nuclides are denoted by crosses. Even-even nuclei, denoted by circles, are included for completeness. Most of the experimental data can be found in ABH. In the heavy element region, we have included the more recent Q_0 determinations by J. O. NEWTON (1957a, 1957b, and private communication; cf. also SHS). The deformations of the Am isotopes are obtained from the hfs measurements of MANNING, FRED, and TOMKINS (1956), Phys. Rev. **102**, 1108.

(cf. Fig. 10 for the A = 25 calculations; see also RAKAVY, 1957, for estimates of δ in this region). It is found that the deformations in the light-element region are greater than in the region $150 < A < 190$ and that the latter deformations are larger than those estimated for the region $A > 220$. This decrease in δ with in creasing A reflects the fact that, in the present model, the deformations are fundamentally of order $A^{-1/3}$.

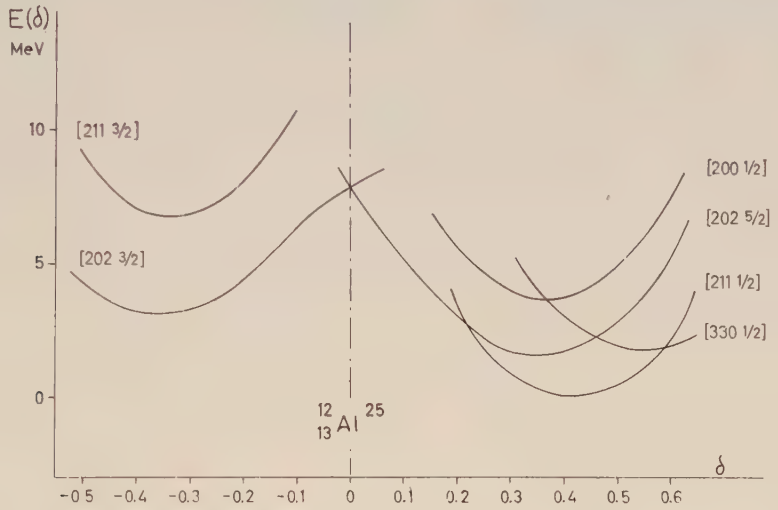

Fig. 10. *Equilibrium calculations corresponding to a number of intrinsic configurations in* Al^{25}. The total energy is plotted as a function of δ based on the sequence of single-particle orbitals according to Fig. 2. The choices of configurations for which $E(\delta)$ is plotted for prolate δ-values correspond to leaving the four neutrons and four protons outside of closed shells in the configuration $[220\ 1/2]^2\ [211\ 3/2]^2$ and placing the fifth proton successively in the orbitals indicated in the figure. These are of course only a few of the possible configurations. For instance, the "hole"-state proton configuration $[220\ 1/2]^2\ [211\ 3/2]^1\ [211\ 1/2]^2$ is thus not considered in this figure.

For a number of nuclei, more detailed calculations have been made, including the possibility of changing the intrinsic configuration with changing δ. Such calculations make it possible to explore the dependence of the nuclear energy on deformation over a larger range of deformations and in particular to compare the energy for prolate and oblate deformations.

The results of some of these calculations are shown in Figs. 10—12. It is found that, in the region around A = 25 as well as $150 < A < 190$ and $A > 230$, the prolate deformations give rise to states of lower energy than do oblate distortions. This is in agreement with the observed positive quadrupole moments reported in all these regions. (The one possible exception to this rule is provided by the reported negative quadrupole moment of Ac^{227}, which is discussed on page 51.) Fig. 11 indicates that the prolate shape is favoured by almost 6 MeV in the region of Tm^{169}. With increasing A this preference for the prolate shape is found to decrease gradually until, in the neighbourhood of Au^{197}, it is found that the calculated prolate and oblate equilibrium distortions have about the same energy. Fig. 12 indicates that, according to the present calculations, the prolate deformation should be favoured by about 2 MeV in the neigh-

bourhood of Ac^{227}. With increasing A beyond Ac the preference for prolate shape increases.

Fig. 12 also illustrates the possibility of two near-lying minima corresponding to two rather different equilibrium shapes. An effect similar to this is also found in the region around Eu, and the shift from one to the other of these two minima in

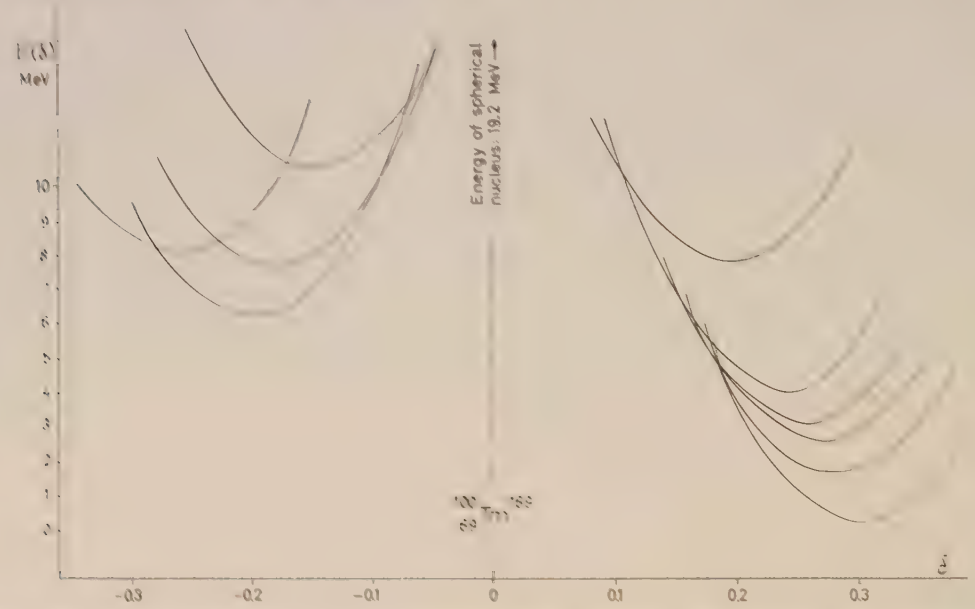

Fig. 11. *Equilibrium calculations for Tm^{169} including different intrinsic configurations.* The calculations indicate a great preference for prolate deformations.

going from Eu^{151} to Eu^{153} leads to a quadrupole moment of the latter about twice as big as that of the former of these isotopes.

Finally, we mention a number of more detailed considerations involved in estimating equilibrium shapes from the present model.

1. In summing the energies of the single-particle orbitals, the kinetic energies may simply be added, while the situation is more complicated for the potential energies. Thus, if the potential energy is assumed to be due to two-body forces, one should take only half the sum of the single-particle potential energies [cf. (SGN)]. This complication is, however, of no importance for the pure harmonic oscillator potential for which $< T_i > = < V_i >$. The total energy then equals a fraction (in the case of two body forces 3/4) of the sum of all the single-particle energies. To the extent that the potential deviates from the pure oscillator, e. g., by the added $\bar{l}\cdot\bar{s}$ and $\bar{l}^2$ terms, one may expect some correction terms in the total energy [cf. Eq. (C.3) of (SGN)]. As, however, the $\bar{l}\cdot\bar{s}$ and $\bar{l}^2$ terms show only a slight δ-dependence at moderately large deformations, the equilibrium deformation corresponding to a given configuration is not significantly affected by these correction terms.

The correction terms might, however, be important for the envelope of the deformation curves. In other words, the ordering between configurations might be changed, such that in the choice between two orbitals α and β, of which β corresponded to a higher single-particle energy, the total energy might still be lower for the con-

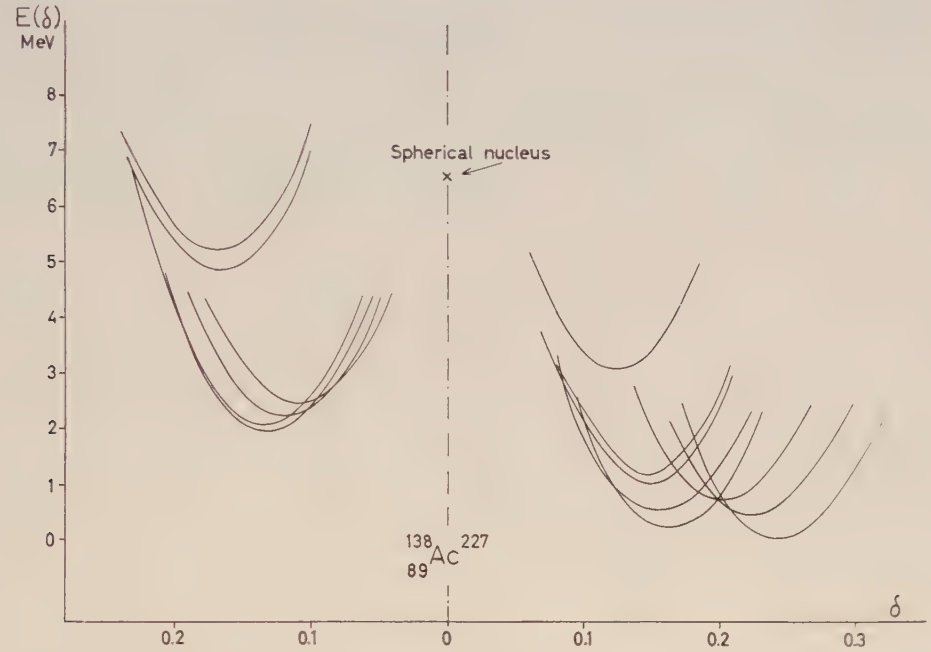

Fig. 12. *Equilibrium calculations for* Ac^{227} *including different available intrinsic configurations.* The preference for prolate deformations amounts here to a relative energy gain of ~ 2 MeV. Another interesting feature is the close competition between two groups of configurations with minima for rather different prolate deformations. These groups correspond alternatively to the i 13/2 shell being completely filled or partially broken.

figuration β instead of α. This would be the case if a very large fraction of E_β were potential energy (in contrast to the case α).

Such a reordering of levels is, however, probably largely taken into account by the fact that the parameters of the potential are determined so as to give the empirical level ordering in actual nuclei (or empirical ground-state configurations of a series of nuclei).

2. The assumption of constant volume within the equipotential surfaces is intended to reflect approximately the incompressibility of nuclear matter. It is, none the less, the most arbitrary element in the present calculations. For a pure harmonic oscillator potential, the equilibrium distortion determined by this condition is also the distortion which makes the eccentricity of the potential and the mass distribution the same, i. e., it is the shape that must be chosen to get a self-consistent field, assuming the nuclear forces to have very short range.

3. The Coulomb energy does not greatly affect the position of the energy minimum

of a particular configuration. The "envelope" curve, giving the ordering of the minima of different configurations, might be more seriously affected. However, the effect of this additional interaction between the protons is probably to some extent taken into account by the choice of a larger μ in calculating the proton orbitals (see the captions to Figs. 2—6).

4. The residual interactions have been entirely neglected in these calculations which assume completely independent particle motion. These interactions are known to mix paired configurations which lie within an energy interval of about 1 MeV of the last filled orbital. At small deformations, this effect is very important and leads eventually to the preference for spherical shape characteristic of configurations in the neighbourhood of closed shells. However, for large deformations, such as those ob-

TABLE VII. *Magnetic moments.* a) *Odd-Z nuclei.*

Nucleus	Energy of isomeric state	I_{exp}	Assigned orbital	Assumed δ	μ_{theo}	μ_{exp}	Ref.
$^{10}_{9}F^{19}$	..	1/2	[220 1/2]	~ 0.4	2.7	2.63	SHS
$^{10}_{9}F^{19}$	197	5/2	[220 1/2]	~ 0.4	3.7	3.5	(a)
$^{12}_{11}Na^{23}$	..	3/2	[211 3/2]	~ 0.5	2.4	2.22	SHS
$^{14}_{13}Al^{27}$	..	5/2	[202 5/2]	~ 0.3	3.7	3.64	SHS
$^{88}_{63}Eu^{151}$	..	5/2	[532 5/2]	0.16	3.1	3.4	SHS
$^{90}_{63}Eu^{153}$	..	5/2	[413 5/2]	0.30	0.9	1.5	SHS
$^{94}_{65}Tb^{159}$	..	3/2	[411 3/2]	0.31	2.2	± 1.5	SHS
$^{98}_{67}Ho^{165}$	..	7/2	[523 7/2]	0.30	4.5	± 3.3	SHS
$^{100}_{69}Tm^{169}$	..	1/2	[411 1/2]	0.29	-0.2	-0.21	SHS
$^{104}_{71}Lu^{175}$	..	7/2	[404 7/2]	0.28	1.4	2.0	(b)
$^{108}_{73}Ta^{181}$	..	7/2	[404 7/2]	0.23	1.5	2.1	SHS
$^{108}_{73}Ta^{181}$	482	5/2	[402 5/2]	0.23	3.7	3.3	(c)
$^{110}_{75}Re^{185}$	..	5/2	[402 5/2]	0.19	3.7	3.14	SHS
$^{112}_{75}Re^{187}$	..	5/2	[402 5/2]	0.19	3.7	3.18	SHS
$^{114}_{77}Ir^{191}$	..	3/2	[402 3/2]	0.14	0.0	0.2	SHS
$^{116}_{77}Ir^{193}$	..	3/2	[402 3/2]	0.12	0.0	0.2	SHS
$^{138}_{89}Ac^{227}$	..	3/2	[530 1/2]	~ 0.2	2.9	1.1	SHS
$^{144}_{93}Np^{237}$	..	5/2	[642 5/2]	0.25	3.0	$\pm 6 \pm 2.5$	SHS
$^{144}_{93}Np^{237}$	60	5/2	[523 5/2]	0.25	1.0	~ 1.4	(d)
$^{146}_{95}Am^{241}$	..	5/2	[523 5/2]	0.27	1.0	1.4	SHS
$^{148}_{95}Am^{243}$	..	5/2	[523 5/2]	0.27	1.0	1.4	SHS

The table lists the odd-A nuclei in the regions of elements which exhibit deformations and for which there exist measured magnetic moments. The first section, a), corresponds to odd-proton nuclei. The first two columns in this table identify the nuclide (and the excitation energy in the case of isomeric states) for which there exists a measurement. Column four gives the state assignment in terms of the quantum numbers $[Nn_z \Lambda K]$. Column five lists the assumed values of the distortion parameter δ, cf. Fig. 9. In the region near A = 25, we have relied mainly on theoretical equilibrium calculations. The calculated and experimental values of the magnetic moments are compared in columns six and seven.

b) *Odd-N nuclei.*

Nucleus	Energy of isomeric state	I_{exp}	Assigned orbital	Assumed δ	μ_{theo}	μ_{exp}	Ref.
$^{11}_{10}Ne^{21}$	..	3/2	[211 3/2]	~ 0.5	-0.8	-0.66	SHS
$^{13}_{12}Mg^{25}$	..	5/2	[202 5/2]	~ 0.4	-1.1	-0.86	SHS
$^{91}_{64}Gd^{155}$	..	3/2	[521 3/2]	0.31	-0.5	-0.30	SHS
$^{93}_{64}Gd^{157}$	..	3/2	[521 3/2]	0.31	-0.5	-0.37	SHS
$^{95}_{66}Dy^{161}$	..	5/2	[642 5/2]	0.31	-0.6	-0.37	(i)
$^{97}_{66}Dy^{163}$	..	5/2	[523 5/2]	0.30	1.1	0.51	(i)
$^{99}_{68}Er^{167}$	..	7/2	[633 7/2]	0.29	-0.8	± 0.5	SHS
$^{101}_{70}Yb^{171}$	..	1/2	[521 1/2]	0.28	0.7	0.46	SHS
$^{103}_{70}Yb^{173}$	..	5/2	[512 5/2]	0.28	-0.8	-0.65	SHS
$^{105}_{70}Yb^{175}$	..	..	[514 7/2]	0.28	1.4	~ 0.15	(e)
$^{105}_{72}Hf^{177}$	..	7/2	[514 7/2]	0.27	1.4	0.6	SHS
$^{107}_{72}Hf^{179}$	..	9/2	[624 9/2]	0.26	-1.0	-0.47	SHS
$^{109}_{74}W^{183}$	..	1/2	[510 1/2]	0.21	0.8	0.12	SHS
$^{111}_{76}Os^{187}$	..	1/2	[510 1/2]	0.18	0.8	0.12	SHS
$^{113}_{76}Os^{189}$	..	3/2	[512 3/2]	0.15	0.9	0.65	SHS
$^{141}_{92}U^{233}$	..	5/2	[633 5/2]	0.23	0.7	0.51	SHS
$^{143}_{92}U^{235}$	..	7/2	[743 7/2]	0.24	-0.6	-0.34	SHS, (f)
$^{145}_{94}Pu^{239}$	..	1/2	[631 1/2]	0.26	-0.1	± 0.02	(g)
$^{147}_{94}Pu^{241}$	..	5/2	[622 5/2]	0.27	-0.5	± 0.1	(h)

(SHS) Strominger, Hollander, and Seaborg (1958).

(a) Lehmann, Leveque, Fiehrer, and Pick (1956), J. Phys. Rad. **17**, 560; W. R. Phillips and G. A. Jones (1956), Phil. Mag. **1**, 576; P. B. Treacy (1955), Nature **176**, 923.

(b) A. Steudel (1957), Naturw. **44**, 371.

(c) Debrunner, Heer, Kündig, and Rüetschi (1957), Helv. Phys. Acta **29**, 463.

(d) Krohn, Novey, and Raboy, as reported in Nucl. Data Cards.

(e) Grace, Johnson, Scurlock, and Taylor (1957), Phil. Mag. **2**, 1079. This experimental magnetic moment disagrees quite badly with the value calculated for this orbital and also with the value observed for the same orbital occurring as the ground state in Hf^{177}. If this value is indeed confirmed it will constitute a rather serious discrepancy with the predictions of the present model.

(f) K. L. Sluis and J. R. McNally (1955), Journ. Opt. Soc. Am. **45**, 56.

(g) Hubbs, Marrus, Nierenberg, and Worcester (1958), Phys. Rev. **109**, 390.

(h) The Pu^{241} moment is calculated from the ratio

$$\left|\frac{\mu(Pu^{241})}{\mu(Pu^{239})}\right|$$

measured by Bleaney, Llewellyn, Pryce, and Hall (1954), Phil. Mag. **45**, 991, and from the Pu^{239} moment given in (g).

(i) J. G. Park (1958), Proc. Roy. Soc. **245**, 118 (*added in proof*).

served in the regions covered by Fig. 9, the calculated equilibrium is usually not sensitive to a mixing of orbitals that lie within a region of 1 MeV, and thus the residual interactions are not important for these calculations. This situation is thus quite different from that in the calculation of the moments of inertia of even-even-nuclei which are changed by more than a factor of two as a result of the residual interactions (cf. § III).

V. CONCLUSION

In the present paper, we have attempted to classify the observed spectra of the odd-A nuclei in those regions of elements where it is known that the nuclear equilibrium shape deviates essentially from spherical symmetry. The spectra consist of a sequence of intrinsic states with each of which is associated a rotational band. The interpretation of the intrinsic excitations is based on a very simple one-particle description, in which each intrinsic state is associated with one of the orbitals of the last odd nucleon assumed to move independently in an average nuclear field. It is an important feature of the independent-particle motion in these nuclei that the binding field deviates considerably from spherical symmetry.

The main results of the classification are presented in § II which treats systematically the available data on the nuclear spectra in the regions of interest. It is found that the one-particle model is able to give correctly the sequence of K and parity values observed for the intrinsic excitations. The interpretation of the intrinsic states, as corresponding approximately to simple one-particle excitations, is further supported by a comparison of the moments and transition probabilities for these states with the values calculated from the one-particle wave functions. The moments of inertia and quadrupole moments are discussed in §§ III and IV. In the present paragraph,

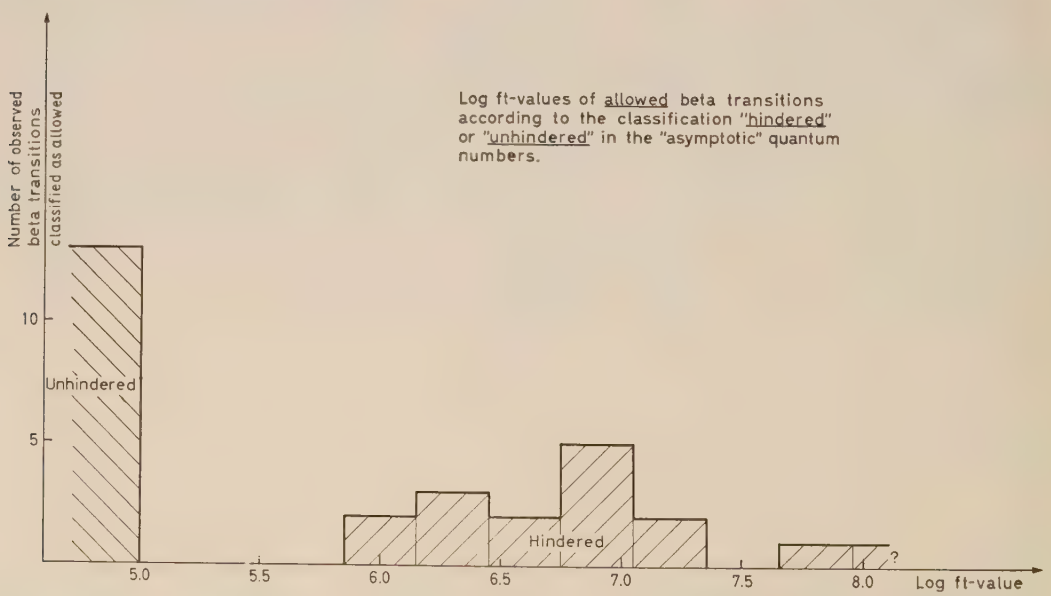

Fig. 13. *Histogram of allowed beta decay ft-values.* The figure is based upon the material collected in Table IX a. One sees that the transitions separate clearly into two groups; those transitions which, according to the classifications of § II, are classified as allowed and unhindered are found to have log $ft \lesssim 5$, while those that are hindered according to this classification have ft-values that are larger by a factor ranging from about 10 to 100.

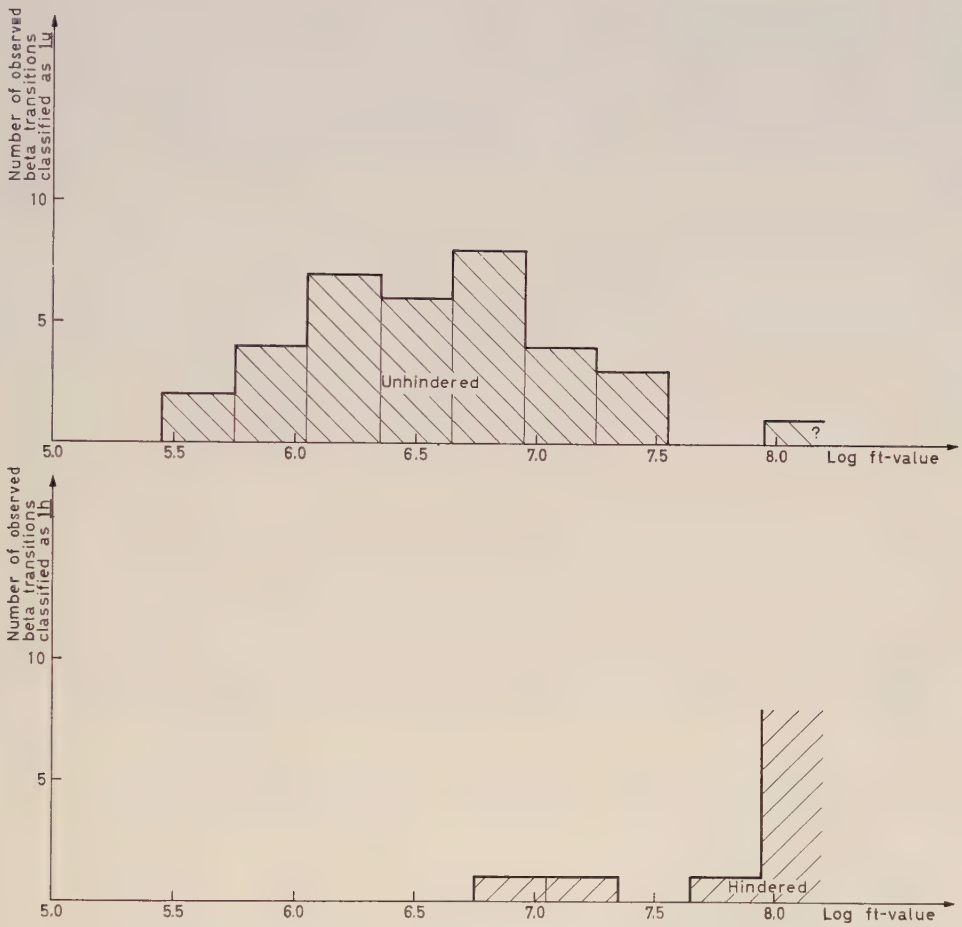

Fig. 14. *Histogram of first forbidden beta decay ft-values.* The figure is based upon the material collected in Table IX:b and plots only those transitions that correspond to $\Delta I = 0$ or 1. One sees that the transitions which, according to § II, are classified as first forbidden and unhindered have log *ft*-values ranging from about 5.5 to 7.5. Only a few transitions have been observed which are classified as first forbidden hindered. The experimental failure to observe these transitions is in agreement with the theoretical expectation that their log *ft*-values should be of the order of, or greater than, ~ 7.5, which often implies intensities too low for detection. Of those first forbidden hindered transitions which are observed two are found to have log $ft \sim 7$. Both these transitions occur in the decay scheme for $A = 153$; one could perhaps attribute this partial breakdown of the asymptotic selection rules to the fact that these nuclei are just on the edge of the region where the present coupling scheme applies.

we give in Tables VII—X and Figs. 13–17 a summary of the comparison of the predictions of the model with data available on magnetic moments, rotational decoupling factors, and beta and gamma transition rates. It is seen that the selection rules implied by the asymptotic form of the one-particle wave function play an important role in influencing the beta- and gamma-ray transition rates. Thus, for example, it is found (cf. Table IX, Figs. 13 and 14) that the overwhelming majo-

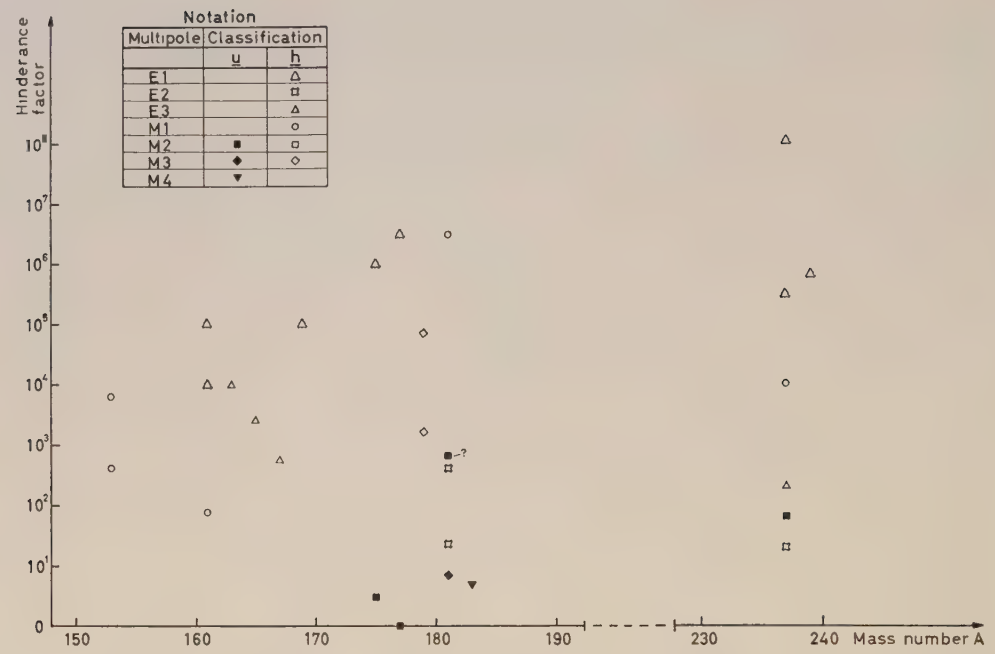

Fig. 15. *Hindrance factors for gamma transitions.* The figure is based on Table X. One sees that transitions which are classified as unhindered in the asymptotic selection rules have transition rates that are within about a factor of 10 of those expected for a single proton moving within a spherical potential. Transitions which are classified as hindered have transition rates that are from 10^2 to 10^8 times slower.

TABLE VIII. *Decoupling factors characterizing rotational bands which have* $K = 1/2$.

Nucleus	Excitation energy of intrinsic state	Orbital assignment	a_{exp}	a_{theo}	Assumed		Dependence of a_{theo} on def.				
					δ	η	$\eta = 0$	2	4	6	∞
$^{12}_{13}Al^{25}$	450	[211 1/2]	−0.02	0.0	0.40	5.0	1.00	0.80	0.14	−0.11	0.00
$^{13}_{12}Mg^{25}$	580	[211 1/2]	−0.20	0.0	0.40	5.0	1.00	0.80	0.14	−0.11	0.00
$^{12}_{13}Al^{25}$	2510	[200 1/2]	−0.56	−0.2	0.37	4.6	−2.00	−1.40	−0.36	0.15	1.00
$^{13}_{12}Mg^{25}$	2560	[200 1/2]	−0.42	−0.2	0.37	4.6	−2.00	−1.40	−0.36	0.15	1.00
$^{12}_{13}Al^{25}$	3090	[330 1/2]	−3.2	− 3	0.54	6.7	−4.00	−3.82	−3.37	−2.91	−1.00
$^{13}_{12}Mg^{25}$	3400	[330 1/2]	−3.5	− 3	0.54	6.7	−4.00	−3.82	−3.37	−2.91	−1.00
$^{99}_{68}Er^{165}$	243	[521 1/2]	1.0	0.9	0.30	6.0	−2.00	0.78	0.95	0.89	0.00
$^{100}_{69}Tm^{169}$	0	[411 1/2]	−0.77	−0.9	0.29	4.8	−2.00	−1.10	−0.93	−0.79	0.00
$^{102}_{69}Tm^{171}$	0	[411 1/2]	−0.87	−0.9	0.29	4.8	−2.00	−1.10	−0.93	−0.79	0.00
$^{101}_{70}Yb^{171}$	0	[521 1/2]	0.85	0.9	0.28	5.7	−2.00	0.78	0.95	0.89	0.00
$^{107}_{74}W^{181}$	515	[510 1/2]	0.22	−0.2	0.23	4.6	3.00	0.16	−0.17	−0.34	−1.00
$^{109}_{74}W^{183}$	0	[510 1/2]	0.17	−0.2	0.21	4.2	3.00	0.16	−0.17	−0.34	−1.00
$^{142}_{91}Pa^{233}$	0	[530 1/2]	−1.38	−2.5	0.23	4.8	−4.00	−3.78	−3.01	−2.08	−1.00
$^{143}_{92}U^{235}$	0.08	[631 1/2]	−0.25	−0.9	0.24	5.0	3.00	−0.20	−0.89	−0.96	0.00
$^{145}_{94}Pu^{239}$	0	[631 1/2]	−0.58	−0.9	0.26	5.3	3.00	−0.20	−0.89	−0.96	0.00

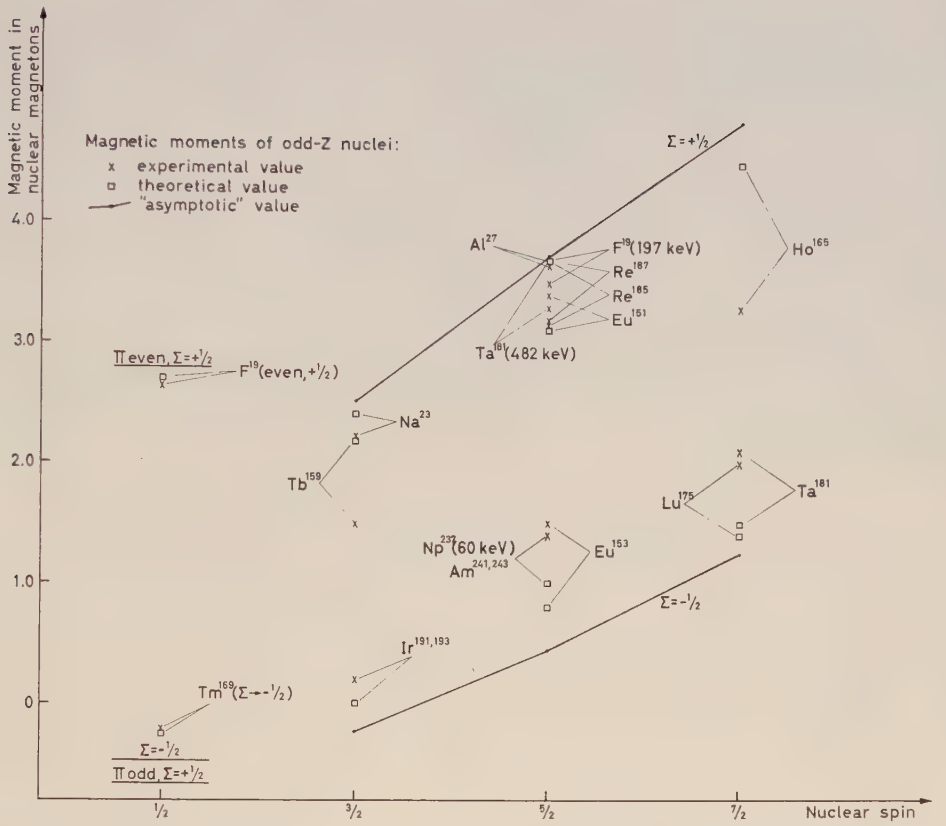

Fig. 16. *Magnetic moments of odd-proton nuclei.* The crosses correspond to the experimental values listed in Table VII:a. The squares represent theoretical values calculated from the detailed wave functions corresponding to single-particle motion in a deformed field. These are compared with one another and with the limiting values (solid line) corresponding to the asymptotic wave functions. These limiting values correspond to the coupling scheme B_1 discussed in A. Bohr (1951), Phys. Rev. **81**, 134. For $I = {}^1/_2$ and $\Sigma = +{}^1/_2$, the asymptotic wave functions yield different magnetic moments corresponding to whether the parity Π is odd or even. One sees from the diagram that the present classification provides a qualitative interpretation of the observed magnetic moments. It is also interesting to note that the detailed wave functions represent the observed moments systematically better than do the asymptotic wave functions. There remain, however, differences of the order of half a magneton (see the discussion in the text). *Added in proof*: A similar figure has recently been given by J. N. I. Gauvin (1958), Nucl. Phys. 8, 213.

← *Caption to Table VIII, p. 84.*

Column two lists the excitation energy at which the lowest state of the rotational band occurs. The orbital assignment, in terms of the quantum numbers $[N n_z \Lambda K]$, is found in column three. The calculated value of a is listed in column five, and the experimental value in column four. The assumed values of the deformation parameters δ and η (cf. Fig. 9 and footnote on p. 7) are listed in columns six and seven. The last five columns show the dependence of a_{theo} on the deformation parameter. The very last column corresponds to the value of a for a pure "asymptotic" state. The value of a in this limit is $a = (-)^N \delta_{\Lambda,0}$.

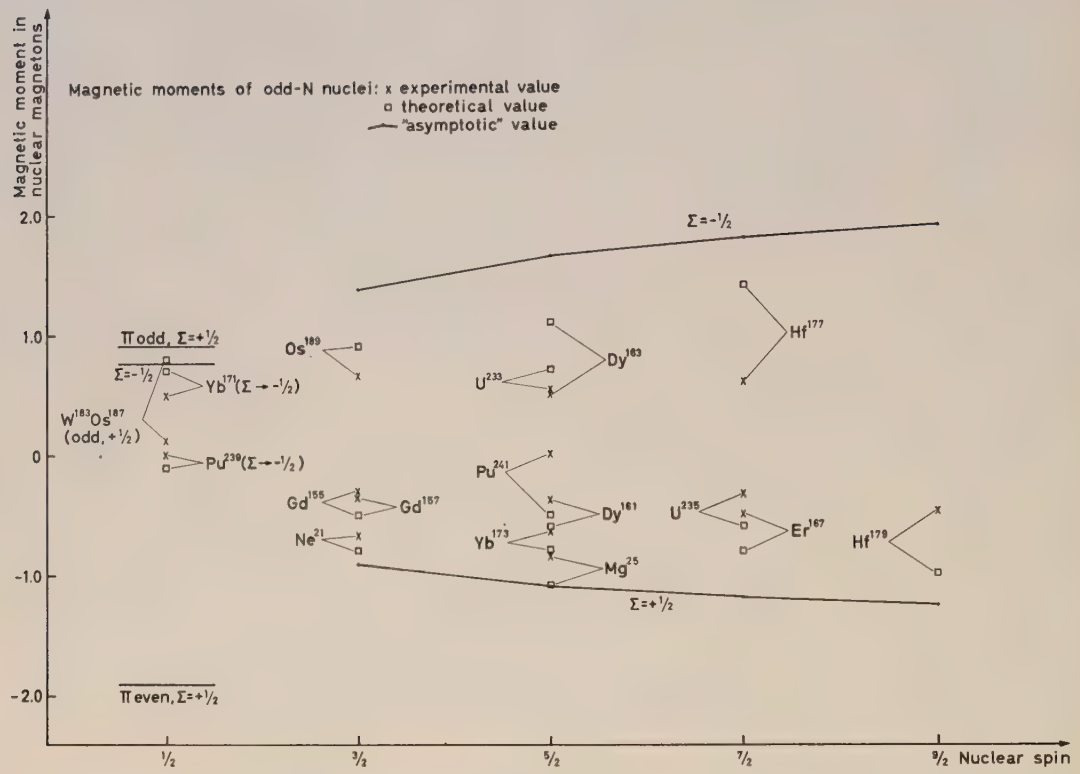

Fig. 17. *Magnetic moments of odd-neutron nuclei.* See caption to Fig. 16.

rity of the observed beta transitions have log ft values which correlate with the classification of the transitions as follows.[1]

$$4.5 < \log ft < 5.0 \quad au$$
$$6.0 < \log ft < 7.5 \quad ah$$
$$5.5 < \log ft \sim 7.5 \quad 1u$$
$$7.5 < \log ft < 8.5 \quad 1h$$

In addition, the model reproduces correctly the main variations in the observed magnetic moments and decoupling factors (cf. Tables VII and VIII, Figs. 16 and 17). However, it is found that, in the case of the magnetic moments, there are deviations between the calculated and predicted values which are in some cases as large as 0.8 nuclear magnetons. These deviations reflect the very great sensitivity of the magnetic moment to the exact orientation of the intrinsic spin with respect to the total angular

[1] It has sometimes been suggested that the selection rules associated with the total number of nodes, N, should be somewhat stronger than the rules connected with the other asymptotic quantum numbers. However, the data collected in Tables IX and X do not seem to indicate such a difference.

momentum. This effect has been observed previously in nuclei which have spherical shapes and has been reasonably accounted for in terms of configuration mixing between the configurations with $j = l + 1/2$ and $j = l - 1/2$ (Blin-Stoyle, 1953; Arima and Horie, 1954).

The success of the simple independent-particle model in describing the non-spherical odd-A nuclei might suggest that it should now be applied to even-even nuclei. It is immediately found, however, that there is a qualitative difference between the observed spectra of these nuclei and what would be predicted by such a model. An independent-particle model would predict that the low-lying intrinsic excitations in even-even nuclei should have an average spacing similar to that observed in the odd-A nuclei. In fact, no intrinsic excitations are found in even-even nuclei up to an energy which is almost an order of magnitude greater than the average spacing in odd-A nuclei[1]. In the regions $150 < A < 190$ and $A > 220$, the first intrinsic excitations

Table IX. *Log ft-values for beta transitions.* a) *Allowed transitions.*

Parent nucleus	Daughter nucleus	Excitation energy of state in daughter	Type of transition	Orbit assignment		Classif.	log *ft*
				Parent	Daughter		
$^{12}_{13}Al^{25}$	$^{13}_{12}Mg^{25}$	0	β^+	[202 5/2]	[202 5/2]	*au*, mirror	3.5
$^{89}_{64}Gd^{153}$	$^{90}_{63}Eu^{153}$	103	*ec*	[651 3/2] †	[411 3/2]	*ah*, †	7.0
$^{92}_{63}Eu^{155}$	$^{91}_{64}Gd^{155}$	87	β^-	[413 5/2] †	[651 3/2]	*ah*	7.3
$^{92}_{63}Eu^{155}$	$^{91}_{64}Gd^{155}$	105	β^-	[413 5/2]	[642 5/2]	*ah*	7.3
$^{95}_{64}Gd^{159}$	$^{94}_{65}Tb^{159}$	364	β^-	[521 3/2]	[532 5/2]	*ah*	6.7
$^{92}_{67}Ho^{159}$	$^{93}_{66}Dy^{159}$	?	*ec*	[523 7/2]	[523 5/2]	*au*	$\lesssim 5$ *if* $\Delta E \leq 2600$
$^{97}_{64}Gd^{161}$	$^{96}_{65}Tb^{161}$	418	β^-	[523 5/2]	[523 7/2]	*au*	~ 4.8
$^{96}_{65}Tb^{161}$	$^{95}_{66}Dy^{161}$	0	β^-	[411 3/2]	[642 5/2]	*ah*	7.8
$^{94}_{67}Ho^{161}$	$^{95}_{66}Dy^{161}$	26	*ec*	[523 7/2]	[523 5/2]	*au*	$\lesssim 4.5$ *if* $\Delta E \lesssim 1000$
$^{95}_{68}Er^{163}$	$^{96}_{67}Ho^{163}$	?	*ec*	[523 5/2]	[523 7/2]	*au*	$\lesssim 5$ *if* $\Delta E \lesssim 1900$
$^{97}_{68}Er^{165}$	$^{98}_{67}Ho^{165}$	0	*ec*	[523 5/2]	[523 7/2]	*au*	≤ 5 *if* $\Delta E \lesssim 600$
$^{100}_{67}Ho^{167}$	$^{99}_{68}Er^{167}$	700	β^-	[523 7/2]	[523 5/2]	*au*	~ 4.8

The first section, (a), exhibits transitions classified as allowed ($\Delta I = 0$ or 1, "no"). The orbitals of initial and final states are here identified by the quantum numbers $[N n_z \Lambda K]$. We have only considered transitions which are not K-forbidden and which involve solely I = K members of the corresponding rotational bands. Column eight gives the log *ft*-value of each transition calculated from the lifetime and branching given in the level schemes of § II. The additional classification in terms of the asymptotic selection rules is introduced in column seven. Transitions that violate the selection rules are classified as *h* (hindered), the others as *u* (unhindered). The second section of Table IX deals with beta transition of first-forbidden type ($\Delta I = 0, 1, 2$, "yes"), denoted (*1*); the last six cases in the table correspond to $\Delta I = 2$, i. e. they have α-type spectra. These latter transitions are denoted (*1**). In section (b) the states are denoted by the quantum numbers $I K \Pi$ $[N n_z \Lambda]$.

[1] This important deviation from the one-particle picture has been known for some time, although a quantitative description has been lacking. For a recent summary of the experimental evidence and a discussion of a possible model for describing the effect, see Bohr, Mottelson, and Pines (1958).

TABLE IX. a) *Allowed transitions* (continued).

Parent nucleus	Daughter nucleus	Excitation energy of state in daughter	Type of transition	Orbit assignment		Classif.	log *ft*
				Parent	Daughter		
$^{97}_{70}Yb^{167}$	$^{98}_{69}Tm^{167}$	?	*ec*	[523 5/2]	[523 7/2]	*au*	$\lesssim 5$ *if* $\Delta E \lesssim 2400$
$^{103}_{68}Er^{171}$	$^{102}_{69}Tm^{171}$	425	β^-	[512 5/2]	[523 7/2]	*ah*	6.3
$^{105}_{70}Yb^{175}$	$^{104}_{71}Lu^{175}$	396	β^-	[514 7/2]	[514 9/2]	*au*	4.5
$^{107}_{70}Yb^{177}$	$^{106}_{71}Lu^{177}$	0	β^-	[624 9/2]	[404 7/2]	*ah*	6.2
$^{106}_{71}Lu^{177}$	$^{105}_{72}Hf^{177}$	326	β^-	[404 7/2]	[624 9/2]	*ah*	6.3
$^{104}_{73}Ta^{177}$	$^{105}_{72}Hf^{177}$	326	*ec*	[404 7/2]	[624 9/2]	*ah*	8.3
$^{106}_{73}Ta^{179}$	$^{107}_{72}Hf^{179}$	0	*ec*	[404 7/2]	[624 9/2]	*ah*	~ 6.9
$^{105}_{74}W^{179}$	$^{106}_{73}Ta^{179}$	30	*ec*	[514 7/2]	[514 9/2]	*au*	< 5 *if* $\Delta E < 2000$
$^{109}_{72}Hf^{181}$	$^{108}_{73}Ta^{181}$	958	β^-	[510 1/2]	[541 1/2]	*ah*	~ 6.5
$^{141}_{94}Pu^{235}$	$^{142}_{93}Np^{235}$	?	*ec*	[633 5/2]	[633 7/2]	*au*	$\lesssim 5$ *if* $\Delta E \lesssim 1000$
$^{143}_{94}Pu^{237}$	$^{144}_{93}Np^{237}$	60	*ec*	[743 7/2]	[523 5/2]	*ah*	6.8
$^{146}_{93}Np^{239}$	$^{145}_{94}Pu^{239}$	286	β^-	[642 5/2]	[622 5/2]	*ah*	6.9
$^{146}_{93}Np^{239}$	$^{145}_{94}Pu^{239}$	512	β^-	[642 5/2]	[633 5/2]	*ah*	6.8
$^{149}_{94}Pu^{243}$	$^{148}_{95}Am^{243}$	84	β^-	[624 7/2]	[642 5/2]	*ah*	6.1
$^{149}_{94}Pu^{243}$	$^{148}_{95}Am^{243}$	465	β^-	[624 7/2]	[633 7/2]	*ah*	~ 6

TABLE IX. b) *First forbidden transitions.*

Parent nucleus	Daughter nucleus	Excitation energy of state in daughter	Type of transition	Orbit assignment		Classif.	log *ft*
				Parent	Daughter		
$^{91}_{62}Sm^{153}$	$^{90}_{63}Eu^{153}$	0	β^-	3/2 3/2− [521]	5/2 5/2+ [413]	$1h$	~ 7.3
$^{91}_{62}Sm^{153}$	$^{90}_{63}Eu^{153}$	103	β^-	3/2 3/2− [521]	3/2 3/2+ [411]	$1u$	6.8
$^{91}_{62}Sm^{153}$	$^{90}_{63}Eu^{153}$	710	β^-	3/2 3/2− [521]	1/2 1/2+ [411]	$1u$	~ 6.5
$^{89}_{64}Gd^{153}$	$^{90}_{63}Eu^{153}$	98	*ec*	3/2 3/2+ [651]†	5/2 5/2− [532]†	$1h$,†	~ 6.8
$^{92}_{63}Eu^{155}$	$^{91}_{64}Gd^{155}$	0	β^-	5/2 5/2+ [413]	3/2 3/2− [521]	$1h$	8.7
$^{94}_{63}Eu^{157}$	$^{93}_{64}Gd^{157}$	0	β^-	5/2 5/2+ [413]	3/2 3/2− [521]	$1h$	8.0
$^{95}_{64}Gd^{159}$	$^{96}_{65}Tb^{159}$	0	β^-	3/2 3/2− [521]	3/2 3/2+ [411]	$1u$	6.7
$^{96}_{65}Tb^{161}$	$^{95}_{66}Dy^{161}$	75	β^-	3/2 3/2+ [411]	3/2 3/2− [521]	$1u$	6.8
$^{99}_{66}Dy^{165}$	$^{98}_{67}Ho^{165}$	0	β^-	7/2 7/2+ [633]	7/2 7/2− [523]	$1u$	~ 6.2
$^{100}_{67}Ho^{167}$	$^{99}_{68}Er^{167}$	0	β^-	7/2 7/2− [523]	7/2 7/2+ [633]	$1u$	~ 6.0
$^{101}_{68}Er^{169}$	$^{100}_{69}Tm^{169}$	0	β^-	1/2 1/2− [521]	1/2 1/2+ [411]	$1u$	6.2
$^{103}_{68}Er^{171}$	$^{102}_{69}Tm^{171}$	688	β^-	5/2 5/2− [512]	3/2 3/2+ [411]	$1u$	8.9 (a)
$^{103}_{68}Er^{171}$	$^{102}_{69}Tm^{171}$	921	β^-	5/2 5/2− [512]	5/2 5/2+ [413]	$1u$	6.9
$^{102}_{69}Tm^{171}$	$^{101}_{70}Yb^{171}$	0	β^-	1/2 1/2+ [411]	1/2 1/2− [521]	$1u$	6.2
$^{105}_{70}Yb^{175}$	$^{104}_{71}Lu^{175}$	0	β^-	7/2 7/2− [514]	7/2 7/2+ [404]	$1u$	6.4

TABLE IX. b) *First forbidden transitions* (continued).

Parent nucleus	Daughter nucleus	Excitation energy of state in daughter	Type of transition	Orbit assigned		Classif.	log *ft*
				Parent	Daughter		
$^{107}_{70}Yb^{177}$	$^{106}_{71}Lu^{177}$	147	β^-	9/2 9/2+ [624]	9/2 9/2− [514]	1*u*	7.2
$^{107}_{70}Yb^{177}$	$^{106}_{71}Lu^{177}$	1230	β^-	9/2 9/2+ [624]	7/2 7/2− [523]	1*u*	5.2—6.2
$^{106}_{71}Lu^{177}$	$^{105}_{72}Hf^{177}$	0	β^-	7/2 7/2+ [404]	7/2 7/2− [514]	1*u*	6.7
$^{104}_{73}Ta^{177}$	$^{105}_{72}Hf^{177}$	0	*ec*	7/2 7/2+ [404]	7/2 7/2- [514]	1*u*	6.6
$^{104}_{73}Ta^{177}$	$^{105}_{72}Hf^{177}$	1070	*ec*	7/2 7/2+ [404]	7/2 7/2- [503]	1*u*	~ 6.5
$^{109}_{72}Hf^{181}$	$^{108}_{73}Ta^{181}$	612	β^-	1/2 1/2− [510]	1/2 1/2+ [411]	1*u*	7.1
$^{110}_{73}Ta^{183}$	$^{109}_{74}W^{183}$	453	β^-	7/2 7/2+ [404]	7/2 7/2− [503]	1*u*	6.9
$^{111}_{74}W^{185}$	$^{110}_{75}Re^{185}$	0	β^-	3/2 3/2− [512]	5/2 5/2+ [402]	1*u*	7.5
$^{142}_{91}Pa^{233}$	$^{141}_{92}U^{233}$	313	β^-	3/2 1/2− [530]	3/2 3/2+ [631]	1*u*	7.0
$^{142}_{91}Pa^{233}$	$^{141}_{92}U^{233}$	400	β^-	3/2 1/2− [530]	1/2 1/2+ [631]	1*u*	6.5
$^{144}_{91}Pa^{235}$	$^{143}_{92}U^{235}$	0.08	β^-	3/2 1/2− [530]	1/2 1/2+ [631]	1*u*	~ 6
$^{142}_{93}Np^{235}$	$^{145}_{92}U^{235}$	0	*ec*	5/2 5/2+ [642]	7/2 7/2− [743]	1*u*	~ 7.5
$^{145}_{92}U^{237}$	$^{144}_{93}Np^{237}$	267	β^-	1/2 1/2+ [631]	3/2 3/2- [521]	1*u*	6.0
$^{143}_{94}Pu^{237}$	$^{144}_{93}Np^{237}$	0	*ec*	7/2 7/2− [743]	5/2 5/2+ [642]	1*u*	6.8
$^{146}_{93}Np^{239}$	$^{145}_{94}Pu^{239}$	392	β^-	5/2 5/2+ [642]	7/2 7/2- [743]	1*u*	6.5
$^{144}_{95}Am^{239}$	$^{145}_{94}Pu^{239}$	286	*ec*	5/2 5/2− [523]	5/2 5/2+ [622]	1*u*	6.0
$^{144}_{95}Am^{239}$	$^{145}_{94}Pu^{239}$	512	*ec*	5/2 5/2− [523]	5/2 5/2+ [633]	1*u*	6.3
$^{147}_{94}Pu^{241}$	$^{146}_{95}Am^{241}$	0	β^-	5/2 5/2+ [622]	5/2 5/2− [523]	1*u*	5.6 (b)
$^{145}_{96}Cm^{241}$	$^{146}_{95}Am^{241}$	480	*ec*	1/2 1/2+ [631]	3/2 3/2− [521]	1*u*	7.4
$^{149}_{94}Pu^{243}$	$^{148}_{95}Am^{243}$	0	β^-	7/2 7/2+ [624]	5/2 5/2− [523]	1*u*	6.1
$^{150}_{95}Am^{245}$	$^{149}_{96}Cm^{245}$	0	β^-	5/2 5/2− [523]	7/2 7/2+ [624]	1*u*	~ 6.2
$^{150}_{95}Am^{245}$	$^{149}_{96}Cm^{245}$	257	β^-	5/2 5/2− [523]	5/2 5/2+ [622]	1*u*	~ 6.2
$^{148}_{97}Bk^{245}$	$^{149}_{96}Cm^{245}$	257	*ec*	3/2 3/2− [521]	5 2 5/2+ [622]	1*u*	7.1
$^{148}_{97}Bk^{245}$	$^{149}_{96}Cm^{245}$	632	*ec*	3/2 3/2− [521]	1/2 1/2+ [631]	1*u*	~ 7.4
$^{152}_{97}Bk^{249}$	$^{151}_{98}Cf^{249}$	0	β^-	7/2 7/2+ [633]	9/2 9/2− [734]	1*u*	6.9
$^{91}_{62}Sm^{153}$	$^{90}_{63}Eu^{153}$	83	β^-	3 2 3/2− [521]	7/2 5/2+ [413]	1*h*	> 8.4
$^{103}_{68}Er^{171}$	$^{102}_{69}Tm^{171}$	0	β^-	5/2 5/2 - [512]	1/2 1/2+ [411]	1*u*	> 8.6
$^{110}_{73}Ta^{183}$	$^{109}_{74}W^{183}$	209	β^-	7/2 7/2+ [404]	3/2 3/2− [512]	1*h*	> 8.7
$^{109}_{76}Os^{185}$	$^{110}_{75}Re^{185}$	0	*ec*	1 2 1/2− [510]	5/2 5/2+ [402]	1*h*	> 9.3
$^{112}_{75}Re^{187}$	$^{111}_{76}Os^{187}$	0	β^-	5/2 5/2+ [402]	1/2 1/2 - [510]	1*h*	~ 11 (c)
$^{145}_{96}Cm^{241}$	$^{146}_{95}Am^{241}$	0	*ec*	1/2 1/2+ [631]	5/2 5/2 - [523]	1*h*	> 9

(†) This single-particle state is associated with a smaller nuclear deformation.

(a) This *ft*-value differs by about a factor of 100 from what is expected according to the assumed classification. This large discrepancy may throw some doubt on the orbital assignments.

(b) This *ft*-value is somewhat smaller than that usually observed for 1*u* transitions. It is possible that this reflects some small error in the transition energy or in the calculated Fermi function for this very low energy transition.

(c) This *ft*-value is calculated from an assumed transition energy of 1.5 keV (JOHNSON and LIBBY, private communication) and a bold extrapolation of the available tables of Fermi functions.

TABLE X. *Hindrance factors for electromagnetic transitions.*

Nucleus	Orbit assignment		Half-life of state	ΔE keV	Mult.	%	Add. class	H
	Initial	Final						
$^{12}_{13}Al^{25}$	1/2− [330]	1/2+ [211]	(a)	..	$E1$	..	h	$\sim 10^2$
$^{12}_{13}Al^{25}$	1/2+ [200]	1/2+ [211]	(a)	..	$M1$	..	h	~ 10
$^{90}_{63}Eu^{153}$	3/2 3/2+ [411]	5/2 5/2+ [413]	4.1×10^{-9} s	103	$M1$	..	h	4×10^2
$^{90}_{63}Eu^{153}$	5/2 3/2+ [411]	5/2 5/2+ [413]	1.5×10^{-10} s	170	$M1$	..	h	$\sim 6\times10^3$
$^{95}_{66}Dy^{161}$	5/2 5/2− [523]	5/2 5/2+ [642]	3×10^{-8} s	26	$E1$	..	h	1×10^4
$^{95}_{66}Dy^{161}$	3/2 3/2− [521]	5/2 5/2− [523]	2×10^{-9} s	49	$M1$	..	h	70
$^{95}_{66}Dy^{161}$	3/2 3/2− [521]	5/2 5/2+ [642]	2×10^{-9} s	75	$E1$	..	h	1×10^5
$^{96}_{67}Ho^{163}$	1/2 1/2+ [411]	7/2 7/2− [523]	0.8 s	305	$E3$	..	h	1×10^4
$^{99}_{66}Dy^{165}$	1/2 1/2− [521]	7/2 7/2+ [633]	1.2 m	108	$E3$	..	h	2×10^3
$^{99}_{68}Er^{167}$	1/2 1/2− [521]	7/2 7/2+ [633]	2.5 s	208	$E3$	..	h	5×10^2
$^{100}_{69}Tm^{169}$	7/2 7/2− [523]	7/2 7/2+ [404]	4.5×10^{-8} s	63	$E1$	..	h	1×10^5
$^{101}_{70}Yb^{171}$	7/2 7/2+ [633]	1/2 1/2− [521]	(b)	75	$E3$	..	h	(b)
$^{104}_{71}Lu^{175}$	9/2 9/2− [514]	7/2 7/2+ [404]	3×10^{-9} s	396	$E1$ $M2$	80 20	h u	1×10^6 1
$^{104}_{71}Lu^{175}$	9/2 9/2− [514]	9/2 7/2+ [404]	3×10^{-9} s	282	$E1$ $M2$	97 3	h u	1×10^6 3
$^{106}_{71}Lu^{177}$	9/2 9/2− [514]	7/2 7/2+ [404]	1.2×10^{-7} s	147	$E1$ $M2$	90 10	h u	5×10^6 1
$^{107}_{72}Hf^{179}$	1/2 1/2− [510]	7/2 7/2− [514]	19 s	160	$M3$	..	h	10^3
$^{105}_{74}W^{179}$	1/2 1/2− [510]	7/2 7/2− [514]	7 m	220	$M3$	..	h	7×10^4
$^{108}_{73}Ta^{181}$	1/2 1/2+ [411]	5/2 5/2+ [402]	1.8×10^{-5} s	132	$E2$	..	h	4×10^2
$^{108}_{73}Ta^{181}$	1/2 1/2+ [411]	7/2 7/2+ [404]	1.8×10^{-5} s	612	$M3$	..	u	7
$^{108}_{73}Ta^{181}$	5/2 5/2+ [402]	7/2 7/2+ [404]	1.1×10^{-8} s	480	$E2$ $M1$	97 3	h h	30 3×10^6
$^{108}_{73}Ta^{181}$	9/2 9/2− [514]	7/2 7/2+ [404]	(c)	152	$E1$ $M2$	85 15	h u	(c)
$^{107}_{74}W^{181}$	5/2 5/2− [512]	9/2 9/2+ [624]	1.4×10^{-5} s	366	$M2$	..	u	7×10^2 (d)
$^{107}_{76}Os^{183}$	1/2 1/2− [510]	9/2 9/2+ [624]	$\sim 10\,\hbar$	171	$M4$	..	u	~ 5
$^{143}_{92}U^{235}$	1/2 1/2+ [631]	7/2 7/2− [743]	26.5 m	$\lesssim 0.08$	$E3$	..	h	(e)
$^{143}_{92}Pu^{237}$	1/2 1/2+ [631]	7/2 7/2− [743]	0.18 s	145	$E3$	..	h	2×10^2
$^{144}_{93}Np^{237}$	5/2 5/2− [523]	5/2 5/2+ [642]	6.3×10^{-8} s	60	$E1$	..	h	3×10^5
$^{144}_{93}Np^{237}$	3/2 3/2− [521]	5/2 5/2+ [642]	5.4×10^{-9} s	267	$E1$ $M2$	~ 100	h u	10^8 (f)
$^{144}_{93}Np^{237}$	3/2 3/2− [521]	7/2 5/2+ [642]	5.4×10^{-9} s	234	$M2$	..	u	70
$^{144}_{93}Np^{237}$	3/2 3/2− [521]	5/2 5/2− [523]	5.4×10^{-9} s	208	$M1$	..	h	1×10^4
$^{144}_{93}Np^{237}$	3/2 3/2− [521]	7/2 5/2− [523]	5.4×10^{-9} s	165	$E2$	..	h	20
$^{145}_{94}Pu^{239}$	7/2 7/2− [743]	5/2 5/2+ [622]	1.9×10^{-7} s	106	$E1$	..	h	6×10^5

Initial and final states for the transition are listed in columns two and three. The states are assigned by listing the quantum numbers $IK\Pi$ $[Nn_z\Lambda]$. The next column gives the experimental half-life. The hindrance factor H of column nine is obtained by correcting the observed half-life for branching and internal conversion and then dividing by the theoretical half-life for a single-proton transition (MOSZKOWSKI, 1955b). Where the conversion coefficients have not been measured we have used theoretical values (SLIV and BAND, 1956, for K-conversion; ROSE, privately circulated tables, for L-conversion). Column eight contains the classification of the transitions as hindered (h) or unhindered (u) with respect to the selection rules in terms of the asymptotic quantum numbers (as given in Table I).

in even-even nuclei are usually not found below about 1 MeV. This energy gap in the even-even nuclei apparently reflects an essential correlation in the motion of a pair of nucleons which fill the degenerate orbits labelled by $+K$ and $-K$. From our present analysis, however, we can conclude that the pairing forces responsible for this correlation in even-even nuclei do not essentially modify the orbit of the unpaired nucleon in an odd-A nucleus[1].

[1] For a discussion of the possible influence of the pairing forces on the absolute magnitude of the spacing of intrinsic levels in odd-A nuclei, see F. BAKKE (to be published).

← *To Table X, p. 90.*

(a) Many transitions between these two bands are observed and the absolute and relative intensities are analyzed in some detail in (LITHERLAND et al., 1958). The hindrance factors quoted in the table represent an average for the several transitions observed between the two bands.

(b) The lifetime of this $E3$ transition is not known, but is expected to be of the order of an hour.

(c) Although no lifetime is known for this transition, the relatively large amount of $M2$ admixture encountered shows a relative hindrance of $E1$ compared to $M2$ of order 10^6, which is in agreement with the classification. Indeed, the situation is similar to Lu^{177}, where we encounter the same orbitals, a similar transition energy, and comparable $E1 - M2$ mixing.

(d) It is possible that the relatively long lifetime of this unhindered transition is associated with a selection rule resulting from the fact that the last odd particle is a neutron. Thus the matrix element, $(x+iy)l_+$, responsible for the transition (cf. Table I) is multiplied by the orbital g-factor, g_l, which is zero for a neutron.

(e) It is not possible to obtain a hindrance factor from the observed lifetime for this transition because of the considerable uncertainty in the conversion coefficient. If we assume the transition matrix element to be the same as for the transition between the same orbitals observed in Pu^{237}, the conversion coefficient is estimated to be of the order of 10^{21}. This value is not inconsistent with a daring extrapolation of the known systematics of conversion coefficients (I. PERLMAN and F. ASARO, private communication).

(f) If the classification of these orbitals is correct, one should probably expect a significant $M2$ admixture in this transition.

ACKNOWLEDGEMENTS

It is a pleasure to acknowledge the stimulation we have derived from the continued interest and support of Professor AAGE BOHR.

We have also benefited greatly from contacts with many experimental workers in the field of nuclear spectroscopy. In this connection, we should especially mention Drs. ASARO, HOLLANDER, NEWTON, PERLMAN, RASMUSSEN, and STEPHENS of the nuclear spectroscopy group at Berkeley, and ELBEK, NATHAN, NIELSEN, and SHELINE of the group in Copenhagen. We are indebted to Mr. O. PRIOR for having carried out a number of calculations involved in the present analysis, and to laborator C. E. FRÖBERG, director of the electronic computor SMIL in Lund, for having programmed and carried through a number of calculations.

One of the authors (SGN) also wishes to take the opportunity of expressing his gratitude to Professor G. SEABORG for his generous hospitality during a visit to the Radiation Laboratory, Berkeley, California, for the academic year of 1956/57.

NORDITA – Nordisk Institut for Teoretisk Atomfysik, København, Danmark
and
Institutionen för Teoretisk Fysik, Lund, Sverige.

APPENDIX I

Most of the wave functions and energy spectra employed in the present analysis have been published previously (SGN). In a few cases, it was necessary to perform additional calculations in order to complete the theoretical spectra. The present appendix contains the results of these additional calculations. The form of the tables and the notation are the same as in (SGN).

Eigenvalues and eigenfunctions of the shell $N = 5$ *with the parameter* $\mu = 0.70$; *valid for the last odd proton of odd Z-nuclei with* $Z > 82$.

The eigenfunctions are given in a representation with N, l, Λ, and Σ diagonal. Base vectors are denoted $|N l \Lambda \Sigma\rangle$. To the right in the table, there are listed the the quantum numbers, $[N n_z \Lambda]$, of the asymptotic wave functions for each orbit.

$N = 5 \quad \Omega = \frac{11}{2}$

eigenvalue: $5/3\,\eta - 26.0$; eigenvector $|555+>$, asymptotic state [505].

$\eta = -6$	-4	-2	0	2	4	6	
−36.000	−33.667	−29.333	−26.000	−22.667	−19.333	−16.000	..

$N = 5 \quad \Omega = \frac{9}{2}$

base vectors: $|554+>$, $|555->$.

$\eta = -6$	-4	-2	0	2	4	6	$+\infty$
−24.000	−21.136	−18.116	−15.000	−11.822	− 8.605	− 5.361	
0.535	0.436	0.359	− 0.302	0.258	0.225	0.198	[505]
− 0.845	− 0.900	− 0.933	0.954	− 0.966	− 0.975	0.980	
−31.000	−29.198	−27.550	−26.000	−24.511	−23.062	−21.639	
0.845	0.900	0.933	0.954	0.966	0.975	0.980	[514]
0.535	0.436	0.359	0.302	0.258	0.225	0.198	

$N = 5 \quad \Omega = \frac{7}{2}$

base vectors: $|553+>$, $|533+>$, $|554->$.

$\eta = -6$	-4	-2	0	2	4	6	$+\infty$
−16.090	−15.493	−14.007	−11.400	− 8.393	− 5.255	− 2.055	
− 0.615	− 0.485	− 0.214	0.000	0.094	0.144	0.177	[503]
− 0.583	− 0.723	− 0.954	1.000	− 0.994	− 0.987	− 0.982	
0.531	0.493	0.210	0.000	− 0.055	− 0.067	− 0.068	
−20.498	−18.153	−16.194	−15.000	−13.961	−12.885	−11.757	
0.082	0.254	0.432	− 0.426	− 0.372	− 0.321	− 0.279	[514]
− 0.717	− 0.655	− 0.285	0.000	− 0.086	− 0.111	− 0.117	
− 0.692	− 0.712	− 0.856	0.905	0.924	0.941	0.953	
−27.812	−26.755	−26.199	−26.000	−26.046	−26.260	−26.588	
0.784	− 0.837	− 0.876	0.905	− 0.924	− 0.936	− 0.944	[523]
− 0.382	0.220	0.092	0.000	− 0.066	− 0.114	− 0.149	
0.489	− 0.501	− 0.473	0.426	− 0.378	− 0.333	− 0.295	

$N = 5 \quad \Omega = \frac{5}{2}$

base vectors: $|552+>$, $|532+>$, $|553->$, $|533->$.

$\eta = -6$	-4	-2	0	2	4	6	$+\infty$
− 5.889	− 6.883	− 6.410	− 4.400	− 1.688	1.293	4.396	
0.442	0.300	− 0.113	0.000	0.042	0.056	0.060	
0.755	0.717	− 0.553	− 0.378	− 0.278	− 0.220	− 0.183	[503]
− 0.311	− 0.271	0.139	0.000	− 0.085	− 0.137	− 0.171	
− 0.370	− 0.568	0.814	0.926	0.956	0.964	0.966	
−13.002	−12.441	−11.766	−11.400	−10.840	−10.022	− 9.039	
− 0.056	0.156	0.158	0.000	0.151	− 0.249	0.312	
− 0.514	0.609	0.806	0.926	− 0.945	0.936	− 0.924	[512]
− 0.525	0.218	− 0.009	0.000	− 0.051	0.074	− 0.077	
− 0.676	0.747	0.571	0.378	− 0.286	0.238	− 0.208	
−16.595	−15.175	−14.743	−15.000	−15.696	−16.559	−17.439	
− 0.533	− 0.526	0.533	− 0.522	0.465	− 0.396	− 0.334	
0.256	0.253	− 0.179	0.000	0.139	− 0.201	− 0.220	[523]
0.557	0.748	− 0.822	0.853	− 0.873	0.890	0.906	
− 0.583	− 0.316	0.092	0.000	− 0.057	0.103	0.139	
−25.314	−24.968	−25.214	−26.000	−27.243	−28.846	−30.718	
− 0.719	0.781	− 0.824	0.853	− 0.872	0.882	0.887	
0.315	− 0.226	0.114	0.000	− 0.103	0.187	0.254	[532]
− 0.563	0.565	− 0.552	0.522	− 0.478	0.428	0.380	
0.258	− 0.143	0.058	0.000	− 0.034	0.053	0.060	

$N = 5 \quad \Omega = \frac{3}{2}$

base vectors: $|551+>$, $|531+>$, $|511+>$, $|552->$, $|532->$

$\eta = -6$	-4	-2	0	2	4	6	$+\infty$
4.556	0.955	− 1.908	− 2.400	0.041	2.966	6.045	
0.291	− 0.210	− 0.097	0.000	− 0.029	− 0.059	− 0.082	
0.754	− 0.710	− 0.581	0.000	0.263	0.343	0.384	[501]
0.477	− 0.534	− 0.669	1.000	− 0.955	− 0.928	− 0.912	
− 0.166	0.147	0.086	0.000	0.020	0.033	0.037	
− 0.303	0.381	0.445	0.000	− 0.135	− 0.129	− 0.115	
− 3.967	− 5.196	− 4.984	− 4.400	− 4.775	− 4.526	− 3.871	
− 0.087	0.100	0.081	0.000	− 0.081	− 0.111	− 0.118	
0.189	− 0.074	0.225	− 0.535	0.374	0.257	0.186	[512]
0.401	− 0.565	− 0.678	0.000	0.234	0.236	0.215	
0.440	− 0.304	− 0.135	0.000	0.135	0.233	0.300	
0.776	− 0.757	− 0.682	0.845	− 0.884	− 0.901	− 0.903	

continued

$\eta=-6$	-4	-2	0	2	4	6	$+\infty$
−11.129	−10.754	−10.555	−11.400	−12.786	−14.144	−15.315	
0.595	− 0.388	0.165	0.000	− 0.183	0.337	− 0.440	
0.273	− 0.552	0.753	0.845	0.863	− 0.822	0.771	
− 0.596	0.579	− 0.301	0.000	0.183	− 0.277	0.327	[521]
− 0.199	0.061	0.026	0.000	0.020	− 0.055	0.069	
0.421	− 0.454	0.561	0.535	0.433	− 0.362	0.317	
−14.878	−13.722	−13.851	−15.000	−16.946	−19.454	−22.221	
− 0.291	0.505	0.599	− 0.603	− 0.551	− 0.460	0.368	
0.454	− 0.362	− 0.176	0.000	− 0.176	− 0.292	0.335	
− 0.480	0.236	0.046	0.000	− 0.028	− 0.073	0.103	[532]
0.642	− 0.716	− 0.771	0.780	0.810	0.818	− 0.830	
− 0.259	0.213	0.120	0.000	0.092	0.166	− 0.230	
−23.782	−23.817	−24.569	−26.000	−28.068	−30.709	−33.838	
0.685	0.735	− 0.773	0.780	0.809	0.812	0.807	
− 0.340	− 0.235	0.121	0.000	0.122	0.236	0.334	
0.162	0.067	− 0.015	0.000	0.011	0.038	0.070	[541]
0.572	0.608	− 0.616	0.603	0.570	0.521	0.464	
− 0.248	− 0.174	0.085	0.000	0.067	0.112	0.134	

$N=5 \quad \Omega=\frac{1}{2}$

base vectors: $|550+>$, $|530+>$, $|510+>$, $|551->$, $|531->$, $|511->$.

$\eta=-6$	-4	-2	0	2	4	6	$+\infty$
15.564	9.484	3.863	0.600	2.383	5.186	8.213	
− 0.141	− 0.100	− 0.046	0.000	0.017	0.030	− 0.035	
− 0.538	− 0.482	− 0.357	0.000	− 0.126	− 0.125	0.114	
− 0.799	− 0.826	− 0.857	− 0.577	0.236	0.154	− 0.118	[501]
0.068	0.058	0.034	0.000	− 0.027	− 0.058	0.081	
0.183	0.208	0.217	0.000	0.250	0.337	− 0.380	
0.120	0.168	0.295	0.816	− 0.930	− 0.918	0.906	
5.511	1.813	− 1.093	− 2.400	− 3.630	− 3.561	− 2.968	
0.096	0.086	0.041	0.000	0.067	− 0.149	0.209	
0.045	0.096	0.114	0.000	− 0.461	0.605	− 0.661	
− 0.317	− 0.371	− 0.433	0.816	0.811	− 0.718	0.669	[510]
− 0.289	− 0.206	− 0.084	0.000	− 0.040	0.072	− 0.082	
− 0.756	− 0.709	− 0.529	0.000	0.160	− 0.145	0.111	
− 0.483	− 0.548	− 0.715	0.577	0.314	− 0.265	0.231	
− 2.958	− 4.023	− 3.773	− 4.400	− 7.253	− 9.946	−11.809	
0.471	0.320	0.143	0.000	0.115	− 0.162	0.166	
0.606	0.629	0.605	− 0.655	− 0.414	0.173	− 0.047	
− 0.426	− 0.326	− 0.185	0.000	− 0.457	0.457	− 0.381	[521]
− 0.191	− 0.187	− 0.130	0.000	− 0.157	0.307	− 0.418	
0.070	− 0.108	− 0.474	0.756	0.748	− 0.761	0.744	
0.433	0.591	0.582	0.000	0.148	− 0.250	0.312	

continued

$\eta=-6$	-4	-2	0	2	4	6	$+\infty$
−10.049	− 9.730	− 9.937	−11.400	−14.005	−17.340	−20.694	
− 0.017	− 0.110	0.120	0.000	0.163	0.373	0.540	
0.412	− 0.499	0.675	0.756	− 0.745	− 0.640	− 0.487	
− 0.249	0.255	− 0.206	0.000	− 0.275	− 0.470	− 0.539	[530]
0.549	− 0.296	0.099	0.000	0.049	0.003	− 0.054	
0.307	− 0.545	0.645	0.655	− 0.571	− 0.457	− 0.395	
− 0.610	0.538	− 0.249	0.000	− 0.121	− 0.148	− 0.149	
−13.672	−12.898	−13.409	−15.000	−17.606	−21.227	−25.701	
0.584	0.625	0.662	− 0.674	0.642	0.538	0.387	
− 0.284	− 0.255	− 0.157	0.000	0.176	0.349	0.434	
0.092	0.074	0.029	0.000	0.042	0.166	0.288	[541]
− 0.440	− 0.638	− 0.717	0.739	− 0.734	− 0.717	− 0.704	
0.452	0.320	0.148	0.000	− 0.128	− 0.213	− 0.282	
− 0.415	− 0.170	− 0.030	0.000	− 0.014	− 0.035	− 0.058	
−22.995	−23.246	−24.250	−26.000	−28.490	−31.711	−35.642	
− 0.638	0.691	− 0.723	0.739	− 0.737	0.722	− 0.698	
0.302	− 0.222	0.117	0.000	− 0.121	0.239	− 0.350	
− 0.095	0.051	− 0.015	0.000	− 0.017	0.066	− 0.141	[550]
− 0.617	0.651	− 0.672	0.674	− 0.657	0.619	− 0.560	
0.303	− 0.207	0.105	0.000	− 0.099	0.181	− 0.233	
− 0.142	0.059	− 0.013	0.000	− 0.009	0.029	− 0.049	

Eigenvalues and eigenfunctions of the shell $N = 7$ with the parameter $\mu = 0.40$ valid for the last odd neutron of odd-N nuclei with $N > 126$.

For the notation, see the caption of the corresponding table for the $N = 5$ shell. In addition, the first column on the left gives the quantum numbers, *ljK*, that characterize the orbital in a spherical potential ($\eta = 0$).

$N = 7 \quad \Omega = \frac{15}{2}$

eigenvalue: $7/3\eta - 29.4$; eigenvector: $|777+>$.

	$\eta=-6$	-4	-2	0	2	4	6	10	$+\infty$
$j\ \frac{15}{2}\ \frac{15}{2}$	−43.400	−38.733	−34.067	−29.400	−24.733	−20.067	−15.400	− 6.067	[707]

$N = 7 \quad \Omega = \frac{13}{2}$

base vectors: $|776+>$, $|777->$.

	$\eta=-6$	-4	-2	0	2	4	6	10	$+\infty$
$j\ \frac{15}{2}\ \frac{13}{2}$	− 38.023	− 35.083	− 32.220	− 29.400	− 26.623	− 23.852	− 21.132	− 15.640	
	.917	.940	.955	.966	.973	.979	.982	9.88	[716]
	.398	.340	.294	.258	.229	.206	.186	.157	
$j\ \frac{13}{2}\ \frac{13}{2}$	−27.778	−23.384	−18.914	−14.400	− 9.838	− 5.281	− 0.668	8.505	
	− .398	− .340	− .294	− .258	− .229	− .206	− .186	− .157	[707]
	.917	.940	.955	.966	.973	.979	.982	.988	

$N = 7 \quad \Omega = \frac{11}{2}$

base vectors: $|775+>$, $|755+>$, $|776->$.

	$\eta=-6$	-4	-2	0	2	4	6	10	$+\infty$
	−34.912	−32.450	−30.726	−29.400	−28.285	−27.293	−26.378	−24.694	
$j\ \frac{15}{2}\ \frac{11}{2}$	.773	.868	.911	.931	.942	.949	.953	.959	[725]
	− .511	− .275	− .104	.000	.064	.106	.136	.173	
	.375	.413	.399	.365	.330	.298	.270	.226	
	−28.731	−25.315	−21.298	−17.000	−12.733	− 9.696	− 7.133	− 2.013	
$h\ \frac{11}{2}\ \frac{11}{2}$	.353	.179	.056	.000	.079	− .242	− .234	− .200	[716]
	.838	.950	.990	1.000	.912	− .364	− .233	− .156	
	.416	.255	.129	.000	− .403	.899	.944	.967	
	−21.158	−19.035	−16.776	−14.400	−11.782	− 7.811	− 3.288	5.907	
$j\ \frac{13}{2}\ \frac{11}{2}$	.527	− .463	− .408	− .365	− .327	.204	− .191	− .203	[705]
	− .189	− .148	− .095	.000	.405	.925	.963	.972	
	.829	.874	.908	.931	.854	.320	.191	.115	

$N = 7 \quad \Omega = 9/2$

base vectors: $|774+>$, $|754+>$, $|775->$, $|755->$.

	$\eta=-6$	-4	-2	0	2	4	6	10	$+\infty$
	−31.773	−30.278	−29.522	−29.400	−29.726	−30.343	−31.148	−33.097	
	.742	.818	.869	.894	.905	.910	.911	.910	
$j\ \frac{15}{2}\ \frac{9}{2}$	− .428	− .295	− .138	.000	.104	.179	.234	.303	[734]
	.456	.475	.473	.447	.411	.373	.337	.279	
	− .241	− .134	− .052	.000	.028	.042	.049	.051	
	−21.537	−20.327	−18.854	−17.000	−15.040	−13.821	−13.191	−12.078	
	.422	.202	.078	.000	.042	− .214	− .236	− .206	
$h\ \frac{11}{2}\ \frac{9}{2}$	.514	.829	.914	.954	.917	− .566	− .382	− .261	[725]
	.178	.289	.165	.000	− .341	.796	.890	.930	
	.725	.435	.362	.302	.205	− .006	.085	.154	
	−20.604	−17.351	15.295	14.400	−13.635	12.000	− 9.665	− 4.618	
	.209	.429	.477	.447	.421	− .353	− .335	− .356	
$j\ \frac{13}{2}\ \frac{9}{2}$	− .580	.165	− .016	.000	.295	.776	.875	.904	[714]
	− .647	.682	.845	.894	.842	.459	.265	.144	
	.449	− .569	− .242	.000	.166	.250	.230	.187	
	−12.887	−12.177	− 9.796	− 6.000	− 1.732	2.698	7.204	16.326	
	− .477	− .325	− .109	.000	.037	.050	.054	.053	
$h\ \frac{9}{2}\ \frac{9}{2}$	− .465	− .446	− .381	− .302	− .248	− .212	− .186	− .149	[705]
	.584	.476	.188	.000	− .085	− .130	− .158	− .190	
	.464	.685	.899	.954	.964	.967	.968	.969	

$N - 7\ \ Q - 7/2$

base vectors: $|773\ \ \searrow\ \ \rangle$, $|753\ \ \searrow\ \ \rangle$, $|733\ \ \searrow\ \ \rangle$, $|774\ \ \searrow\ \ \rangle$, $|754\ \ \searrow\ \ \rangle$.

	−6	4	2	0	2	4	6	10	$-\infty$	
$i\ \frac{15}{2}\ \frac{7}{2}$	29.686	28.625	−28.580	−29.400	−30.919	−32.954	−35.344	−40.775		[743]
	.680	.771	.828	.856	.864	.861	.854	.839		
	− .444	− .312	− .157	.000	.136	.242	.320	.422		
	.244	.091	0.18	.000	.010	.029	.048	.079		
	.464	.518	.532	.516	.481	.438	.394	.318		
	.257	− .179	− .083	.000	.056	.088	.103	.108		
$h\ \frac{11}{2}\ \frac{7}{2}$	− 21.834	18.902	− 17.304	− 17.000	− 17.032	− 17.610	− 18.819	− 21.626		[734]
	.242	.169	.090	.000	.000	.139	− .195	− .179		
	− .373	.616	.835	.905	.896	.700	− .508	− .352		
	.802	− .671	− .282	.000	.133	.156	− .132	− .104		
	.397	.311	.182	.000	− .291	− .681	.819	.874		
	.049	.211	.428	.426	.307	.052	.124	.263		
$i\ \frac{13}{2}\ \frac{7}{2}$	16.302	14.960	− 14.133	− 14.400	− 15.250	− 15.730	− 15.545	− 14.588		[723]
	.570	− .537	− .535	− .516	− .497	− .477	− .467	− .498		
	− .060	− .005	.023	.000	.179	.563	.713	.752		
	− .123	− .047	− .018	.000	.031	.141	.217	.283		
	.457	.601	.796	.856	.815	.543	.312	.147		
	.669	− .590	− .283	.000	.237	.376	.360	.290		
$f\ \frac{7}{2}\ \frac{7}{2}$	− 12.602	12.894	− 11.276	− 7.800	− 4.783	− 2.647	− 0.370	4.471		[714]
	.011	− .071	− .029	.000	.058	.092	.102	.100		
	.337	.443	.147	.000	− .223	− .216	− .185	− .140		
	.476	.696	.938	1.000	− .567	− .348	− .275	− .205		
	.509	.390	.102	.000	− .121	− .216	− .271	− .332		
	.475	.403	.294	.000	.781	.882	.898	.904		
$h\ \frac{9}{2}\ \frac{7}{2}$	4.177	− 5.886	− 6.640	− 6.000	− 3.282	1.008	5.478	14.585		[703]
	− .393	− .289	− .141	.000	.049	.058	.068	.083		
	− .610	− .571	− .507	− .426	− .311	− .296	− .311	− .336		
	− .236	− .233	− .198	.000	.812	.913	.926	.928		
	.399	.349	.201	.000	− .074	− .063	− .057	− .047		
	.508	.643	.802	.905	.485	.266	.195	.131		

$N = 7 \quad \Omega = 5/2$

base vectors: $|772+>$, $|752+>$, $|732+>$, $|773->$, $|753->$, $|733->$.

	$\eta=-6$	-4	-2	0	2	4	6	10	$+\infty$
	−27.974	−27.399	−27.886	−29.400	31.843	35.058	−38.859	−47.584	
	.645	.730	.788	.817	.819	.804	.783	.742	
$j\frac{15}{2}\frac{5}{2}$	− .416	− .311	− .164	.000	.156	.287	.388	.514	
	.188	.095	.024	.000	.019	.060	.107	.185	[752]
	.505	.556	.582	.577	.545	.497	.442	.345	
	− .312	− .219	− .109	.000	.087	.142	.169	.177	
	.153	.060	.012	.000	.006	.017	.026	.033	
	−17.491	−16.294	−16.128	−17.000	−18.672	−20.975	−23.955	−30.615	
	− .436	.233	.106	.000	− .043	.039	.113	− .117	
$h\frac{11}{2}\frac{5}{2}$	− .142	.591	.775	.853	.850	.747	.586	− .405	
	.280	− .459	− .282	.000	.221	.314	.297	− .240	[743]
	− .142	.298	.182	.000	− .250	− .570	− .734	.796	
	− .421	.391	.500	.522	.400	.122	− .134	.356	
	.717	− .380	− .157	.000	.064	.046	− .001	.060	
	−16.019	−13.920	−13.307	−14.400	−16.570	−18.934	−20.841	−23.929	
	− .158	− .488	− .579	− .577	− .560	− .564	− .573	− .615	
$j\frac{13}{2}\frac{5}{2}$	.539	.283	.092	.000	.060	.315	.476	.508	
	− .468	− .123	− .016	.000	.026	.168	.315	.446	[732]
	.606	.611	.756	.817	.777	.574	.334	.129	
	− .274	− .445	− .284	.000	.279	.466	.470	.369	
	.153	.311	.066	.000	.033	.090	.115	.113	
	− 9.194	− 8.675	− 7.884	− 7.800	− 7.552	− 7.720	− 7.650	− 7.029	
	− .536	.349	.010	.000	− .070	.128	.143	.137	
$f\frac{7}{2}\frac{5}{2}$	− .254	.378	.202	.000	.140	− .136	− .099	− .051	
	.328	− .131	.748	.926	.740	− .528	− .430	− .321	[723]
	.371	− .286	.050	.000	.140	− .287	− .373	− .465	
	− .256	.057	.268	.000	− .636	.767	.778	.765	
	− .581	.795	.570	.378	.061	.124	.201	.274	
	− 3.775	− 6.163	− 6.338	− 6.000	− 5.805	− 4.052	− 1.875	2.920	
	− .065	− .112	− .159	.000	.099	.131	.157	.194	
$h\frac{9}{2}\frac{5}{2}$	.263	.148	− .416	− .522	− .470	− .480	− .510	− .551	
	.559	.701	.304	.000	.579	.741	.766	.768	[712]
	.404	.323	.209	.000	− .127	− .123	− .111	− .089	
	.627	.584	.602	.853	.561	.308	.207	.119	
	.242	.169	− .550	.000	.321	.306	.270	.214	
	5.053	1.051	− 1.856	− 0.800	3.041	7.339	11.780	20.836	
	.279	.202	− .082	.000	− .013	− .022	− .027	− .029	
$f\frac{5}{2}\frac{5}{2}$	.619	.556	− .386	.000	.091	.103	.100	.088	
	.497	.506	− .517	− .378	− .261	− .205	− .170	− .128	[703]
	− .241	− .207	.100	.000	.021	.042	.058	.078	
	− .439	− .507	.473	.000	− .187	− .255	− .290	− .327	
	− .207	− .307	.586	.926	.942	.938	.934	.928	

$N = 7 \quad \Omega = \frac{3}{2}$

base vectors: $|771+\rangle$, $|751+\rangle$, $|731+\rangle$, $|711+\rangle$, $|772-\rangle$, $|752\ \ \rangle$, $|732-\rangle$.

	$\eta = -6$	-4	-2	0	2	4	6	10	$+\infty$
$j\frac{15}{2}\frac{3}{2}$	−26.942	−26.599	−27.428	−29.400	−32.475	−36.569	−41.533	−53.292	[761]
	.609	.693	.749	.775	.769	.740	.699	.619	
	− .408	− .305	− .164	.000	.165	.310	.423	.557	
	.214	.102	.027	.000	.026	.091	.173	.317	
	− .121	− .035	− .004	.000	.003	.016	.039	.088	
	.522	.590	.628	.633	.605	.553	.486	.356	
	− .331	− .248	− .130	.000	.117	.201	.246	.252	
	.147	.074	.019	.000	.014	.043	.069	.092	
$h\frac{11}{2}\frac{3}{2}$	−17.640	−15.485	−15.394	−17.000	−19.883	−23.755	−28.480	−39.004	[752]
	.177	.189	.122	.000	− .086	− .065	.002	− .023	
	.320	.534	.719	.780	.780	.704	.577	− .382	
	− .544	− .508	− .289	.000	.279	.455	.480	− .396	
	.627	.386	.089	.000	.048	.119	.149	− .142	
	.408	.327	.176	.000	− .213	− .470	− .634	.693	
	− .045	.306	.553	.603	.490	.206	− .113	.421	
	− .090	− .266	− .200	.000	.135	.126	.021	.134	
$j\frac{13}{2}\frac{3}{2}$	−13.875	−12.836	−12.765	−14.400	−17.534	−21.522	−25.432	−32.534	[741]
	.583	− .573	− .619	− .633	− .609	− .609	− .633	.684	
	− .155	.175	.143	.000	− .058	.061	.186	− .179	
	− .025	− .082	− .035	.000	− .003	.107	.294	− .472	
	.050	.088	.014	.000	− .001	.031	.101	− .195	
	− .279	.528	.719	.775	.733	.561	.323	− .088	
	.583	− .522	− .273	.000	.290	.516	.548	− .410	
	− .465	.276	.068	.000	.057	.178	.252	− .250	
$f\frac{7}{2}\frac{3}{2}$	9.104	− 9.079	− 7.497	7.800	− 9.935	−12.490	−14.650	−18.200	[732]
	− .085	.109	.031	.000	− .070	.151	.170	.150	
	.439	− .323	− .120	.000	.034	.006	.063	.106	
	.027	− .285	− .634	.845	.787	− .601	− .477	− .329	
	− .565	.721	.642	.000	.263	− .274	− .253	− .206	
	.553	− .368	− .100	.000	.141	− .341	− .460	− .578	
	.251	− .343	− .334	.000	− .516	.627	.604	.538	
	− .333	.173	− .221	.535	.139	.179	.316	.438	
$h\frac{9}{2}\frac{3}{2}$	1.744	− 3.792	− 4.958	− 6.000	8.012	− 8.733	− 8.817	8.270	[721]
	− .464	.349	− .184	.000	.152	.224	.275	.343	
	− .515	.542	− .552	− .603	.566	.592	.626	.663	
	.193	− .078	.007	.000	.297	.441	.444	.405	
	.293	− .213	− .026	.000	.122	.267	.335	.395	
	.288	− .276	.193	.000	.169	− .181	.164	− .126	
	.002	− .155	.476	.780	.541	.256	.132	.034	
	− .560	.658	− .630	.000	.481	.485	.424	.325	

continued

	$\eta=-6$	-4	-2	0	2	4	6	10	$+\infty$
	5.411	0.954	− 2.425	− 1.800	− 0.927	0.712	2.795	7.467	
	− .092	− .096	− .060	.000	− .030	− .056	− .067	− .069	
$p\,\frac{3}{2}\,\frac{3}{2}$	.021	− .052	− .155	.000	.158	.173	.159	.127	
	.412	.442	.323	.000	− .192	− .106	− .064	− .027	[712]
	.306	.421	.684	1.000	− .478	− .366	− .303	− .229	
	.281	.209	.094	.000	.044	.098	.137	.185	
	.627	.566	.413	.000	− .298	− .424	− .484	− .542	
	.505	.502	.469	.000	.786	.795	.788	.773	
	14.693	8.303	2.600	− 0.800	2.233	6.491	10.917	19.966	
	.165	.119	.053	.000	.015	− .029	− .039	.054	
$f\,\frac{5}{2}\,\frac{3}{2}$	.500	.436	.306	.000	.119	.158	.182	.212	
	.671	.665	.638	.535	.121	.454	.474	.496	
	.300	.316	.333	.000	.828	.839	.836	.826	[701]
	− .123	− .105	− .055	.000	.016	.025	.028	.028	
	− .305	− .333	− .305	.000	− .117	− .113	− .103	− .084	
	− .273	− .363	− .538	.845	.332	.225	.175	.122	

$N=7\quad \Omega=\frac{1}{2}$

base vectors: $|770+>$, $|750+>$, $|730+>$, $|710+>$, $|771->$, $|751->$, $|731->$, $|711->$.

	$\eta=-6$	-4	-2	0	2	4	6	10	$+\infty$
	− 26.392	− 26.200	− 27.200	− 29.400	− 32.797	− 37.378	− 43.098	− 57.413	
	.577	.657	.710	.730	.717	.673	.608	.471	
	− .380	− .291	− .158	.000	.160	.300	.408	.515	
	.183	.097	.027	.000	.027	.103	.211	.418	
$f\,\frac{15}{2}\,\frac{1}{2}$	− .063	− .025	− .004	.000	.004	.033	.095	.264	[770]
	.553	.624	.670	.683	.662	.610	.531	.352	
	− .365	− .273	− .146	.000	.142	.258	.328	.325	
	.187	.091	.024	.000	.022	.077	.137	.189	
	− .103	− .030	− .004	.000	.002	.014	.031	.053	
	16.200	11.669	15.023	17.000	20.554	25.623	32.110	46.822	
	.426	.286	.142	.000	− .128	− .166	− .108	.090	
	.003	.438	.664	.739	.689	.577	.449	− .236	
$h\,\frac{11}{2}\,\frac{1}{2}$	− .153	− .381	− .268	.000	.284	.506	.579	− .461	
	.097	.161	.066	.000	.083	.280	.421	− .417	[761]
	.141	.246	.159	.000	− .173	− .369	− .512	.554	
	.343	.458	.611	.674	.585	.314	− .062	.438	
	− .538	− .433	− .244	.000	.217	.256	.081	.219	
	.599	.313	.073	.000	.038	.072	.037	.055	

continued

	γ 6	4	2	0	2	4	6	10	− ∞
	13.789	−12.505	−12.500	−14.400	−18.063	−23.313	−29.142	−40.249	
	.185	− .508	− .652	− .683	− .651	− .609	− .626	.676	
	− .536	.416	.199	.000	− .169	− .176	− .099	.183	
	.480	− .223	− .051	.000	− .044	− .052	.113	− .257	
$\frac{13}{2}\frac{1}{2}$	.230	.081	.012	.000	− .014	− .027	.109	− .338	[750]
	.091	.588	.686	.730	.689	.523	.266	− .022	
	.212	− .328	− .239	.000	.259	.505	.567	− .385	
	.040	.192	.066	.000	.065	.250	.408	− .400	
	.012	− .149	− .020	.000	.010	.061	.122	− .143	
	7.942	7.628	6.394	7.800	−11.684	16.940	21.485	−29.147	
	.063	− .506	− .064	.000	− .047	.159	.174	− .119	
	.202	.342	− .300	.000	− .078	.177	.276	− .291	
	− .315	.171	.130	.756	.703	.482	.294	.113	
$\frac{7}{2}\frac{1}{2}$	.154	− .027	.257	.000	.496	− .575	− .509	.377	[741]
	− .209	.178	.002	.000	.115	− .367	− .526	.656	
	.376	− .220	− .171	.000	− .399	.456	.365	− .219	
	.096	.349	− .574	.655	.257	.192	.356	− .481	
	.580	.725	.545	.000	.113	.024	.105	− .192	
	− 1.621	3.886	− 4.897	6.000	9.793	13.004	−15.329	−18.958	
	.169	.192	.187	.000	.198	.322	− .409	− .511	
	.176	.044	.415	.674	.593	.590	.597	.582	
	.113	.564	.522	.000	− .018	− .063	− .000	.109	
$\frac{9}{2}\frac{1}{2}$	.395	− .417	− .227	.000	.036	− .285	− .383	− .451	[730]
	.469	.360	.213	.000	− .191	.217	.198	.143	
	.519	.541	.572	.739	.466	− .110	.031	.114	
	.194	− .097	− .246	.000	.571	− .584	− .478	− .328	
	294	− 193	.188	.000	.166	− .251	− .247	.208	
	6.347	2.068	1.059	1.800	4.829	5.922	− 6.149	− 5.746	
	.325	2.38	.094	.000	.056	.109	.123	− .115	
	629	.586	411	.000	.211	.194	.144	.079	
	.241	.317	.427	.000	.032	.178	.207	.195	
$\frac{3}{2}\frac{1}{2}$	.406	− .333	− .168	.816	− .671	− .483	− .378	− .265	[721]
	.179	− .165	− .082	.000	.075	.180	.250	.333	
	.133	− .221	− .272	.000	− .381	− .549	− .612	− .659	
	.348	.341	.139	.000	.575	.524	.477	.414	
	325	.444	745	.577	.141	.277	.337	.395	
	14.908	8.299	2.360	− 0.800	− 1.324	0.238	2.294	6.952	
	− .081	− .073	− .043	.000	− .041	− .084	.115	.156	
	− .130	− .166	− .189	.000	.254	.350	− .402	− .459	
	.095	.054	− .089	− .655	− .615	− .657	.675	.687	
$\frac{5}{2}\frac{1}{2}$	.375	.460	.594	.000	.499	.503	− .491	− .469	[710]
	.165	.120	.056	.000	.037	.061	− .069	− .067	
	.502	.439	.315	.000	− .198	− .191	.165	.123	
	.675	.668	.636	.756	.274	.129	− .070	− .023	
	.303	.316	.309	.000	.437	.358	− .302	− .231	

continued

	$\eta = -6$	-4	-2	0	2	4	6	10	$+\infty$
	24.689	15.854	7.379	1.200	4.379	8.608	13.019	22.050	
	.072	.051	.023	.000	.009	.018	.022	.024	
	.291	.247	.167	.000	− .068	− .082	− .082	− .072	
	.613	.587	.527	.000	.206	.173	.147	.112	
$p\,\frac{1}{2}\,\frac{1}{2}$	.670	.685	.705	− .577	− .216	− .145	− .112	− .078	[701]
	− .047	− .039	− .021	.000	− .012	.026	− .037	− .053	
	− .154	− .160	.138	.000	.097	.148	.177	.210	
	− .221	.273	− .350	.000	− .388	− .444	− .470	− .495	
	− .104	− .142	− .234	.816	.864	.850	.840	.827	

REFERENCES

Alaga, G. (1955), Phys. Rev. **100**, 432.

— (1957), Nuclear Phys. **4**, 625.

Alaga, Alder, Bohr, and Mottelson (1955), Mat. Fys. Medd. Dan. Vid. Selsk. **29**, no. 9.

Alder, Bohr, Huus, Mottelson, and Winther (1956), Revs. Mod. Phys. **28**, 432, referred to as ABH.

Arima, A. and Horie, H. (1954), Progr. Theor. Phys. **11**, 509.

Asaro, Perlman, and Stephens (1957), private communication.

Bakke, F. (1958), to be published.

Bés, D. (1958), Nuclear Phys. (in press).

Blin-Stoyle, R. J. (1953), Proc. Phys. Soc. (London) A **66**, 1158.

Bohr, A. (1952), Mat. Fys. Medd. Dan. Vid. Selsk. **26**, no. 14.

Bohr, Fröman, and Mottelson (1955), Mat. Fys. Medd. Dan. Vid. Selsk. **29**, no. 10.

Bohr, A. and Mottelson, B. (1955a), Mat. Fys. Medd. Dan. Vid. Selsk. **30**, no. 1.

Bohr, A. and Mottelson, B. (1955b), Chapter 17 of *Beta- and Gamma-Ray Spectroscopy*, ed. K. Siegbahn (North Holland Publishing Company, Amsterdam).

Bohr, Mottelson, and Pines (1958), Phys. Rev. **110**, 936.

Bromley, Gove, and Litherland, Can. Journ. Phys. (to be published).

Chase, D. and Wilets, L. (1956). Phys. Rev. **101**, 1038.

Chasman, D. and Rasmussen, J. O. (1956), University of California Radiation Laboratory Report UCRL-3629.

Elliot, J. P. (1958, in press).

Elliot, J. P. and Flowers, B. H. (1955), Proc. Roy. Soc. London A **229**, 536.

Fred, Tompkins, and Meggers (1955), Phys. Rev. **98**, 1514.

Fröman, P. O. (1957), Mat. Fys. Skr. Dan. Vid. Selsk. **1**, no. 3.

Gallagher, Sweeney, and Rasmussen (1957), Phys. Rev. **108**, 108.

Ghiorso, Thompson, Higgins, Harvey, and Seaborg (1954), Phys. Rev. **95**, 293.

Gottfried, K. (1956), Phys. Rev. **103** 1017.

Helm, R. C. (1956), Phys. Rev. **104**, 1466.

Hollander J., (1957), Phys. Rev. **105**, 1518.

Hubbs, J. C. and Marrus, R. (1958), Phys. Rev. **110**, 287.

Inglis, D. (1954), Phys. Rev. **96**, 1059.

Kerman, A. (1955), Mat. Fys. Medd. Dan. Vid. Selsk. **30**, no. 15.

Litherland, Mc. Manus, Paul, Bromley, and Gove (1958), Can. Journ. Phys. **36**, 378.

McGowan, F. K. and Stelson, P. H. (1957, to be published).

Moszkowski, S. (1955a), Phys. Rev. **99**, 803.

— (1955b), Chapter 13 of *Beta- and Gamma-Ray Spectroscopy*, ed. K. Siegbahn (North Holland Publishing Company, Amsterdam).

— (1956), Phys. Rev. **103**, 1328.

Mottelson, B. R. and Nilsson, S. G. (1955a), Phys. Rev. **99**, 1615, referred to as MN.
Mottelson, B. R. and Nilsson, S. G. (1955b), Zs. f. Physik, **141**, 217.
Newton, J. O. (1955), Progress in Nuclear Physics (ed. O. Frisch).
— (1957a), Nuclear Phys. **3**, 345.
— (1957b), Nuclear Phys. **5**, 218.
Nilsson, S. G. (1955a), Mat. Fys. Medd. Dan. Vid. Selsk. **29**, no. 16, referred to as SGN.
— (1955b), dissertation (Berlingska boktryckeriet, Lund).
Nilsson, S. G. and Rasmussen, J. O. (1958), Nuclear Phys. **5**, 617.
Paul, E. B. (1956), Physica **22**, 1140.
Perlman, I. and Rasmussen, J. (1957), Chapter on Alpha Radiactivity in *Handbuch der Physik*, vol. 42 (Springer Verlag, Berlin), referred to as PR.
Rasmussen, Canavan, and Hollander (1957), Phys. Rev. **107**, 141.
Rakavy, G. (1957), Nuclear Phys. **4**, 375.
Redlich, M. (1955), Phys. Rev. **99**, 1427.
Reiner, A. S. (1958), Nuclear Phys. **5**, 544.
Sharenberg, R. P. and Goldring, G. (1958), Bull. Am. Phys. Soc. **II**:**3**, 55.
Sheline, R. K. (1956), Nuclear Phys. **2**, 382.
Sliv, L. A. and Band, I. M., Coefficients of Internal Conversion of Gamma Radiation (Acad. of Sciences, USSR, 1956); Translation issued in U.S.A. as Report 57, ICCKI (Phys. Dept., Univ. of Illinois., Urbana, Ill. 1956).
Stelson, P. H. and McGowan, F. K. (1957), Phys. Rev. **105**, 1346.
Strominger, Hollander, and Seaborg, Table of Isotopes (1958), Revs. Mod. Phys. **30**, 505, often referred to in the text as SHS.
Toth, K. and Rasmussen, J. O. (1957), Bull. Am. Phys. Soc. **II**:**2**, 386.

Indleveret til selskabet den 9. juni 1958.
Færdig fra trykkeriet den 2. februar 1959.

Det Kongelige Danske Videnskabernes Selskab

Matematisk-fysiske Skrifter

Mat. Fys. Skr. Dan. Vid. Selsk.

Bind 1

(uafsluttet / in preparation) kr. ø.

1. Brodersen, Svend, and Langseth, A.: The Infrared Spectra of Benzene, sym-Benzene-d_3, and Benzene-d_6. 1956 14,00
2. Nörlund, N. E.: Sur les fonctions hypergéométriques d'ordre supérieur. 1956 .. 15,00
3. Fröman, Per Olof: Alpha Decay of Deformed Nuclei. 1957 20,00
4. Brodersen, Svend: A Simplified Procedure for Calculating the Complete Harmonic Potential Function of a Molecule from the Vibrational Frequencies. 1957 10,00
5. Brodersen, Svend, and Langseth, A.: A Complete Rule for the Vibrational Frequencies of Certain Isotopic Molecules. 1958 6,00
6. Källén, G., and Wightman, A.: The Analytic Properties of the Vacuum Expectation Value of a Product of three Scalar Local Fields. 1958 15,00
7. In preparation.
8. Mottelson, Ben R., and Nilsson, Sven Gösta: The Intrinsic States of Odd-A Nuclei having Ellipsoidal Equilibrium Shape. 1959 22,00

Formerly was published:

Niels Bjerrum: *Selected Papers.* Edited by Friends and Coworkers. Copenhagen 1949. 295 pages. Bound 18,00

This publication is sold by the agent of the Academy,
and it is not obtainable on an exchange basis.

On direct application to the agent of the Academy, EJNAR MUNKSGAARD, Publishers, 6 Nörregade, Köbenhavn K., a subscription may be taken out for the series *Matematisk-fysiske Skrifter*. This subscription automatically includes the *Matematisk-fysiske Meddelelser* in 8vo as well, since the *Meddelelser* and the *Skrifter* differ only in size, not in subject matter. Papers with large formulae, tables, plates etc., will as a rule be published in the *Skrifter*, in 4to.

For subscribers or others who wish to receive only those publications which deal with a single group of subjects, a special arrangement may be made with the agent of the Academy to obtain the published papers included under one or more of the following heads: *Mathematics, Physics, Chemistry, Astronomy, Geology*.

In order to simplify library cataloguing and reference work, these publications will appear without any special designation as to subject. On the cover of each, however, there will appear a list of the most recent paper dealing with the same subject.

The last published numbers of *Matematisk-fysiske Skrifter* within the group of **Physics** are the following:

Vol. **1**, nos. 3, 6, 8.

Printed in Denmark
Bianco Lunos Bogtrykkeri A/S